M-Pos247

WATER CHANNEL ACTIVITY OF WILD TYPE AND MUTANT NODULIN-26 EXPRESSED IN *XENOPUS LAEVIS* OOCYTES.
((G. Chandy[1], D.M. Roberts[2], James Hall[1])) [1]Department of Physiology and Biophysics, U.C. Irvine, Irvine CA, 92717-4560; [2]Department of Biochemistry, University of Tennessey, Knoxville, TN 37996.

MIP-related proteins (MRPs) are a relatively new growing family of integral membrane proteins. MRPs are found in diverse phyla from man to archaebacteria. Nodulin-26, is a plant-encoded symbiosome-membrane MRP, whose physiological function has not been established. Since MIP and most of its relatives have been demonstrated to increase membrane water-permeability, we investigated whether Nodulin-26 and its site directed mutants (S262A and S262A) also increased oocyte membrane water-permeability. We have expressed the recombinant proteins in *Xenopus* oocytes and have compared their water fluxing properties to MIP and Aquaporin-1, a known water channel. Nodulin-26 and the mutants increase oocyte membrane water-permeability more than MIP but less than Aquaporin-1. To further characterize the water channel properties of Nodulin-26 we will determine whether Nodulin-26 is inhibited by $HgCl_2$ and measure the activation energy of the induced water-permeability.

SYNAPTIC TRANSMISSION AND PLASTICITY

M-Pos248

RELEASE OF CAGED BIOEFFECTOR MOLECULES BY TWO PHOTON EXCITATION: EXCITATION SPECTRA, ABSORPTION CROSS SECTIONS AND PRACTICALITIES OF SOME COMMON CAGING GROUPS.
((Warren R. Zipfel, Rebecca M. Williams and Watt W. Webb)) Developmental Resource for Biophysical Imaging and Opto-Electronics (DRBIO), Applied and Engineering Physics, Cornell University, Ithaca, NY 14853.

Photolysis of photoactivatable or "caged" compounds provides a means of spatially and temporally controlling the release of biologically active molecules such as metabolites, neurotransmitters or calcium. The use of two photon excitation provides 3D spatial control and limits the region of potentially deleterious effects of UV light. The two photon excitation spectra and cross-sections were measured for carboxy-2-nitrobenzl ester caged GABA over the wavelength range 630 to 700nm using HPLC analysis of photoproduct, and for 4,5 - dimethoxy-2-nitrobenzl ester caged fluorescein over the wavelength range 680nm to 760nm using a calibrated fluorescence standard. In addition, several aspects related to the practical use of these caged compounds were measured, including pH dependence of photorelease, stability at 37C, percent initial uncaged effector (especially important to the use of caged neurotransmitters), and potential for membrane damage from focused illumination.

Supported by NSF (DIR8800278), NIH (RR04224) and NIH (R07719) at DRBIO.

M-Pos249

INDUCTION OF LTD BY PHOTOLYTIC RELEASE OF INOSITOL TRISPHOSPHATE IN PURKINJE NEURONES.
((Kamran Khodakhah)) University of Pennsylvania, Department of Physiology, PA 19104.

Repeated concurrent activation of excitatory inputs of a Purkinje neuron, the Climbing and Parallel fiber inputs, results in the long term depression (LTD) of the Parallel fiber synaptic strength. It is thought that activation of the $InsP_3$-mobilizing glutamate metabotropic receptors by Parallel fibers is necessary for the induction of LTD. Whole cell patch clamp technique was combined with intracellular flash photolytic release of $InsP_3$ and microspectrofluoremitry to study the role of $InsP_3$ in the induction of LTD in Purkinje neurones. Caged $InsP_3$ and a fluorescent Ca indicator (Furaptra or Fluo-3) were introduced into the cell *via* the patch pipette and the cell was voltage clamped at the chloride reversal potential (set between -70 to -100 mV). Parallel fibers were stimulated by an extracellular electrode and a stable synaptic response was recorded for 10-30 min before a 1ms pulse of UV light (300-350nm) was used to photolytically release 5-80μM $InsP_3$. Photolytic release of $InsP_3$ >10μM evoked calcium release from intracellular stores which when combined with a 50ms depolarization of the Purkinje neuron, was effective in producing 25-50% depression in the Parallel fiber response persisting >80 min. Succeeding "depolarization+$InsP_3$" pulses produced further depression only if the previously-induced depression was less than 50%. Flash photolytic release of $InsP_3$ without depolarization occasionally resulted in LTD, but was not as effective (5-20% depression) or reproducible as that combined with depolarization. Inclusion of 10mM BAPTA in the patch pipette inhibited the induction of LTD. The results demonstrate the ability of $InsP_3$-evoked calcium release to substitute for the Parallel fiber activation during induction of LTD. Further, it appears that $InsP_3$-evoked calcium release combined with calcium entry *via* the voltage activated calcium channels is sufficient to produce LTD in the cerebellum.

M-Pos250

POPULATION DYNAMICS OF SYNAPTIC RELEASE SITES.
((Richard Bertram, Arthur Sherman)) NIDDK, NIH, Bethesda, MD 20892.

There is substantial evidence that Ca^{2+} channels and transmitter release sites are co-localized in the synaptic terminal. A recent model for synaptic transmission [Bertram et al, *Biophys. J.* 68:A396,1995] proposes that the release time course is determined by the kinetics of Ca^{2+} binding to these sites rather than diffusion of Ca^{2+} or membrane potential. Neglecting diffusion simplifies the model but obligates consideration of the stochastic nature of Ca^{2+} channel opening, because each release site has a different history of exposure to Ca^{2+}. We derive a system of partial differential equations for the probability distributions of bound sites under open and closed channels in a nerve terminal. The expected values of these distributions are given by a system of ordinary differential equations (ODEs), which can be used to determine release over long pulse trains. Although the instantaneous time course of binding is complex, binding averaged over a pulse is simple, allowing derivation of approximate formulas and the almost complete invariance of the normalized release time course to changes in quantal content. We suggest several approximations that can dramatically reduce the number of ODEs while retaining many or all of the phenomenological characteristics of the model, making it adaptable for use in applications ranging from studies of single terminals to large networks of neurons.

M-Pos251

PREPULSE FACILITATED NEURONAL L-TYPE CA CHANNEL AND CARDIAC α_{1L} IS MEDIATED BY TWO DISTINCT PHOSPHORYLATION SITES.
(Gl. Lee[2*], A.. Bibikova[2], A. Sculptoreanu[2] and M. Chahine[1]). Laval Hospital Research Center[1], Laval Univ., Ste-Foy, Qc., and Depts. of Exptl. Med. and Surgery[2], Lady Davis Institute for Med. Res. of SMBD- Jewish General Hospital, McGill University, Montreal, Qc, H3T 1E2 (**Sponsor GI Lee**).

Calcium currents in primary cultures of parasympathetic neurons isolated from major pelvic (MPG) ganglia of rats are predominantly L-type and are facilitated by prepulses. Facilitation of the neuronal currents is similar to prepulse facilitation in oocytes injected with mRNA encoding for the rabbit cardiac α_1-subunit in several aspects: inhibition by Rp-CAMPS (50 μM), enhancement by low concentrations of okadaic acid (0.1-1 μM) and occlusion by higher concentrations of okadaic acid (5-10 μM) and Sp-CAMPS (100 μM). Enhancement and occlusion of facilitation by okadaic acid was blocked by the dihydropyridine antagonist isradipine (PN200-110) and 200 μM Cd^{2+} and prevented by pre-exposure to Rp-CAMPS. Higher concentrations of Rp-CAMPS (500 μM) were required to block facilitation in oocytes. Pre-exposure of neurones to Sp-CAMPS (100 μM) for several minutes before establishing whole cell configuration also lead to rapid occlusion of facilitation, however the irreversible increase in control currents (before prepulse) lagged the apparent runup of facilitated currents by several seconds. The dual action of okadaic acid and Sp-CAMPS can be attributed to two effects: a significant (10 fold) speeding up of in the time dependent onset of facilitation and a slowing in the recovery immediately following the facilitating prepulse. The latter is probably responsible for the eventual occlusion with high concentrations of okadaic acid. This data suggests that at least two phosphorylation sites may be involved -one responsible for the initial rapid enhancement by prepulse and another responsible for occlusion of facilitation with high cAMP-dependent protein kinase activity. In addition, the dual concentration dependent effect of okadaic acid suggests that different and specific phosphatases may be involved in the reversal of prepulse facilitation of L-type calcium channel currents in parasympathetic neurons. *(Supported by grants from MRC to AS and MC and Heart Foundation to MC and AS. PN200-110 was a gift from Sandoz Canada.)*

M-Pos252

A MODEL OF PRESYNAPTIC CALCIUM TRANSIENTS AND NEUROTRANSMITTER RELEASE FROM TERMINALS IN THE MAMMALIAN CENTRAL NERVOUS SYSTEM
((S.R. Sinha*, L.-G. Wu^ and P. Saggau*)) *Baylor College of Medicine, Houston, TX 77030 and ^University of Colorado Health Science Center, Denver, CO 80262, (Spon. by J.A. Dani)

The development of techniques for selectively loading calcium indicators into presynaptic terminals of mammalian brain slices now allows for the investigation of the nonlinear relationship between presynaptic calcium ($[Ca^{2+}]_{pre}$) and neurotransmitter release in these preparations. However, several questions remain about the exact nature and the accuracy of the signals measured. To address these questions, we have developed a simple model of a mammalian presynaptic terminal. The model consists of concentric spherical shells with radial diffusion only. In addition to diffusion, the dynamics of Ca^{2+} binding to intrinsic buffers and to calcium indicators is also included. Transmitter release is modelled as a power function of $[Ca^{2+}]_{pre}$ and a saturable process with a finite number of release sites. Model parameters were based on literature values and on our own experimental data from hippocampal brain slices.

Using this model, we investigated the dynamics of $[Ca^{2+}]_{pre}$ upon influx of Ca^{2+} into a presynaptic terminal and the ability of the calcium indicators fura-2 (high affinity) and furaptra (low affinity) to measure these transients. We also tested the fidelity with which the indicators could measure the degree of nonlinearity between $[Ca^{2+}]_{pre}$ and transmitter release. Furaptra reflected the amplitude and kinetics of the volume-averaged $[Ca^{2+}]_{pre}$ much more accurately than fura-2; however, in agreement with our experimental results, for a certain range of parameters, both indicators were equally able to measure the degree of nonlinearity. The model was also used to compare the efficacy of changes in duration of Ca^{2+} influx as opposed to amplitude in causing transmitter release. A change in amplitude was much more effective, *i.e.*, transmitter release was a higher power function of $[Ca^{2+}]_{pre}$. This is in agreement with experimental results obtained with application of 4-aminopyridine, a K^+-channel blocker.

Implications of the model and its parameters for neurotransmitter release and $[Ca^{2+}]_{pre}$ dynamics in the mammalian central nervous system will be discussed.

M-Pos253

SHORT FIRST LATENCY OF NMDA RECEPTOR CHANNELS IN PATCHES.
((Jeffrey A. Dzubay, Dawn Shepherd, and Craig E. Jahr)) The Vollum Institute, Oregon Health Sciences University , Portland, Oregon 97201. (Sponsored by Craig E. Jahr)

The single channel behavior underlying the slow timecourse of the NMDA EPSC has been explained by two contrasting schemes. In one scheme the receptor channels open quickly after binding glutamate, have a moderately high peak open probability, and continue to re-open while the agonist remains bound for several hundred milliseconds (Jahr, 1992). The second scheme requires a very low open probability and long first latencies (Edmonds and Colquhoun, 1992). The goal of this study was to determine which scheme best describes NMDA channel behavior by looking at the speed with which the channels first open after binding agonist. Outside-out patch recordings from cultured rat hippocampal neurons were used in conjunction with fast application techniques and the open channel blocker MK-801. The amount of block produced by either a brief pulse of 10 mM L-glutamate and 20 uM MK-801 (62±10%, n=7) or a pulse of the rapidly dissociating low affinity agonist L-cysteate (10 mM) in the continuous presence of 20 uM MK-801 (79±11%, n=7), was comparable (p>0.1, Student's t-test) to that produced by a brief pulse of 10 mM L-glutamate in the continuous presence of 20 uM MK-801 (70±10%, n=8)). Thus, the majority of the channels that open, do so for the first time early (< 20 ms) in the response. These results, along with our findings that MK-801 does not block desensitized receptors, support the first scheme in which the channels have short first latencies. It follows from this high open probability scheme that relatively few channels are required at each synaptic site to account for the amplitude of miniature EPSCs.

Edmonds B, Colquhoun D (1992) Rapid decay of averaged single-channel NMDA receptor activations recorded at low agonist concentration. Proc. R. Soc. Lond. B. 250: 279-286.
Jahr CE (1992) High probability opening of NMDA receptor channels by L-glutamate. Science 255: 470-472.

M-Pos254

A NEURONAL G PROTEIN-GATED K^+ CHANNEL IS A MULTIMER OF INWARD RECTIFIER CHANNEL SUBUNITS
((Bratislav M. Velimirovic, Eric A. Gordon, Nancy F. Lim, Betsy Navarro and David E. Clapham)) Department of Pharmacology, Mayo Foundation, Rochester, MN 55905

G protein-activated inward rectifying potassium channel clones GIRK1, GIRK2, and CIR were expressed individually or in combination in *Xenopus laevis* oocytes and CHO cells. Expression of any of these single inward rectifier clones yielded relatively small currents. However, when GIRK1 was coexpressed with CIR or GIRK2, up to 10-fold larger currents were recorded. No such clear synergistic effects were observed after coexpression of CIR/GIRK2 under the same conditions. G protein βγ dimer (Gβγ) subunits purified from bovine brain increased channel activity 50 to 1000-fold in oocytes and CHO cells expressing GIRK1/GIRK2. Expressed channels had a conductance of 32 pS, a mean open time of 0.9 ms at -70 mV, and sharply inwardly rectified in the presence of Mg^{2+} or polyamines. $G\beta_1\gamma_2$ coexpressed with GIRK2 alone yielded large net currents in the basal state. Purified Gβγ strongly activated single GIRK2 channels which exhibited the same properties as CIR channels expressed in oocytes, Sf9 and CHO cells: channels were short-lived and of variable conductance. The GIRK2 subunit, in addition to the proposed role for interaction with GIRK1, may play an important role in the activation of the native heteromultimeric channel by Gβγ. We propose that a neuronal G protein activated inward rectifier K+ channel is a heteromultimer formed by GIRK1/GIRK2 potassium channel clones and that Gβγ activation may involve both subunits. This work was supported by an NIH grant to DE Clapham, an American Heart Association fellowship to B Velimirovic, an NIH NRSA to EA Gordon, an NIH NHLBI training grant to NF Lim, and a grant from Colciencias to B. Navarro.

M-Pos255

LIPID- AND ANESTHETIC-PROTEIN INTERACTIONS IN THE NICOTINIC ACETYLCHOLINE RECEPTOR PROBED BY FTIR DIFFERENCE SPECTROSCOPY
((Stephen E. Ryan, Caroline N. Demers, and John E. Baenziger)) Dept. of Biochemistry, University of Ottawa, Ottawa, Canada K1H 8M5

The effects of different lipids and several local anesthetics on the carbamylcholine induced structural changes in the nicotinic acetylcholine receptor (nAChR) have been explored using FTIR *difference* spectroscopy. The difference of spectra acquired in the presence and absence of Carb from native, native alkaline extracted, and affinity purified nAChR reconstituted into PC/PA/Chol exhibit a similar pattern of positive and negative bands indicating an essentially identical structure and resting-to-desensitized conformational change in all three lipid membranes. In contrast, the difference of spectra recorded in the presence and absence of Carb from the nAChR in membranes lacking Chol and/or PA exhibit subtle variations that are essentially identical to those observed in difference spectra recorded in the continuous presence of the local anesthetic, dibucaine, from the nAChR in PC/PA/Chol. The results suggest that both Chol and PA exert their effects on nAChR function through a similar mechanism of action and that in the absence of both lipids, the nAChR is stabilized in a conformation that is essentially identical to that stabilized by dibucaine. The implications of the variations detected in the difference spectra on the mechanisms of lipid and ligand action at the nAChR are discussed.

M-Pos256

THE DYNAMICS OF MITOCHONDRIA CA^{2+} REMOVAL AND ITS EFFECT ON NEUROPEPTIDE TRANSMISSION AT INTACT NERVE TERMINALS.
((Y-Y. Peng)) Dept. of Pharmac.\Physiol. Sci., Univ. of Chicago, 947 E. 58th St, Chicago, IL. 60637. (Spon. by Amy Beth Harkins)

The preganglionic nerve terminals in bullfrog sympathetic ganglia release neuropeptide LHRH with a slow time course and they are rich with mitochondria. As LHRH release is controlled quantitatively by nerve-evoked intraterminal Ca^{2+} transients, effects of mitochondria uncoupler CCCP (10 μM) on these transients were monitored by fura-2 fluorimetry while the presynaptic nerves were stimulated electrically.

CCCP increased the rate of Ca^{2+} rise and the peak amplitude of $[Ca^{2+}]_i$ during nerve firing (ranging from 30 to 1500 nM). In normal Ringer, many responses to prolonged stimulation (> 300 stimuli at 20 Hz) had a plateau and sometimes even a decay phase during the stimulation. In CCCP the $[Ca^{2+}]_i$ increased monotonically during stimulation. CCCP also slowed down the Ca^{2+} decay after the cessation of the stimulation. Thus, Ca^{2+} removal by the mitochondria had a limiting effect on both the amplitude and the duration of the nerve evoked Ca^{2+} elevation and should therefore had limited the total amount of peptide release. Effects of CCCP were produced directly by blockade of the uniporter which sustained the nerve-evoked intraterminal Ca^{2+} elevation. The sustained Ca^{2+} elevation enhanced the Ca-induced-Ca release (CICR) from the ryanodine-sensitive store which further amplified the Ca^{2+} signal. At rest, intraterminal mitochondria removed Ca^{2+} at such a low rate that when the process was blocked by CCCP, the resting $[Ca^{2+}]$ was increased by as little as 5 nM. In contrast, after prolonged nerve firing (e.g. 800 action potentials at 20 Hz), CCCP produced $\Delta[Ca^{2+}]_i$ as high as 2.7 μM.

This work was supported by the Alfred Sloan Foundation and the NINDS of NIH.

M-Pos257

GLOBAL ELECTROSTATIC PROPERTIES IN CHOLINESTERASES
D. Ripoll, C. Faerman (Cornell Theory Center, and Dept. of Biochemistry, Molecular and Cell Biology -Cornell University, Ithaca NY 14853, USA) I. Silman, J. Sussman (Dept. of Neurology, and Dept. of Structural Biology, Weizmann Institute of Science, Rehovot 76100 ISRAEL)

Acetylcholinesterase and butyrylcholinesterase from humans have a high degree of sequence identity with acetylcholinesterase from Torpedo Californica. We calculated the electrostatic properties of these two human enzymes, using the molecular models recently reported by Harel et al. We found out that the global electrostatic properties are well conserved within the family. Furthermore, a puzzling observation of an area spanning across the dimer of Tc AChE, also present in the two model of the human enzymes, is documented here. This novel site could potentially have important consequences in the design of new inhibitors of these relevant enzymes.

M-Pos258

LATENT COUPLING BETWEEN CA1 NEURONS IN HIPPOCAMPUS ((T.Tsintsadze, A.Klishin, N.Lozovaya, O.Krishtal)) Bogomoletz Institute of Physiology, Bogomoletz str.4, Kiev, Ukraine.

When performed temporary block of A_1 adenosine receptors in hippocampus (by 8-cyclopentyltheophylline, CPT) at increased external $[Ca^{2+}]/[Mg^{2+}]$ ratio (2.5 mM/0.5 mM), leads to a dramatic and irreversible change in the EPSC evoked by Schaffer collateral/commissural (SCC) stimulation and recorded by *in situ* patch clamp in CA1 pyramidal neurons. The duration of the EPSC becomes stimulus-dependent, increasing with increase in stimulus strength. The later occurring component of the EPSC is carried through NMDA receptor-operated channels, but disappears under either the NMDA antagonist, APV, or the nonNMDA antagonist CNQX. These findings indicate that the late component of the SCC evoked EPSC is polysynaptic: predominantly nonNMDA receptor-mediated SCC inputs excite CA1 neurons that recurrently excite each other by predominantly NMDA receptor-mediated synapses. These recurrent connections are normally silent but become active after CPT treatment, leading to enhancement of the late component of the EPSC. When all functional NMDA receptors are blocked by MK-801, subsequent application of CPT leads to a partial reappearance of NMDA receptor-mediated EPSCs evoked by SCC stimulation indicating that latent NMDA receptors are recruited.

M-Pos259

MOLECULAR MODELING OF THE NICOTINIC ACETYLCHOLINE RECEPTOR TRANSMEMBRANE REGION IN THE OPEN STATE. ((M.O. Ortells, G.E. Barrantes and F.J. Barrantes)) Instituto de Investigaciones Bioquímicas de Bahía Blanca, CONICET, CC 857, 8000 Bahía Blanca, Argentina.

The nicotinic acetylcholine receptor is the best studied member of all the ligand gated ion channels. On the basis of a previous closed-state model of its transmembrane region (Ortells & Lunt, *J. Neurochem.*. 1995, *65*:S72, and *Prot. Engng., submitted*), we have now generated a model of the open-state by replacing the M2 helical regions surrounding the ion-channel proper with kinked helices. This opening was done in such a way as to match the positions of the M2's observed in the electron microscope images produced by Unwin (Nature, 373:37, 1995). In both models (open and closed), M1 is built as a three-strand β-sheet, M3 is half β-sheet and half helical, and M4 is an α-helix. In the construction of the new model, due account was taken of those residues labeled, or known by other means (e.g. mutational or electrophysiological studies) to have a strong influence on ion permeation properties, the assumption being made that such residues are accesible from the lumen of the channel. Following the *Torpedo* α subunit nomenclature, the residues E241, T244, L245, S248, L250, L251, S252, T254, V255, L258, V259, I260, and E262 face the ion channel in one or more of the three ion-channel states (open, closed and desensitized). All of them with the exception of L250, are visible from the lumen in our open-state model. In the upper half of the channel, the M2's are widely separated and their side chains are readily visible from the lumen, and hence all labeling can be explained by the probes having access to the M2's from the channel itself. The lower half of the channel is more closely packed, and because of the inclination imposed by the kink in the M2s, the side chains of three residues labeled by chlorpromazine (T244, S248 and L251) are at the almost the same level, in a plane parallel to the membrane surface.

Supported by CONICET and Fundación Antorchas from Argentina, and the European Union grant No. CII-CT94-0127.

M-Pos260

A MATHEMATICAL DESCRIPTION OF mPSC GENERATION AT CENTRAL SYNAPSES: INFLUENCE OF SYNAPTIC GEOMETRY. ((V. Uteshev and P. Pennefather)). Dept of Physiology, Univ. Toronto, M5S 2S2.

We have developed an analytical description of the generation of miniature postsynaptic currents (mPSCs) at individual punctate synapses commonly found on CNS neurons and have considered the influence of synaptic geometry on mPSC generation. By synaptic geometry we mean the shapes and relative positions of the cluster of postsynaptic receptors (hot spot) and of the presynaptic region where evoked vesicular release can occur (active zone) as well as the width of the synaptic cleft. We also consider explicitly diffusion of neurotransmitter out of the vesicle (non-instantaneous release) and diffusion in the synaptic cleft as well as the pharmacodynamics of ion channel activation by neurotransmitter. The amplitude of mPSCs recorded in both cultured neurons and in brain slices exhibits considerable variation (C.V.~0.5) and the distribution of amplitudes is skewed towards smaller values. Our analysis provides an explanation for this observation. If release of successive mPSCs can occur with equal probability anywhere within the contours of an active zone, the distance from that point to the center of the postsynaptic hot spot of receptors will vary sufficiently to influence the concentration of transmitter at the hot spot. With realistic parameters, this effect is sufficient to generate the observed variability mPSC amplitude. Only a few release sites will be optimally positioned just over the center of the hot spot and thus generate mPSCs with the largest observable amplitude; for most release sites the diffusional distance will be larger and the resulting mPSCs smaller. Guassian amplitude distributions are not expected, these distributions will be skewed towards smaller values. Supported by NCE Neuroscience Network and MRC (Canada).

M-Pos261

SPECIFIC UP-REGULATION OF NMDA COMPONENT OF HIPPOCAMPAL EPSC IN ISCHEMIA. T.Tsintsadze, N. Lozovaya, A.Klishin and O.Krishtal

Electrophysiological recording were made from the hippocampal slices exposed to *in vitro* ischemic conditions in which the superfused medium was hypoxic and deprived of glucose. The excitatory postsynaptic current (EPSC) recorded from CA1 pyramidal neurons were initially depressed. Reoxigenation with normal solution for 2 hours after brief (10 min) ischemia led to a dramatic and irreversible change in the EPSC. Kinetics acquired stimulus-dependence and markedly slowest down with the increase in the stimulus strength. The stimulus-dependent fraction of EPSC is carried through NMDA receptor-operated channels and disappears under NMDA antagonist. When slices were exposed to a severe ischemic conditions for 40 min initially inhibited EPSC transiently increased and after few minutes disappeared. This transient increase was accompanied with predominant enhancement of NMDA component and was prevented by the antagonist of NMDA receptors, APV, and antagonist of metabotropic receptors RS-α-Methyl-4-carboxyphenylglycine.

EPITHELIAL

M-Pos262

TWO TYPES OF INTRACELLULAR CA^{2+} POOLS IN THE PORCINE TRACHEAL EPITHELIAL CELLS. ((Young-Kee Kim and Hyoung-Jin Cho)) Department of Agricultural Chemistry, Chungbuk National University, Cheung-Ju, Chungbuk, 360-763, Korea.

Membrane vesicles prepared from the epithelial cells of porcine trachea were tight-sealed vesicles since they showed a saturation in $^{45}Ca^{2+}$ uptake experiment and spontaneous release of stored $^{45}Ca^{2+}$ by the addition of Ca^{2+} ionophores. It has been known that the tracheal epithelial cells have intracellular $InsP_3$-sensitive Ca^{2+} stores. We have found that $InsP_3$ indirectly increases the activity of microsomal Ca^{2+}-ATPase through the release of luminal Ca^{2+}. $InsP_3$-induced increase in the activity of microsomal Ca^{2+}-ATPase was dose-dependent up to 20% of the total activity; however, more than 30% of total activity were thapsigargin-sensitive and $InsP_3$-independent. In order to characterize the $InsP_3$-insensitive activity of Ca^{2+}-ATPase, total activity of microsomal ATPases was monitored at various concentrations of free Ca^{2+} in the absence of $InsP_3$. The activity showed a bell-shape change dependent on the Ca^{2+} concentration and the maximal activity was observed at 100 nM Ca^{2+}. The biphasic change of the activity was appeared only in the intact vesicles and was sensitive to thapsigargin. Since Ca^{2+}-dependent biphasic change in the activity of caffeine-sensitive Ca^{2+} release channel is well-known, we examined the caffeine sensitivity of the vesicles. The microsomes released 30~40% of the stored $^{45}Ca^{2+}$ by 10 mM caffeine while $InsP_3$ (10 μM) released ~20% of the stored $^{45}Ca^{2+}$. The caffeine-induced release was inhibited by procane, an antagonist of ryanodine receptor channel, and was biphasic on various concentrations of free Ca^{2+} with a maximal release at 0.1~1 μM. $^{45}Ca^{2+}$ releases from these two types of stores were additive indicating that these two types of intracellular Ca^{2+} stores are physically independent. These results suggest that the tracheal epithelial cells have at least two types of intracellular Ca^{2+} stores, $InsP_3$-sensitive store and caffeine-sensitive store.

M-Pos263

CLONING OF A HOMOLOGUE OF THE INWARD RECTIFYING K^+-CHANNEL, IRK1, FROM REPTILIAN COLON ((L. Thomas, D. C. Dawson and J. Offord)) Dept. of Physiology, University of Michigan and Dept. Biotechnology, Parke-Davis Pharmaceutical Res. Div. of Warner-Lambert Co., Ann Arbor, MI 48105 (Spon. by J Jacquez)

The colon of the fresh water turtle absorbs K and secretes Na, activities that depend on the function of basolateral and apical K channels. Although functional assays provide evidence for at least four distinct K channel types in colonic cells, an understanding of the molecular basis for K channel function in these epithelial cells has been hampered by the absence of molecular probes for channel proteins. Recently, a new class of K channels has been identified, typified by ROMK1 and IRK1. Northern blot analysis of turtle colon RNA revealed the presence of an IRK1-channel homologue. Using cDNA probes for macrophage K^+-channel (IRK1) and nested PCR of turtle colon cDNA we were able to clone and sequence an inward rectifying K-channel with high sequence homology to the macrophage IRK1. (NIH Support)

M-Pos264

DIVERSITY OF PLASMA MEMBRANE CALCIUM PUMP ISOFORMS (rPMCAs) ALONG THE RAT NEPHRON

((Ariel Caride, Eduardo Chini, Sumiko Homma, John Penniston, and Thomas Dousa)) Dept. Biochem. & Molec. Biol. & Nephrology Res. Unit, Mayo Clinic, Rochester, MN 55905.

The three major divisions of the rat kidney (cortex, outer medulla and papilla) were macrodissected and assayed for the presence of mRNA codifying for rPMCA 1, 2, 3, and 4 by RT-PCR. Both cortex and outer medulla showed all rPMCAs, although semiquantitative comparisons indicated that cortex is enriched in rPMCA2 compared to the outer medulla, and rPMCA3 is more abundant in the outer medulla. In contrast, papilla showed only message for rPMCAs 1 and 4. The primers used allowed us to study their alternative splices at site C. All isoforms expressed the variant b, except rPMCA3, which expressed primarily variants a and c in the cortex and variants a, b, and c in the outer medulla. The nephron segments corresponding to the cortex and outer medulla were microdissected and analyzed by RT-PCR. rPMCA4 was present all along the nephron. rPMCA1 and 2 were found in all nephron segments, but more frequently in glomerulae, PCT, DTL, CTAL, DCT and CCD. rPMCA3 was primarily found in DTL, although it was also detected in glomerulae and CTAL. The ubiquity of rPMCA4 is in keeping with the idea that this isoform is constitutive. The simultaneous presence of message for rPMCA1 and 2 in segments where Ca^{2+} is reabsorbed suggests that these isoforms are involved in such function. Since very little is known about Ca^{2+} metabolism in DTL, the variety of isoforms present in this segment is intriguing. With support of NIH grants DK 44902 and DK 16105.

M-Pos265

CHARACTERIZATION OF BASOLATERAL K^+ CHANNELS IN PRIMARY CULTURED RAT TRACHEAL EPITHELIA.

((T.H. Hwang, D.J. Suh*, H.R. Bae*, S.H. Lee and J.S. Jung)) Dept of Physiology, Pusan National University & Dong-A University*, Pusan, Korea

Basolateral K^+ channels in epithelia have been considered to play an important role in cAMP-mediated chloride secretion. To characterize K^+ channels in the basolateral membrane of tracheal epithelia, rat tracheal epithelial monolayers cultured on permeable filters were mounted into an Ussing chamber system and the mucosal membrane was permeabilzed with nystatin (180 μg/ml). During measurement of the macroscopic K^+ conductance properties of the basolateral membrane under a transepithelial voltage clamp, we detected at least two types of K^+ currents: One is an inwardly rectifying K^+ current and the other is a slowly activating K^+ current. The inwardly rectifying K^+ current was inhibited by 0.1 mM Ba^{2+}. The slowly activating K^+ current, which shows strong outward rectification, was activated by cAMP and inhibited by clofilium, PMA and lowering temperature, which is consistent with the biophysical characeristics of Isk channel. RT-PCR analysis releaved the presence of Isk cDNA in the rat trachea epithalia. Although 0.1 mM Ba^{2+} minimally affected I_{sc} induced by cAMP in intact epithelia, 0.1 mM clofilium strongly inhibited it, indicating that Isk channel is important for maintaining cAMP-induced chloride secretion in the rat trachea epithelia.

M-Pos266

NON-SELECTIVE CATION CHANNELS FROM APICAL PLASMA MEMBRANES OF HUMAN TERM PLACENTA RECONSTITUTED ON PLANAR LIPID BILAYERS.

((Claudio Grosman and Ignacio L. Reisin)) Departamento de Química Analítica y Fisicoquímica, Facultad de Farmacia y Bioquímica, Universidad de Buenos Aires, Junín 956 2 p (1113), Buenos Aires, Argentina.

We reconstituted ionic channels from the apical (maternal blood-facing) surface of corionic villi from freshly delivered human term placentae. Membrane fragments from this syncytial epithelium were isolated by an isotonic agitation step followed by differential centrifugation and the selective $MgCl_2$-precipitation of non-apical membranes. The purity of the fractions was assessed by marker enzyme analysis, the enrichment factor of alkaline phosphatase being 21.6 ± 3.1, and those of contaminants less than 1.6. Most frequently, we reconstituted non-selective cation channels ($P_{Cl}/P_K<0.1$) with multiple and identical conductance levels of 40 pS (symmetric 150 mM KCl). Single, 40-pS units were seldom observed in spite of vesicle dilution, vesicle sonication, vesicle fusion with bare liposomes or treatment of crude villi with a chaotropic agent (150 mM KI). Such clusters displayed frequent synchronous current transitions which spanned several conductance levels, strongly suggesting the occurrence of cooperative gating of 40-pS channels or a multi-substate channel. The observed human placental channels share many properties with syncytial, non-selective cation channels of helminth parasite origin (Grosman and Reisin, *Biophys. J.* 68:148*a*, 1995 and *Exp. Parasitol.*, in press)

M-Pos267

LASER INTERFEROMETRIC MEASUREMENT OF CELL VOLUME: DETERMINATION OF EPITHELIAL CELL MEMBRANE WATER PERMEABILITY.

((Javier Farinas and A.S. Verkman)) Graduate Group in Biophysics, UCSF, San Francisco, CA 94143-0521.

The development of strategies to measure osmotic water permeability of plasma membranes in epithelial cell layers has been motivated by the identification of a family of molecular water channels. A general approach utilizing laser interferometry was developed and applied to measure osmotic water permeability coefficients (P_f) in cell layers. Because of the refractive index difference between cytoplasm and extracellular solution, a change in cell volume produces a change in the optical path length normal to a cell layer. A HeNe laser (λ = 633 nm) was used as the light source of a Michelson interferometer in which one arm passed through a flow chamber containing a cell layer. In response to a change in extracellular osmolality, cell volume changes. The resulting change in optical path length was detected as a change in the interferometric signal. A mathematical model was developed to deduce the time course of osmotically-induced cell volume change from the interferometric signal for cells of arbitrary shape and size. The model predicts a large change in interferometric signal which does not strongly depend on cell shape. The method was applied to measuring P_f of adherent MDCK cells. This method should permit measurement of apical and basolateral P_f for intact epithelia.

M-Pos268

CHARACTERIZATION OF A G PROTEIN-ACTIVATED NON-SPECIFIC CATION CURRENT IN RAT RETINAL PIGMENT EPITHELIAL CELLS

((J.S. RYAN, J.F. POYER, AND M.E.M. KELLY*)) Departments of Pharmacology and Ophthalmology*, Dalhousie University, Canada, B3H 4H7.

We used patch-clamp recording techniques to investigate G protein-activated currents in cultured rat retinal pigmented epithelial (RPE) cells. Using 140 mM KCl in the pipette and 140 mM NaCl Ringers, rat RPE cells possessed both inward and outward K^+ currents. Inclusion of a non-hydrolyzable guanine triphosphate (GTP) analogue, GTPγS or Gpp(NH)p, in the recording electrode elicited a cation-selective current. In contrast, the inactive guanine diphosphate (GDP) analogue, GDPβS, failed to elicit any change in whole-cell current. The GTPγS-activated cation current had a mean reversal potential of +5.7 mV in 140 mM extracellular NaCl and was not affected by alterations in the Cl^- concentration gradient. Removal of extracellular Ca^{2+} and inclusion of 10 mM BAPTA in the pipette did not block GTPγS activation of the cation current, suggesting that this conductance was not dependent on Ca^{2+}. The GTPγS-activated cation current was found to be permeable to several monovalent cations with a rank order of permeability: $Na^+ \geq K^+ >$ choline > TRIS > NMDG. The cation current was insensitive to amiloride and gadolinium, and was unaffected by the chloride channel blocker 4-acetamido-4'-isothiocyanato stilbene-2,2'-disulfonic acid (SITS) and the K^+ channel blocker Ba^{2+}. Our results demonstrate the presence of a G protein regulated non-specific cation current in rat RPE cells. Activating the NSC current may depolarize RPE cells to allow activation outward K^+conductances.This would provide a mechanism by which these cells could rid themselves of accumulated K^+.Supported by NSERC OGP0121657

M-Pos269

HIDDEN MARKOV ANALYSIS OF NOISY SINGLE CHANNEL CURRENT RECORDINGS. ((L. Venkataramanan, R.Kuc and F.J.Sigworth)) Departments of Electrical Engineering and Cellular and Molecular Physiology, Yale Univ., New Haven, CT 06510.

Traditional hidden Markov modeling techniques have been applied in the past few years to model single channel current events at low signal to noise ratios (e.g. Chung et al, Phil. Trans. R.Soc. B 329:265, 1990 and 334:357, 1991). We have extended the traditional algorithms to include background noise that is non-white and state dependent. We propose a k^{th} order ARN (Auto Regressive Noise) model to account for the correlated noise and additional white Gaussian noise sources to model excess noise in partially open and open states. Along with the estimation of the rate constants and the current amplitudes, the parameters of the ARN model are also estimated. We have also implemented modifications to the algorithms to extend the analysis to continuous time anti-aliased data.

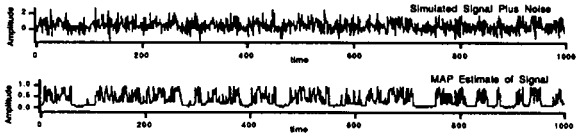

M-Pos270

ANALYSIS OF MULTICHANNEL PATCH-CLAMP DATA FROM VOLTAGE OPERATED CHANNELS: STATISTICAL APPROACHES APPLIED TO L-TYPE Ca^{++}-CHANNELS ((W. Baumgartner, C. Romanin, P. Weiß* and H. Schindler)) Institute for Biophysics and *Department of Stochastic, J.-Kepler University of Linz, A-4040 Linz, Austria

Several new statistical methods were developed for analyzing patch-clamp traces with N<10 identical channels. In a first step the removal of artifacts such as capacitive currents, drift or pick up from traces showing channel activity was performed by an algorithm based on the principle of least squares. The accuracy of artifact removal was verified by a test. Undisturbed traces were then used to calculate the number of channels, their open probability and availability, applying a maximum likelihood estimator. The result is approved when passing a test for consistency between these data and predictions for statistics of channel occurrance. Furthermore, a method was developed to calculate the first latency from multichannel traces and to approach run analysis. In addition, a nonparametric test was constructed, evaluating whether data from different experiments belong to the same, unknown statistical ensemble. These methods were put to test using simulated single channel traces as well as records obtained from cardiac L-type Ca^{++}-channels.

(Supported by the Austrian Research Funds, projects S6607, S6606-MED)

M-Pos271

EFFECT OF Mg^{2+} ON SINGLE-CHANNEL PROPERTIES OF THE IP_3 RECEPTOR IN *XENOPUS* OOCYTE OUTER NUCLEAR MEMBRANE ((D. D. Mak and J. K. Foskett)) Dept. of Physiology, School of Medicine, University of Pennsylvania, Philadelphia, PA 19104, USA.

Single-channel properties of the inositol-1,4,5-trisphosphate (IP_3) receptor (IP_3R) in its native membrane environment have been studied by patch clamping nuclei isolated mechanically from *Xenopus* oocytes. Since previous similar studies used buffers containing Mg^{2+}, we investigated specifically the effects of Mg^{2+} on IP_3R channel properties. In symmetric KCl buffer, conductance substates and single channel kinetics, e.g. long open duration and high open probability, were similar when free [Mg^{2+}] was varied from 0 to 9.5 mM. In 0 Mg^{2+}, however, a wide, continuous range of channel conductance (G) were observed (180 to 380 pS at 20 mV), with the most frequent G ≈ 320 pS at 20 mV. Fluctuations in G were sometimes observed during single channel openings. G was essentially ohmic. As [Mg^{2+}] was increased, both the range of G fluctuations and the most-frequently observed G decreased: at 20 mV, G ranged from 210 to 270 pS in 0.5 mM Mg^{2+}, and became constant at 120 pS and 90 pS in 2.5 mM and 9.5 mM Mg^{2+}, respectively. The presence of Mg^{2+} contributed a new short kinetic state in the open-channel dwell time histogram, and G became non-ohmic (dV/dI = 300 pS at 50 mV in 2.5 mM Mg^{2+}). In asymmetric buffer conditions, Mg^{2+} was shown to have a high permeability through the IP_3R channel ($P_{Mg}/P_K = 3$). Stabilization and reduction of G were observed with Mg^{2+} on either side of the channel. This study revealed a new and complex form of regulation of the IP_3R by Mg^{2+}, and suggests that changes in cytoplasmic [Mg^{2+}] may be expected to modulate permeability of the IP_3R, with important consequences for $[Ca^{2+}]_i$ signalling in cells.

M-Pos272

CELL-FREE EXPRESSION AND FUNCTIONAL RECONSTITUTION OF A NEURONAL NICOTINIC ACETYLCHOLINE RECEPTOR. ((L.K. Lyford and R.L. Rosenberg)) Department of Pharmacology, University of North Carolina at Chapel Hill, Chapel Hill, NC 27599

As an alternative to the expression of ion channel proteins in target cells, we have developed a system for the cell-free expression of functional ion channels (Rosenberg and East, *Nature* 360: 166-169, 1992). This system utilizes endoplasmic reticulum microsomes from secretory cells which are fused into artificial membranes. We have expressed a non-desensitizing mutant of the α7 neuronal nicotinic acetylcholine receptor (Revah *et al.*, *Nature* 353: 846-849, 1991) and studied its electrophysiological properties in planar lipid bilayers. A 40 kD protein was translated in the absence of microsomes and a 50 kD glycosylated protein was synthesized in the presence of microsomes. A proteinase K protection assay reveals a 36 kD intramicrosomal fragment, consistent with a large extracellular domain as predicted by most models. Sucrose gradient sedimentation revealed a ~3.6 S protein in the absence of microsomes. Solubilized proteins translated in the presence of microsomes sedimented at >11 S, suggesting oligomerization. Cell-free expressed α7 receptors incorporated into planar lipid bilayers had a unitary conductance of 48 to 51 pS, were non-selective between K^+ and Na^+ and were blocked by α-bungarotoxin. These properties are similar to those displayed by this mutant α7 nAChR expressed in *Xenopus* oocytes.

M-Pos273

ION CHANNEL ACTIVITY IN ARHABDOMERAL MEMBRANE OF ISOLATED *LIMULUS* PHOTORECEPTOR CELLS. ((D. Chaves[1], L. Kass[2], G.H. Renninger[1])) [1]Department of Physics, University of Guelph, Guelph Canada, N1G 2W1. [2]Department of Zoology, University of Maine, Orono ME 04469

Ion channels from the lateral eye of the horseshoe crab, *Limulus polyphemus*, were investigated using the technique of patch-clamping. The cells were dissociated into isolated ommatidia and photoreceptor cells. Only the arhabdomeral membrane was used for electrophysiological recording. Some permeability and gating properties of various ion channels in cell-attached patches were studied; ion exchange experiments were carried out in the inside-out patch configuration.

Preliminary experiments indicate the presence of a chloride channel which has not been described previously in the eyes of *Limulus*. Channel conductance in symmetrical solutions was 130 pS and did not appear to be voltage dependent. A putative fast transient potassium channel with a conductance of 10 pS in symmetrical solutions appears to be voltage dependent. Research supported in part by NSERC Canada.

M-Pos274

A NEW STATISTICAL TEST FOR ANALYSIS OF PATCH-CLAMP DATA. ((V.Ph.Pastushenko, H.Schindler, H.Waldl* and R.Hafner*)) Inst. for Biophysics and *Inst. for applied Statistics, J.-Kepler Univ. of Linz, A-4040 Linz, Austria.

We have developed a new statistical test (Joint Gaussian, JG), for finding abrupt jumps in the records of ion channel currents. It is defined as maximum of absolute values of all Gaussian tests within the testing window. The distribution of JG-test for testing null-hypothesis is simulated numerically for different testing windows and positions within the window. Comparison of JG with standard G- and Student T-tests was made within the same algorithm with moving dynamic window. The averaging was made over 100 independently simulated records of HMM-type (200 epochs in each record, average dwell time 30 points, levels at 0 and 1, noise amplitude 0.5). The average numbers of erroneous (i.e. false found and real lost) transitions are shown in dependence on numbers of transitions found by each method. The minimum number of erroneous transitions for JG is 1.4±0.3 less than that for G. Scattering is shown relative to JG-test. Analogous procedure may be recommended for analysis of real data with unknown number of levels in the case of arbitrary noise as an alternative for low-pass filtering.

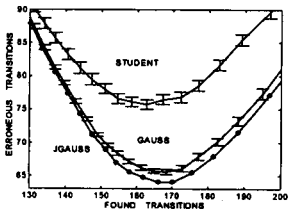

M-Pos275

ALGORITHM FOR CONSTRUCTION OF IDEALIZED CURRENT TRACES.
D. Restrepo[1,2], M.M. Zviman[1], F.W. Lischka[1] and J.H. Teeter[1,2]. [1]Monell Chemical Senses Center and [2]Department of Physiology, University of Pennsylvania, Philadelphia, PA 19104.

Recording of single channel currents by patch clamping is a powerful technique for characterization of the kinetics of ion channels. For recordings with low levels of noise, half-amplitude algorithms provide a convenient way to construct idealized current traces for use in determining kinetic parameters. However, when channels have multiple subconductance states, or significant amounts of open channel noise, the half-amplitude algorithm makes a significant number of mistakes that must be corrected by the investigator in a subjective manner. These problems can be alleviated by using the mean-variance (MV) algorithm of Patlak (Biophys. J., 65:29-42, 1993) where the mean current and the variance are computed within a fixed time window for each point. An MV histogram can then be constructed where different subconductance states are easily visualized as peaks. This algorithm provides a more objective determination of the number of states. However, determination of kinetic parameters is tedious because it entails computation of the volume under each peak in the MV histogram for different size windows. This is a problem particularly when the kinetics involve more than one time constant. We have designed an algorithm to construct idealized current traces. Each point is assigned to a particular state based on its location within the MV histogram. The resulting idealized trace can be used to determine time constants, sequence of transitions, open channel noise, etc. The algorithm is being implemented in a Windows program written in Borland C++.

This work was supported by NIH grants DC 00566 and DC01838.

M-Pos276 *(See Tu-Pos330a)*

DISSECTING SKM1 SODIUM CHANNEL STEADY-STATE INACTIVATION: CONTRIBUTIONS FROM FAST AND SLOW INACTIVATION.
(D. Featherstone and P. Ruben) Department of Biology, Utah State University, Logan, UT 84322-5305

Room-temperature macropatch recordings of Skm1 alpha subunits expressed in *Xenopus* oocytes show that channels inactivate with a voltage dependent, two-exponential time course. Steady-state inactivation curves are best fit by the sum of two Boltzmann equations. Our data show that one of the two curves (V_0=-115mV, z=3.5*e*) is created by inactivation following the slow (several tens of milliseconds) time course, while the other curve (V_0=-95mV, z=5.2*e*) is created by inactivation following the fast (a few hundred microseconds to a few milliseconds) time course. We conclude that steady-state inactivation is produced by both fast and slow inactivation mechanisms and that their separate contributions to steady-state inactivation can be reliably dissociated. The apparent voltage dependence of fast inactivation is higher than that of activation (5.2*e* vs. 3.3*e*), and is substantially hyperpolarized (-95mV vs. -38mV), thus representing either missed slow activation openings or fast inactivation from closed states.

(Supported by PHS Grant R-01 NS29204 to PCR)

M-Pos277

ION CHANNELS FORMED FROM CYCLIC PEPTIDES WITH ACYL CHAINS.
((M.Sokabe, Q.Zhi, *K.Donowaki, *H.Ishida, *K.Okubo)) Dept. Physiol. Nagoya Univ. Sch. Med., Nagoya 466, Japan and *Dept. Appl-Chem. Fac. Engineer. Kumamoto Univ., Kumamoto, 860, Japan

We designed cyclic peptides based on a non-natural amino acid with a long acyl chain, N'-acylated diamino benzoic acid (Daba(C_m)). In the present study dipeptides (Ala-Daba(C_{16})) were polymerized to form cyclic peptides ((Ala-Daba(C_{16}))n) with three different ring size (n = 3,4,5). The ring size, acyl chain length and species of natural amino acid of the peptide would systematically be changed. Lipid bilayer membranes were formed from *n*-decane solution containing soybean lecithin and the peptides. All the peptides successfully produced single channel currents under voltage clamp condition whilst no significant difference among different peptides was observed. The single channel conductances were ca. 9pS at 100mM KCl. The ion selectivity determined by the permeability ratio fell in the order of $K^+ > Na^+ > Cl^- >> Li^+, Ca^{2+}$. The conductance-activity relationship of K^+ followed the simple Michaelis-Menten's law and the permeability ratio of Na^+ to K^+ was constant in a wide range of salt concentrations, suggesting that these channels behave as a cation selective single ion channel. Taken together it seems that the rate limiting step of the ion permeation through the channels is the translocation across the hydrophobic acyl chain cavity. Interesingly the channel was blocked by Ca^{2+}, probably via the binding to the peptide ring that may form channel entrance.

M-Pos278

A P2X RECEPTOR FROM GASTRIC SMOOTH MUSCLE CELLS.
((Mehmet Ugur, Joshua J. Singer and John V. Walsh Jr.)) Department of Physiology, University of Massachusetts Medical School, Worcester, MA 01655.

Recently four types of P2X receptors have been cloned ($P2X_{1-4}$) and identified as ligand-gated cation channels activated by extracellular adenosine 5'-triphosphate (ATP). We report here an ATP-gated cation channel found in amphibian smooth muscle cells with properties different from the channels cloned so far. It is insensitive to α,β methylene-ATP and shows no desensitization; it is also much less sensitive to Mg-ATP than are $P2X_{1-4}$. We suggest that this channel is a fifth type of P2X receptor. -- Whole-cell currents activated by extracellular ATP in isolated gastric smooth muscle cells from *Bufo marinus* were present in all cells and showed no sign of desensitization even after 5 minutes of continuous application; ion substitutions indicated that the current was carried by cations. In outside-out patches ATP promptly activated single channel currents, again with no sign of desensitization and with many different conductance levels. Guanosine 5'-O-(2-thio di-phosphate) (GDP-β-S) (300 μM) or BAPTA (5 mM) in the internal solution did not abolish the whole-cell current; and with inside-out patches excised into a GTP-free, divalent-free solution, extracellular ATP still activated the channel, indicating a direct mode of ATP action. Removal of 1 mM Mg^{++} from the extracellular solution greatly increased the whole-cell ATP responses; but external Mg^{++} had only a small effect on the single-channel conductance, suggesting a possible Mg^{++} effect on gating. In bathing solutions with physiological levels of divalent ions (Ca^{++} 1.8, Mg^{++} 1 mM), a minimum ATP concentration of about 1 mM was required for activation. In whole-cell mode at 1 mM concentration, α,β methylene-ATP had almost no effect; and 3-O-(4'-benzoyl) benzoyl-ATP and 2-Methylthio ATP had a potency at least as great as ATP.
(Supported by NIH HL 47530 and DK 31620)

CARRIERS, EXCHANGERS, COTRANSPORTERS

M-Pos279

FUNCTIONAL ANALYSIS OF THE HUMAN CARDIAC Na/Ca EXCHANGER EXPRESSED IN SF9 CELLS.
((M. Egger, P. Lipp, B. Schwaller#, W. J. Lederer*, D.H. Schulze¶, E. Niggli)). Dept. of Physiology, University of Bern, Switzerland; *Dept. of Physiology & ¶Dept. of Microbiology and Immunology, UMAB, School of Medicine, Baltimore, USA, #Dept. of Histology, University Fribourg, Switzerland.

The cardiac Na^+/Ca^{2+} exchanger (NCX) was expressed in SF9 insect cells infected with the recombinant baculovirus 3E3A3. The level of protein expression and exchanger activity at an MOI of 2-5 (plaque assay: 0.25-1.6 10^7/ml) reached its maximum at 3 days after infection. The cellular localization of the Na^+/Ca^{2+} proteins in infected cells was examined by immuno-fluorescence. Functional characterization of the Na^+/Ca^{2+} protein under whole cell voltage-clamp conditions involved examination of the voltage-dependence of I_{NCX} creep-currents. Intracellular Ca^{2+} concentration jumps were generated by flash-photolysis of caged Ca^{2+} (DM-nitrophen). In infected cells at a fixed membrane potential of -40 mV, photolysis of caged Ca^{2+} activated I_{NCX} up to 20 pA while a similar photolysis in native SF9 cells produced no measurable I_{NCX}. With ratiometric confocal measurements using fura-red and fluo-3, reducing extracellular Na^+ to 0 mM increased $[Ca^{2+}]_i$ to about 700 nM. Extracellular $[Ni^{2+}]$ blocked the electrical activity of the Na^+/Ca^{2+} exchanger in SF9 cells.
This work was supported by SNF to EN and by NIH (WJL,DHS).

M-Pos280

CLONING OF A SQUID Na^+-Ca^{2+} EXCHANGER: NCX-SQ1
((Z. He, A. Doering, L. Lu, and K.D. Philipson)) UCLA, Los Angeles, CA, 90095-1760.

The Na^+/Ca^{2+} exchanger (NCX) is an electrogenic transporter that translocates Na^+ and Ca^{2+} in opposite directions across the plasma membrane. Four isoforms of this exchanger have been cloned, NCX1 from canine heart, NCX 2 and NCX3 from rat brain, and CalX from Drosophila. We now report the cloning of a Na^+/Ca^{2+} exchanger from squid giant axon (NCX-SQ1). The squid exchanger was identified by PCR using degenerate primer pairs derived from the conserved transmembrane segments 6 and 9 of NCX1 and NCX2. The PCR product was used to screen a squid optic lobe cDNA library. A partial clone was obtained and was used as a probe to screen a squid stellate ganglion cDNA library. Two clones (SG12 and SG14), each containing the complete coding sequence for the squid exchanger were obtained. The squid clone has an open reading frame of 2.6 kb encoding for a protein of 892 amino acids. The squid exchanger is 64% identical to NCX3, 58% identical to NCX1 and NCX2 and 51% identical to CalX at the amino acid level. The SG12 clone was expressed in *Xenopus* oocytes, and exchanger activity was detected by Na^+-dependent $^{45}Ca^{2+}$-uptake into intact cells and electrophysically using the giant excised patch technique. NCX-SQ1 is regulated by Ca^{2+} at an intracellular site; further characterization is underway.

M-Pos281

CLONING OF A THIRD MAMMALIAN Na^+-Ca^{2+} EXCHANGER: NCX3 ((D.A. Nicoll, B. Quednau, Z. Qiu, Y.-R. Xia, A.J. Lusis, and K.D. Philipson)) UCLA, Los Angeles, CA, 90095-1760.

NCX3 is the third mammalian Na^+-Ca^{2+} exchanger protein to be cloned. NCX3 was identified by PCR using degenerate primers derived from the conserved transmembrane segment 2 and XIP regions of NCX1 (Nicoll, D.A., *et al.* (1990) Science **250**: 562) and NCX2 (Li, Z., *et al.* (1994) JBC **269**: 17434). The NCX3 PCR product was used to probe a rat brain cDNA library. Two overlapping clones totalling 4.8 kb were isolated, sequenced, and joined at a unique Bsp106 restriction enzyme site to form a full length cDNA clone. The NCX3 cDNA clone has an open reading frame of 2.8 kb encoding for a protein of 927 amino acids. At the amino acid level, NCX3 shares 73% identity with NCX1 and 75% identity with NCX2. NCX1 and NCX2 share 68% identity. The 5' UTR of NCX3 is at least 833 bp and contains 17 ATGs and a GC-rich region. The 3' UTR is at least 1.2 kb and does not end in a polyA$^+$ tail. NCX3 exchanger activity can be expressed in *Xenopus* oocytes and in the mammalian BHK cell line. NCX3 transcripts are 6 kb in size and, like NCX2 transcripts, are detected only in skeletal muscle and brain on Northern blots. NCX3 maps to mouse chromosome 12.

M-Pos282

TISSUE-SPECIFIC EXPRESSION OF THE Na/Ca EXCHANGER ISOFORMS NCX1, NCX2, AND NCX3 ((B.D. Quednau, D.A. Nicoll, and K.D. Philipson)) Cardiovascular Research Laboratory, UCLA, Los Angeles, CA 90095

The Na/Ca exchanger NCX1 was first cloned from heart where it plays a major role in excitation-contraction coupling. A second Na/Ca exchanger, NCX2 (Li et al., JBC 269: 17434, 1994), as well as a third isoform, NCX3 (see adjacent poster), have been cloned from rat brain. We have investigated the tissue-specific expression of all three Na/Ca exchanger isoforms in rat using Northern blot and RT-PCR analysis. By Northern blot, we could detect NCX1 specific mRNA in a variety of different tissues, whereas NCX2 and NCX3 transcripts are present only in brain and skeletal muscle. The far more sensitive RT-PCR shows that NCX3 transcripts are restricted to a small number of tissues whereas NCX1 and NCX2 mRNAs can be amplified from almost every tissue except liver. NCX1 mRNA undergoes alternative splicing which generates many tissue-specific splicing isoforms. NCX2 and NCX3 mRNAs both lack a stretch of 111 nts at the position where alternative splicing in NCX1 occurs. However, RT-PCR using primer pairs that span the missing nucleotide sequence did not detect any additional splice variants for NCX2 or NCX3. Transcripts of all three isoforms can also be detected in cultured neurons, astrocytes, and oligodendrocytes. Previously undescribed NCX1 splicing isoforms are present in astrocytes and oligocytes. Comparison of the alternative splicing pattern of NCX1 from several different neonatal and adult tissues shows a developmentally regulated switch to different splicing isoforms only in skeletal muscle. No differences could be detected between NCX2 and NCX3 neonatal/adult tissues.

M-Pos283

THE EXCHANGE INHIBITORY PROTEIN DOMAIN OF THE CARDIAC NA-CA EXCHANGE PROTEIN IS CLEAVED BY CHYMOTRYPSIN DIGESTION. ((S. Bliler and C.C. Hale)) Dalton Cardiovascular Research Center and Department of Biomedical Sciences, University of Missouri, Columbia, MO 65211. (Spon. by M. Rovetto)

The exchange inhibitory peptide (XIP), a potent inhibitor of Na-Ca exchange (NCX) activity, is homologous to a putative regulatory region at amino acid residues 219-238 on cytoplasmic loop f of the NCX protein. Synthetic XIP was used to raise a polyclonal antibody. On Western blot analysis of bovine cardiac sarcolemmal (BSL) vesicles prepared in the presence of a protease inhibitor cocktail, the anti-XIP antibody recognizes major proteins with apparent Mr of 200+, 120, and 70 kDa. BSL vesicles prepared in the absence of a protease inhibitor cocktail produces a significant decrease in the 120 kDa protein. While 120 and 70 kDa forms of NCX have been widely described, the nature of the 200+ kDa protein is unknown. Mild chymotrypsin digestion of BSL vesicles resulted in a 3-fold stimulation of NCX activity while abolishing recognition by the anti-XIP antibody of all three proteins. We conclude that the 120 and 70 kDa protein contain the XIP domain which is cleaved during proteolytic stimulation of NCX activity by chymotrypsin. (Supported by the American Heart Association).

M-Pos284

PREFERENCE IN NCX1 ISOFORM EXPRESSION IN RAT ASTROCYTE AND NEURON CULTURES ((S.He, L.L.Bambrick, B.K.Krueger, W.J.Lederer, D.H.Schulze. Departments of Microbiology/ Immunology and Physiology, University of Maryland, School of Medicine, Baltimore, MD 21201))

Na^+-Ca^{2+} exchanger is a transmembrane protein that regulates intracellular calcium levels. The NCX1 gene has been shown to undergo alternative splicing in the C-terminus of the intracellular loop of the protein to produce multiple isoforms; identified by exons labeled A,B,C,D,E and F. Cultured rat cortical astrocytes display a Na-dependent Ca flux, inhibited by 5mM Ni^{2+} suggesting that it may arise from transport by the Na^+/Ca^{2+}exchanger. We have quantified the relative expression of the different isofoms found in rat astrocyte cultures using γ^{32}P-ATP end-labeled RT-PCR and separating the products on a sequencing gel. Three predominant isoforms BDEF, BDF and BD were identified in rat astrocyte cultures (each representing about 23% of the total PCR product). When this quantitive analysis is extended to cultured neonatal hippocampal neurons, we show that the NCX1 isoforms that predominate include exons ADF and AD (representing nearly 95% of the transcripts). The clear predominance of A isoforms in hippocampal neurons and B isoforms in astrocytes suggest cell-type preference of NCX1 isoforms in neurons and astrocytes, the two main cell types in rat brain.

M-Pos285

STRIKING HOMOLOGY IN THE 3' UNTRANSLATED REGION OF NCX1 cDNAs. ((S. Luo, W.J. Lederer, D. H. Schulze)) Departments of Microbiology/Immunology and Physiology, University of Maryland School of Medicine, Baltimore MD 21201.

The Na^+/Ca^{2+} exchanger, an important transporter in regulating intracellular Ca^{2+}, is present in many tissues and in various species. In our study of cDNAs that code for the NCX1 gene, we describe surprising sequence conservation in the 3' untranslated region of cDNAs of the Na^+/Ca^{2+} exchanger across species. The coding region of mammalian Na^+/Ca^{2+} exchangers are known to be highly conserved at the nucleic acid level as is the case for the coding region of other transporter protein cDNAs (such as the Na and Ca pumps). Coding regions that correspond to the mature protein are between 94-97% identical at the nucleic acid level depending on the species and the regions compared. The nucleic acids that code for the putative leader peptide region for the exchanger in mammalian species is less conserved (75-83%) as might be expected. But the first 224 bp of sequence 3' of the stop codon are conserved, demonstrating between 87-96% identity depending on the mammalian cDNA sequence studied. We and others have used anti-sense oligonucleotides complementary to part of this region to inhibit the functional expression of the Na^+/Ca^{2+} exchanger. This AT rich region in the 3' untranslated region appears not to code for a protein and thus the remarkable degree of conservation across species suggests that this part of the 3' untranslated region must be important. One hypothesis is that it may stabilize the RNA, proloning its half-life and another is that this region may play a role in regulating transcription.

M-Pos286

CHARACTERIZATION AND EXPRESSION OF THE *DROSOPHILA* Na^+/Ca^{2+} EXCHANGER cDNA IN *XENOPUS* OOCYTES. ((A. Ruknudin, S. Wisel, C. Valdivia, P. Kofuji,, W. J. Lederer and D. H. Schulze)) Departments of Microbiology/Immunology and Physiology , University of Maryland School of Medicine, Baltimore, MD 21201.

We have cloned the full length cDNAs for the Na^+/Ca^{2+}exchanger from *Drosophila* using a human cDNA as a probe. The *Drosophila* Na^+/Ca^{2+} exchanger has a similar structure of previously characterized mammalian exchangers containing a series of N terminal and C terminal hydrophobic regions and a large intracellular loop between these putative trans-membrane regions. The overall homology between the human and *Drosophila* cDNAs is 44% identity at the amino acid level providing the most diversity observed to date between cloned Na^+/Ca^{2+} exchangers. Independent cDNA clones from *Drosophila* displayed sequence variation at the equivalent position in the mammalian cDNAs where alternative splicing has been demonstrated, suggesting a further parallel between the *Drosophila* and mammalian Na^+/Ca^{2+} exchangers. Also the *Drosophila* cDNA was used to map the Na^+/Ca^{2+}exchanger gene to chromosome 3 (A-B) using polytene chromosomes. Na^+/Ca^{2+}exchanger activity (in the reverse mode) was measured in oocytes injected with *Drosophila* cRNA by measurement of Ca^{2+}-activated chloride current using two-electrode voltage clamp. 4 mM Ni^{2+} abolished the Na^+/Ca^{2+}exchanger dependent current. Functional differences between the human cardiac and *Drosophila* Na^+/Ca^{2+} exchangers were observed in this assay system.

M-Pos287

SIMULTANEOUS RECORDING OF Na^+/Ca^{2+} EXCHANGE CURRENT AND SWELLING ACTIVATED Cl^- CURRENT FROM ISOLATED GUINEA-PIG ATRIAL MYOCYTES
((A.R. Wright, S.A. Rees, J.I. Vandenberg, V.W. Twist and T. Powell)) University Laboratory of Physiology, Parks Road, Oxford, UK

Hypo-osmotically induced cell swelling has been found to decrease Na^+/Ca^{2+} exchange current ($I_{Na,Ca}$) in voltage clamped guinea-pig ventricular cells, but in atrial cells the hyposmotic whole cell current is often dominated by a swelling activated Cl^- current ($I_{Cl,swell}$) which obscures $I_{Na,Ca}$. We have estimated changes in $I_{Na,Ca}$ in atrial cells by fitting whole cell current, measured during a 20 mV to -110 mV ramp repeated every 4 seconds, to a sum of scaled $I_{Na,Ca}$ (■), background current ($I_{background}$;+) and $I_{Cl,swell}$ (□). $I_{Na,Ca}$ and $I_{background}$ are, respectively, the nickel-sensitive and nickel-insensitive components of isosmotic whole cell current. $I_{Cl,swell}$ is the difference between isosmotic and hyposmotic nickel-insensitive currents, or, in cases where the giga-ohm seal was lost before nickel could be applied, the difference between two hypo-osmotic I-V curves measured at different times. In 8 atrial cells, the reduction in $I_{Na,Ca}$ could be described by an exponential relaxation of time constant 79±15s and amplitude 41±6% of initial $I_{Na,Ca}$. The reduction began 66±16s after the switch to hyposmotic solution, whereas the foot of the $I_{Cl,swell}$ activation curve occurred 165±36s after switching, and showed higher order kinetics than the change in $I_{Na,Ca}$; data from one cell is shown in the figure.

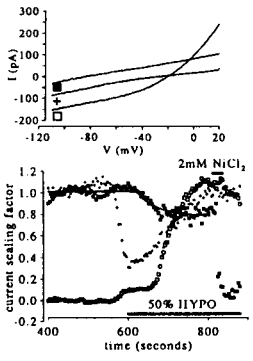

M-Pos288

CURRENT-VOLTAGE RELATIONSHIPS AND STEADY-STATE CHARACTERISTICS OF SODIUM-CALCIUM EXCHANGE: TEST OF THE EIGHT-STATE CONSECUTIVE MODEL
((A. Omelchenko and L.V. Hryshko)) Div. Cardiovasc. Sci., St. Boniface Gen. Hosp. Res. Ctr., Univ. Manitoba, Winnipeg, Canada, R2H 2A6 (Sponsored by R. Bose)

An analytical expression for Na^+-Ca^{2+} exchange currents in cardiac cells and X. laevis oocytes expressing the cardiac Na^+-Ca^{2+} exchanger, NCX1, has been obtained for the eight-state model proposed by Hilgemann, D.W. *et al.* (Nature, 352:715, 1991). A solution was derived on the basis of the following assumptions: 1) Na^+/Ca^{2+} exchange is electrogenic and moves one net positive charge per cycle; 2) the exchanger translocates Na^+ and Ca^{2+} in separate consecutive steps; 3) movement of one positive charge corresponds to the Na^+ translocation step; 4) the exchange cycle has a 3:1 Na^+/Ca^{2+} stoichiometry; 5) all binding reactions are treated as instantaneous equilibria and voltage-independent; 6) transitional states with "occluded" Na^+ and Ca^{2+} may exist; and 7) electrogenicity occurs exclusively with "occlusion-deocclusion" of Na^+ on the extracellular side. The equation obtained has been employed to derive theoretical expressions for current-voltage relationships, maximum Na^+-Ca^{2+} exchange currents, and half-saturating concentrations for Na^+ and Ca^{2+}. These equations were analyzed over a wide range of cytoplasmic and extracellular Na^+ and Ca^{2+} concentrations, including "zero-*trans*" and inverse "zero-*trans*" conditions. Correspondence of theoretical results with those obtained from giant excised patch experiments and mathematical details of the modeling procedures will be presented.

M-Pos289

THE SAME REGULATORY Ca^{2+} BINDING SITE IS EMPLOYED BY NCX1 AND Calx FOR OPPOSITE Ca_i^{2+} REGULATION PHENOTYPES.
((J. Buchko, M. Hnatowich, and L.V. Hryshko)) St. Boniface Hosp. Res. Ctr., Univ. Manitoba, Winnipeg, Manitoba, Canada, R2H 2A6.

The cardiac Na^+-Ca^{2+} exchanger (NCX1) is regulated by Ca^{2+}, in addition to transporting this ion. When reverse mode Na^+-Ca^{2+} exchange currents are examined, Ca^{2+} regulation appears as the augmentation of outward currents by micromolar cytoplasmic [Ca^{2+}]. The regulatory Ca^{2+} binding site has been identified for NCX1 and comprises two highly acidic clusters of amino acids within the large intracellular loop. Specific mutations within the loop result in two relatively distinct phenotypes. First, mutations within the acidic clusters reduce both $^{45}Ca^{2+}$ binding affinity to fusion proteins expressing portions of the cytoplasmic loop (Levitsky et al., J Biol Chem, 269:22847, 1994) and functional regulation as assessed by the giant excised patch technique (Matsuoka et al., J Gen Physiol, 105:403, 1995). Second, certain mutations produce exchangers which are relatively Ca_i^{2+} insensitive. In contrast, the *Drosophila* Na^+-Ca^{2+} exchanger, Calx, exhibits an opposite regulatory phenotype to that of NCX1. Calx is *inhibited* by Ca_i^{2+} over the same concentration range which stimulates NCX1. NCX1 and Calx amino acid sequence comparison suggests that the same regulatory site may be employed by both exchangers. To test this possibility, the putative Ca^{2+} binding site of Calx was studied using site-directed mutagenesis and the giant excised patch technique. Analogous mutations which reduce the regulatory Ca^{2+} affinity for NCX1 lead to an equivalent reduction in the inhibitory potency of Ca_i^{2+} for Calx. Similarly, mutations which lead to Ca^{2+}-insensitive NCX1 exchangers also render Calx Ca^{2+}-insensitive. Thus, the contrasting regulatory phenotypes of NCX1 and Calx appear to be mediated by the same Ca_i^{2+} binding site.

M-Pos290

Na^+/Ca^{2+} EXCHANGE IN FROG SKELETAL MUSCLE AND ITS ALTERNATE Ni^{2+}/Ca^{2+} MODE.
((R.A. Venosa and A. Hoya)). Cát. de Fisiología y Biofísica y Ctro. de Investigaciones Cardiovasculares, Facultad de Ciencias Médicas, UNLP, La Plata, Argentina.

The Na^+ dependent Ca^{2+} efflux ($^{45}Ca^{2+}$) in intact frog sartorii from *Leptodactylus ocellatus* was studied. Under resting normal conditions the activity of the Na^+/Ca^{2+} exchange was not readily detectable. The exposure of muscles to 4 mM caffeine, roughly doubled the Ca^{2+} efflux rate coefficient (k_o). This increase exhibits characteristics typical of the Na^+/Ca^{2+} exchanger (forward mode) being decreased by: a) 72% in the absence of external Na^+; b) 73% in Na^+ loaded muscles ($[Na^+]_i$ = 98 mM); c) 70% upon depolarization to -27 mV ($[K^+]_o$ = 50 mM); d) and 80% in the presence of 5 mM amiloride. Ni^{2+} (5 mM) an inhibitor of the exchanger current (Kimura et al. 1987. J. Physiol. 384:199-122), surprisingly increased the caffeine promoted rise in k_o (P=0.002). This effect was blocked by 5 mM amiloride. Caffeine, on the other hand, produced a 3-fold increase in Ni^{2+} ($^{63}Ni^{2+}$) influx. Under similar experimental conditions 5 mM Ca^{2+} also produced an increase in k_o but it was amiloride-insensitive. We conclude that: a) in frog skeletal muscle Na^+/Ca^{2+} exchange activity becomes apparent when $[Ca^{2+}]_i$ is substantially increased by caffeine; and b) the inhibition of the exchanger current by Ni^{2+} probably represents a shift from an electrogenic Na^+/Ca^{2+} antiport mode toward an electroneutral $1Ni^{2+}/1Ca^{2+}$ exchange.

M-Pos291

ELECTROGENIC FLUX MEDIATED BY A CLONED H^+/*MYO*-INOSITOL SYMPORTER EXPRESSED IN *XENOPUS* OOCYTES.
((E.M. Klamo[1], M.E. Drew[2], S.M.Landfear[2], and M.P. Kavanaugh[1])) Vollum Institute[1] and Department of Molecular Microbiology and Immunology[2], OHSU, Portland, OR 97201

A gene related to the facilitative glucose transporter gene family cloned from the parasitic protozoan *Leishmania donovani* was expressed in *Xenopus* oocytes and demonstrated to encode a *myo*-inositol transporter (Drew et al. *Mol. Cell. Biol.* 15; 5508 1995). Superfusion of *myo*-inositol on voltage-clamped oocytes expressing this transporter resulted in inward currents which were increased by membrane hyperpolarization and did not reverse at positive potentials. The transport current was not affected by replacement of Na^+ with choline in the bath solution, but was influenced by pH as described below. In the presence of *myo*-inositol, a hyperpolarizing jump from +20 mV to -80 mV activated an inward current concomitant with an alkalinization of the extracellular space as measured with a pH-sensitive electrode placed near the oocyte. Simultaneous measurement of charge transfer and tracer flux during a 200 s pulse of [^{3}H]*myo*-inositol superfused on voltage-clamped oocytes revealed that 0.97± 0.09 fundamental charges were translocated per molecule of *myo*-inositol. Together these results suggest that the one proton is cotransported with one molecule of *myo*-inositol. Analysis of the kinetic parameters K_m and I_{max} revealed an interaction between *myo*-inositol and protons. Increasing the extracellular proton concentration increased the apparent affinity of the transporter for *myo*-inositol, while I_{max}^{MI} remained unchanged. However, increasing the extracellular *myo*-inositol concentration resulted in an increased apparent affinity for protons as well as an increase in I_{max}^{H+}. Voltage jumps performed in the absence of *myo*-inositol revealed non-linear capacitive currents which were proportional to the transporter expression level. These charge movements were well fit by a Boltzmann function ($V_{0.5}$=-98mV, zδ=0.52, pH 7.5). By estimating the transporter density from these fits, a turnover rate of 1.4 ± 0.08/sec at -60mV was obtained. The $V_{0.5}$ of the charge movement was shifted -17 mV by a 1 unit decrease in pH. These data are consistent with a model in which most of the charge movement occurs during a conformational transition of the protein, with proton binding in a shallow ion well followed by *myo*-inositol binding and translocation of the complex.

M-Pos292

LARGE SCALE PURIFICATION OF AN ABC-TYPE PROTEIN COMPLEX, THE MALTOSE TRANSPORTER OF *E. coli* AND PRELIMINARY CRYSTALLIZATION RESULTS.
((W.v. Gustedt, May Chan, Hiroshi Nikaido, Bing K. Jap)) Life Sciences Division, LBNL, Berkeley, CA, 94720.

The (ATP-binding-cassette) ABC-family of proteins are ubiquitous membrane proteins, which can be found from bacteria to animals. They are responsible for the transport of a variety of substrates (e.g. peptides, proteins, aminoacids, sugars) across cell membranes. Well known representatives of this family are the cystic fibrosis transmembrane conductor and the multidrug resistance protein.

The ABC-transporters are composed of four domains. Two are transmembrane proteins ,which probably form a transport channel. The others contain a nucleotide binding site. Transport of a substrate seems to be unidirectional and energy dependent.

We have sucessfully purified the maltose transporter of E. coli, a member of the ABC-family to high purity and homogeneity. It could be shown that the purified protein is highly active and functional in its solubilized and reconstituted state. The purification method is reproducible and provides milligram amounts of homogenous protein.

Three dimensional crystals have been obtained from the purified protein. Preliminary crystallization results will be presented.

M-Pos293

CLONING, SEQUENCING, AND INITIAL CHARACTERIZATION OF A PUTATIVE ION COTRANSPORT PROTEIN FROM CYANOBACTERIUM SYNECHOCOCCUS SP. PCC 7002. ((Christopher M. Gillen, Veronica L. Stirewalt, Donald A. Bryant, and Bliss Forbush III)) Dept. of Cell. and Mol. Physiology, Yale Univ. Sch. Med., New Haven, CT 06520 and Dept. of Biochem. and Mol. Biology, The Pennsylvania St. Univ., University Park, PA 16802.

We have cloned and sequenced a putative ion cotransport protein (ORF738) from the cyanobacterium Synechococcus sp. PCC 7002. ORF738 was originally recognized as an open reading frame (ORF128) downstream from the psaA and psaB genes of the Photosystem I complex. The complete open reading frame encodes a peptide of 738 amino acids (a.a.) with extensive sequence and structural homology to ion cotransport proteins of the Na-K-2Cl (NKCC) and Na-Cl family. Hydropathy analysis predicts twelve membrane-spanning domains with a 300 a.a. C-terminal cytoplasmic tail. The predicted peptide is 33% identical to both the human bumetanide-sensitive NKCC and the rat thiazide - sensitive Na-Cl cotransporter. ORF738 is about 80% identical to NKCC in a region between predicted transmembrane domains 2 and 3, an area that is highly conserved among members of the NKCC family. An insertionally inactivated Synechococcus mutant has been constructed by interposon mutagenesis and will be characterized with respect to its growth requirements and capacity to transport ions. We have overexpressed ORF738 in both wild type E. Coli (BL21) and E. Coli deficient in K transport systems (TK401). BL21 cells which express ORF128 grow more slowly than controls in high sodium growth medium (400 mM) but have growth rates similar to control in high sucrose growth media (800 mM). TK401 cells which express ORF738 demonstrate a 20-30% increase in ^{86}RB uptake compared to control cells. Together, these results suggest that ORF738 is a transport protein capable of ion translocation. (supported by DK47661).

M-Pos294

THE DIMERIC STATE OF THE MITOCHONDRIAL OXOGLUTARATE CARRIER (OGC) IS A PREREQUISITE FOR THE FORMATION OF A DISULFIDE CROSS-LINK BETWEEN THE MONOMERS. ((F. Bisaccia, V. Zara, L. Capobianco, V. Iacobazzi and F. Palmieri)) Dept. Pharmaco-Biology, University of Bari, Italy. (Spon. by C. Mannella)

Isolated OGC can be cross-linked to dimers by disulfide-forming reagents like Cu^{2+}-phenanthroline and diamide. Acetone and other solvents increase the extent of Cu^{2+}-phenanthroline-induced cross-linking. Cross-linked OGC re-incorporated in proteoliposomes fully retains oxoglutarate transport activity. Under optimal conditions formation of cross-linked OGC dimer amounts to 75% of total protein. Cross-linking is prevented by SH reagents and reversed by SH-reducing reagents, indicating it is mediated by disulfide bridge(s). Formation of S-S bridge(s) requires the native state of the protein since it is suppressed by SDS and by heating. Furthermore, the extent of cross-linking is independent of OGC concentration indicating that S-S bridge(s) form between subunits of native dimers. The number and localization of S-S bridge(s) in cross-linked OGC were examined by peptide fragmentation and subsequent cleavage of disulfide bond(s) by b-mercaptoethanol. Cross-linking of OGC is through a single S-S bond between cysteines 184 of the two subunits, indicating that these residues in putative transmembrane helix four are near the twofold axis of the native dimer structure.

M-Pos295

NOREPINEPHRINE TRANSPORTERS HAVE CHANNEL MODES OF CONDUCTION. ((A. Galli, R. D. Blakely, and L. J. DeFelice.)) Pharmacology, Vanderbilt, Nashville TN 37232. We report the direct measurement of unitary events from an electrogenic ($1NE^+$:$1Na^+$:$1Cl^-$) transporter, hNET (human norepinephrine transporter). NE-induced currents in transfected HEK-293 cells exceed predictions based on stoichiometry, transporter number, and NE uptake; fluctuation analysis suggests 2 pS events. Patches stimulated by NE or guanethidine reveal channels with 2.4 ± 0.4 pS that are blocked by hNET antagonists. These data indicate that hNETs have two functional modes of conduction: a classical transporter mode (T-mode) and a novel channel mode (C-mode). T-mode is weakly electrogenic and transports transmitter and co-ions under stoichiometric conditions. C-mode occurs with low probability compared with T mode but carries essentially all transmitter-induced current. Both modes are sensitive to cocaine and antidepressants, suggesting a common pathway. The existence of a channel in a previously-established fixed-stoichiometry transporter has mechanistic implications, and transitions between modes may constitute a novel regulatory mechanism.

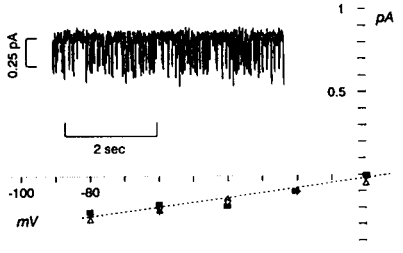

M-Pos296

FOR THE LLC-PK$_1$ NA$^+$/ALA COTRANSPORTER, TRANSLOCATION AND BINDING/DISSOCIATION OF SODIUM ARE POTENTIAL INDEPENDENT. ((J.J. Wilson, G.A. Kimmich)) Dept. of Biophysics, Univ. of Rochester School of Medicine, Rochester, NY 14642. (Spon. by I.H. Sarelius)

Sodium-coupled alanine transport in LLC-PK$_1$ cells occurs via a simultaneous and ordered mechanism in which sodium binds to the cotransporter prior to alanine at the extracellular surface of the plasma membrane. Alanine and sodium are cotransported with 1:1 coupling and glide symmetry. The relative simplicity of this system makes it a useful model for studying the potential dependence of specific steps in the transport cycle.

When binding of extracellular alanine is made rate limiting, the expression for the K_m for sodium simplifies to include only four rate constants which relate to translocation of the free protein and to extracellular sodium binding/dissociation. A potential dependent K_m for sodium under these conditions suggests that one or both of these steps is potential dependent. Likewise, lack of potential dependence for the K_m implies that both of these steps are potential independent.

We have evidence that the K_m for sodium (5μM extracellular alanine) remains constant at 143mM when the membrane potential is changed from approximately -60mV to +10mV. Over the same membrane potential range, the maximal velocity changes two-fold. This suggests that neither translocation of the free protein nor binding/dissociation of sodium at the extracellular surface of the membrane are potential dependent steps.

M-Pos297

EFFECTS OF NO_2 ON K-CL COTRANSPORT AND CELL VOLUME IN HIGH POTASSIUM (HK) DOG RED BLOOD CELLS (DRBCs) WITH HIGH AND LOW GLUTATHIONE (HG/LG). (H. Fujise, K. Higa, A. Nishimaki, H. Ochiai, and P.K. Lauf) Departs. Pathol., School of Vet. Medicine, Azabu Univ., Sagamihara, Kanagawa 229, Japan, and Physiol. and Biophys., Wright State Univ., Dayton, OH, 45435, USA.

Hemoglobin oxidation by NO_2 is more efficient in HK-LG than in HK-HG DRBCs (Ogawa et al., Jpn.J. Vet. Sci. 51(6),1185.1989). Both HK D RBCS also possess a strong ouabain-insensitive K-Cl cotransport (Fujise et al. Am. J. Physiol. 260:C589, 1991). We tested the hypothesis whether NO_2, like other oxidants such as diamide, would also activate K-Cl cotransport, yet differently in HG and LG HK DRBCs. We measured ouabain-insensitive Rb influx in Cl and NO_3 in presences and absence of NO_2. In HG-HK DRBCs NO_2 stimulated Rb influx in Cl 6 fold and in NO_3 1.5 fold. The difference between the two, i.e. Cl-dependent Rb influx, was half maximum activated by 0.8 to 1 mM NO_2 in both HG and LG cells, and the Vmax of NO_2-treated HG-HK DRBCs was increased by 18fold over controls, at 2-4 mM NO_2. NO_2 did not alter the affinity of the transporter for K (apparent Km values were identical). At concentrations of >3 mM NO_2 inhibited Rb influx in Cl but not in NO_3. In low potassium (LK) DRBCs NO_2 stimulated Rb uptake in both Cl and NO_3, the relative effects dependent on the oxidant concentration. NO_2 treatment decreased cell volume in Cl but not in NO_3. Thus K-Cl cotransport present in both HK and LK DRBCs responds different to NO_2 whereas the stimulation in HK cells was apparently independent of the HG and LG levels. Stimulation at low and inhibition at high NO_2 concentrations point to effects at the regulatory and at the transporter levels (Supp. in part by a Visiting Professor Fellowship from Azabu University and NIH DK 37,160 to P.K.L).

M-Pos298

SARCOLEMMAL SODIUM-CALCIUM EXCHANGE IN MYOCARDIAL ISCHEMIA. ((Malcolm M. Bersohn)) Veterans Affairs Medical Center and University of California, Los Angeles, CA 90073

Alterations in sarcolemmal Ca^{2+} efflux mechanisms may have an important pathophysiologic role in ischemic injury. Therefore, the effects of 90 and 120 minutes of ischemia on the sarcolemmal Na^+-Ca^{2+} exchanger were investigated and compared to previous data for up to 1 hour of ischemia. Sarcolemmal vesicles were purified from control rabbit hearts and rabbit hearts made globally ischemic for 20, 30, 60, 90, and 120 minutes.

Purification of K^+-pnitrophenylphosphatase activity was about 30 fold compared to the initial homogenate and was the same for control and ischemic hearts. The initial velocity of Na^+-Ca^{2+} exchange was measured at 37° as Na^+_i-dependent $^{45}Ca^{2+}$ uptake after 1 sec. There was no inhibition after 20 minutes of ischemia, a 22% reduction in Vmax after 30 minutes of ischemia, and approximately a 50% reduction in Vmax after 60, 90, and 120 minutes of ischemia. At no duration of ischemia was there any change in the Ca^{2+} affinity of the Na^+-Ca^{2+} exchanger. Solubilization and reconstitution of the Na^+-Ca^{2+} exchanger into asolectin vesicles restored the velocity to the same level as control reconstituted vesicles after 60 minutes of ischemia but not after 90 or 120 minutes of ischemia despite the same degree of Na^+-Ca^{2+} exchange inhibition in the native vesicles.

The inhibition of Na^+-Ca^{2+} exchange activity in sarcolemmal vesicles is reversible by altering the membrane lipid environment for the first hour of ischemia, but not thereafter.

M-Pos299

ELECTRICAL PROPERTIES OF PORINS FROM *BORRELIA BURGDORFERI*.

((1)Tajib A. Mirzabekov, [2]Jonathan T. Skare, [2]Ellen S. Shang, [2]David R. Blanco, [2]James N. Miller, [2]Michael A. Lovett, [1]Bruce L. Kagan)) [1]Department of Psychiatry and Biobehavioral Sciences and [2]Department of Microbiology and Immunology, UCLA School of Medicine, 760 Westwood Plaza, Los Angeles, CA 90095.

Electrical properties of porins from *Borrelia burgdorferi* (the agent of Lyme disease) were studied. The porins formed channels in a planar lipid bilayer with conductances 220 pS, 600 pS and 9.5 nS in 1 M KCl, respectively. While the 220 pS and 600 pS channels had three subconducting states (approx. 70%, 30% and less than 7% of full open state), as shown by other porin channels, the 9.5 nS channel had more than ten subconducting states. The 220 pS and 600 pS channels had slight and asymmetric voltage dependence. Asymmetry of single channel voltage dependencies was the same as that of multichannel membranes which shows that porins incorporate into the bilayer in an oriented manner. In contrast to known porin channels the 9.5 nS channel had strong and symmetric voltage dependence. In current recordings from a membrane containing a single channel, slow (minutes) as well as fast (milliseconds) transition kinetics were observed. Application of +/-120 mV transformed all three channel to closed states with conductances less than 10% of full open states. Transition of channels to these low conductive states could irreversibly change channel properties (single channel conductance, voltage dependence, ion selectivity). Such voltage induced 'inactivation' of ion channels was previously observed with mitochondrial VDAC channels (J. Membr. Biol, 1993; 133:129-143). Gating charges of the 9.5 nS channel were titrated at acidic (3.0) and basic (9.9) pHs. Lowering of pH to 3.0 greatly enhanced the channel voltage-dependence. By analog to VDAC (BBA, 1990; 1021:161-168) we propose that the voltage sensor of 9.5 nS channel is composed of tens of negatively and positively charged amino acid residues.

M-Pos300

SODIUM/CALCIUM EXCHANGE ACTIVITIES IN CULTURED LYMPHOCYTE AND MONOCYTE CELL LINES. ((M. Balasubramanyam, M. Condrescu, J.P. Reeves and J.P. Gardner)) UMDNJ-New Jersey Medical School, Newark, NJ 07103. (Spon. by F.P.J. Diecke)

The Na/Ca exchanger (NCX) reportedly modulates plasmamembrane Ca flux during lymphocyte activation and ATP or cytolysin/perforin exposure. We examined putative "forward" and "reverse" mode NCX activities in cultured lymphocytes (Jurkat, Molt YAC-1 and EBV-transformed B cells), the promyelocytic cell line HL-60, THP-1 monocytes and Jurkat cells transfected with the bovine cardiac NCX (17-3J cells). Of cells treated with 5(6)-carboxyeosin (5-10 μM for 20 min, to inhibit Ca pump activity) and thapsigargin (Tg, 100 nM) and exposed to Ca-free media, only THP-1 and 17-3J cells showed rapid decreases in cytosolic Ca (Ca_i) in Na-free solution. Reverse mode NCX activity was examined in ouabain-treated cells exposed to +/- Na-solution; ^{45}Ca uptake was significantly enhanced in low Na-solution in HL-60 (28.8%), THP-1 (56.9%) and 17-3J (31.3%) cells. Tg-mediated Ca entry in the presence of $LaCl_3$ or SK&F 96365 (JCI; 94:2002) similarly showed enhanced rates in low Na-solution in HL-60 (0.4±0.1-fold), THP-1 (2.9±0.3-fold) and 17-3J (1.6±0.3-fold) cells, with little or no changes in other cell lines (-0.4±0.2-0.2±0.1-fold). 5(6)-carboxyeosin treatment increased Ca_i in Jurkat cells, however ^{45}Ca uptake and Tg/Ca_i activity were not enhanced in the absence of extracellular Na. This protocol did increase NCX-mediated ^{45}Ca uptake and Tg-mediated increases in Ca_i in HL-60, THP-1 and 17-3J cells and was additive with ouabain-treatment. These results suggest the Ca pump can affect measured rates of NCX activity. The lack of demonstrable Na/Ca exchange activity in lymphocyte cell lines indicates this transport system is not present or is down-regulated as a result of transformation or culture conditions.

M-Pos301

ISOLATION OF A PARTIAL REACTION OF ROD NA:CA,K EXCHANGER CYCLE ((A. Navangione, V. Vellani and G. Rispoli)) Dipartimento di Biologia, Sezione Fisiologia Generale, Via Borsari 46, Ferrara, Italy 44100.

The reaction cycle of photoreceptor Na:Ca,K exchanger was studied in isolated rod outer segment (OS) recorded in whole cell voltage clamp. To this purpose, it was looked for an electrogenic step that could be forced to occur by rapidly changing the extracellular solution (<50 msec) and which was slow enough to be resolved by this experimental protocol. An inward current transient (amplitude 12.2±0.6 pA, integral 0.40±0.03 pC, n=18) was observed upon switching an OS intracellularly perfused with 139 mM K (K_i) and 20 mM Ca_i from Isotonic extracellular Li (Li_o)+0 Ca_o to Isotonic Li_o+5 mM Ca_o. Transients up to 7 pA were observed upon switching from Li_o+0 Ca_o to Li_o+1 μM free Ca_o. Such transients were not observed in the opposite solution change, nor if the OS was perfused with K_i or Ca_i only. This indicates that the simultaneous presence of K_i and Ca_i orientates an high affinity Ca binding site to the extracellular side, where Ca_o binds to it electrogenically. The kinetics of current reactivation upon switching from Li_o+1 μM Ca_o to isotonic Na_o+0 Ca_o was slower in respect to the one recorded upon switching from Li_o+0 Ca_o to Isotonic Na_o+0 Ca_o. This kinetics change was shown previously using larger Ca_o concentrations in the Li_o solution and from which it was deduced that the exchanger density was about 10^4 mol·μm^{-2} (Bioph. J. 68, A414, 1995). The Ca binding to the exchanger site, recruited by the presence of Ca and K at the opposite side of the membrane, results then weakly electrogenic; the Ca affinity of the site in the absence of Na is in the μM range; the Ca binding to this site is faster than its unbinding.

M-Pos302

REVERSE OPERATION OF THE GAT1 (Na,Cl,GABA) COTRANSPORTER IN GIANT XENOPUS OOCYTE MEMBRANE PATCHES. ((C.-C. Lu[+], S. Mager[#], & D.W. Hilgemann[+])), [+]Dept. of Physiology, UTSW, Dallas, TX, 75235 and [#]Division of Biology, Cal-Tech, Pasadena, CA 91125.

We have studied cytoplasmic ion and substrate dependencies of reverse (outward) current generated by the expressed GAT1 (Na,Cl,GABA) cotransporter in giant excised membrane patches from *Xenopus* oocytes. With 20 mM Cl_o, reverse GAT1 current does not require extracellular monovalent cations. Cl_i and GABA activate no GAT1 current in the absence of Na_i. In most cases, Na_i does not induce outward current at 0 mV in the absence of $GABA_i$ and Cl_i. With 150mM Na_i and Cl_i, the K_d for $GABA_i$ is 3.3 mM. The n_{Hill} for Na_i is 2.16±0.2 and for Cl_i is 1.05 ±0.06. As Cl_i is decreased from 150 mM to 5 mM, the K_d for Na_i shifts progressively from 36 mM to 140mM, while the maximum current decreases by 30%. As Na_i is decreased from 150 to 20 mM, the K_d for Cl_i shifts progressively from 1.9mM to 13mM, while the maximum current decreases by 7-fold. As Na_i is decreased from 150 to 20 mM, the normalized slopes of current-voltage relations increase by about 2 fold. Minimum transport models are being evaluated in relation to these results, as well as additional studies of fast (30,000 s^{-1}) and slow (25 s^{-1}) GAT1-mediated charge movements.

M-Pos303

CHANNEL-LIKE NOISE OF CARDIAC Na,Ca EXCHANGE CURRENT PREDICTED BY KINETICS OF PARTIAL EXCHANGE REACTIONS. ((Donald W. Hilgemann)), Department of Physiology, UTSW Medical Center at Dallas, Dallas, TX, 75235-9040.

Recent studies suggest that single cardiac Na,Ca exchangers could generate electrical currents of about 1 fA (6000 elementary charges s^{-1}) which would flicker between 'off' and 'on' levels similar to single ion channel currents. These predictions have been verified by analysis of exchange current noise in small cardiac membrane patches. Noise frequency spectra correlate well with inactivation kinetics of exchange current, and the noise has a predicted bell-shaped dependence on the activation state of the exchanger. Maximum unitary currents are calculated to be 0.6-1.6 fA. These results are verified independently in giant membrane patches by isolating charge movements for both Na,Na and Ca,Ca exchange modes of the 'chymotrypsin-deregulated exchanger'. Results with cardiac membrane and oocyte membrane expressing NCX1 are very similar. Charge densities are consistent with 300-400 exchangers per μm^2 in cardiac membrane, and the slowest transport rates are about 5000 s^{-1} with half-maximal ion concentrations (37°C). The charge movements of Na,Na exchange are immobilized by exchanger inactivation reactions, and they appear to consist of three components. In addition, a small steady state current with bell-shaped dependence on Na concentration (in the complete absence of calcium) suggests significant Na,Na exchange with a stoichiometry other than 3-to-3 (e.g. 3-to-2).

M-Pos304

CALCIUM INFLUX BY SODIUM-CALCIUM EXCHANGE IS TIGHTLY LINKED TO MITOCHONDRIAL CALCIUM ACCUMULATION IN TRANSFECTED CHO CELLS. ((M. Condrescu and J.P. Reeves)) Dept. Physiology, UMDNJ, Newark, NJ 07103

Transfected CHO cells expressing the bovine cardiac Na/Ca exchanger accumulate > 1 mmol Ca/liter cell water in a Na-free medium when pre-treated with ouabain to elevate $[Na]_i$. Mitochondrial inhibitors (Cl-CCP, oligomycin + rotenone, Na azide) inhibit ^{45}Ca accumulation by 50% or more. Pretreatment of the cells with BAPTA-AM (50 μM) to chelate cytosolic Ca initially inhibited ^{45}Ca uptake by ouabain-treated cells, reflecting loss of secondary Ca activation of exchange activity. After 5 min in the Na-free medium, however, ^{45}Ca accumulated to higher levels in the BAPTA-treated cells than in controls. Mitochondrial inhibitors reduced the 5-min levels of ^{45}Ca uptake by 60% in the BAPTA-treated cells. ^{45}Ca uptake by BAPTA-treated cells was stimulated by ouabain-pretreatment and inhibited by Na_o, indicating that reverse Na/Ca exchange was the primary influx mechanism. Simultaneous loading of cells with BAPTA and fura-2 showed that BAPTA loading completely suppressed changes in $[Ca]_i$ associated with Na/Ca exchange activity. Thus, Ca entering cells via reverse Na/Ca exchange is coupled to mitochondrial Ca accumulation via a novel Ca sequestration pathway that does not involve a major increase in bulk cytosolic [Ca].

M-Pos305

REGULATION OF THE NCX-2 SODIUM-CALCIUM EXCHANGER BY PROTEIN KINASES IN CHO CELLS. ((M. Condrescu, D. Nicoll*, K.D. Philipson* and J. P. Reeves)) Physiology Dept., UMDNJ, Newark, NJ 07103 and *Cardiovascular Research Laboratory, UCLA School of Medicine, Los Angeles, CA 90024 (Spon. J. Fu)

CHO cells were permanently transfected with an expression vector (pcDNA3) containing an insert coding for the NCX-2 isoform of the Na/Ca exchanger. The rate of ^{45}Ca uptake under Na-free conditions in ouabain-treated cells was inhibited by pretreatment (30 min) with the tyrosine-kinase inhibitor genistein; maximal inhibition was 75% and half-maximal inhibition occurred at 100 μM genistein. ^{45}Ca uptake was unaffected by 200 μM daizrein, an inactive analog of genistein. Genistein (200 μM) treatment had no effect on the apparent K_m for Ca, or the concentration dependence of inhibition by Na_o (IC_{50} = 50 mM at 100 μM Ca). Activation of protein kinase C with 100 nM phorbol 12-myristate 13-acetate (PMA) produced a small (20 $\pm$ 4%) but significant ($p<0.01$) inhibition of ^{45}Ca uptake; down-regulation of protein kinase C by overnight incubation with PMA stimulated ^{45}Ca uptake 50-80% ($p<0.03$) and eliminated any effect of acute PMA administration. Neither genistein nor PMA had any effect on ^{45}Ca uptake in CHO cells expressing NCX-1. The results suggest that NCX-2 is activated by tyrosine kinase activity and inhibited by protein kinase C activity in these cells.

M-Pos306

BARIUM INFLUX VIA SODIUM-CALCIUM EXCHANGE IS STIMULATED BY INTRACELLULAR STORE DEPLETION IN TRANSFECTED CHO CELLS. ((G. Chernaya, V. G. Patel, M. Condrescu and J. P. Reeves)) Department of Physiology, UMDNJ, Newark, NJ 07103

Ba influx was measured with fura-2 in transfected CHO cells expressing the bovine cardiac Na/Ca exchanger. Ba influx was accelerated by Na-removal and by pretreatment of the cells with ouabain; similar results were obtained in ^{133}Ba flux assays. Vector-transfected control CHO cells do not express Na/Ca exchange and showed no change in Ba influx with Na-removal or ouabain treatment. Ba is not sequestered by the ER, nor does Ba efflux occur in a Na-free medium, suggesting that Ba is not a substrate for either the SERCA or PMCA Ca pumps. Treatment of the transfected cells with Tg (200 nM) or ionomycin (200 nM) released Ca^{2+} from intracellular stores and accelerated subsequent Ba uptake in a Na-free medium (Li substitution). Gramicidin (1 μM) blocked the effects of Tg and ionomycin under these conditions, presumably by lowering $[Na]_i$. Tg or ionomycin had little or no affect on Ba uptake at $[Na]_o$ = 140 mM or in vector-transfected control cells. Removal of ionomycin with bovine serum albumin reversed its stimulating effects on Ba uptake. The results suggest that Ca release from intracellular stores stimulates Na/Ca exchange activity. We hypothesize that activation of the exchanger by increased $[Ca]_i$ is responsible for the accelerated exchange activity.

M-Pos307

STIMULATION OF SODIUM-CALCIUM EXCHANGE ACTIVITY IN TRANSFECTED CHO CELLS BY THE PURINERGIC AGONIST ATP. ((M. Vázquez, G. Chernaya and J. P. Reeves)) Physiology Dept., UMDNJ, Newark, NJ 07103 (Spon. J. Durkin)

ATP interacts with a P_{2U} receptor in CHO cells to stimulate Ca release from $InsP_3$-sensitive stores. Transfected CHO cells expressing the bovine cardiac Na/Ca exchanger were loaded with fura-2 and placed in Ca-free media containing either Na or Li as the principal cation. The $[Ca]_i$ transient elicited by ATP was slightly reduced in the Li- compared to the Na-medium. Simultaneous addition of ATP (0.3 mM) + Ca (0.7 mM) produced a greatly enhanced, prolonged $[Ca]_i$ response in the Li-medium compared to the Na-medium. The addition of Ca 1 min after the addition of ATP also elicited an enhanced rise in $[Ca]_i$ in Li- compared to the Na-medium but when Ca was added 2 or 3 min after ATP, the response in the Li-medium was greatly reduced. Vector-transfected control cells showed little or no difference between the Li- and Na-media in similar experiments. When exchange activity was measured using Ba instead of Ca (cf. Chernaya *et al.*, this conference) Ba influx was also stimulated by ATP in Li- compared to Na-media when Ba was added 0 or 1 min after ATP, but not at 2 min after ATP. The results indicate that Ca release from $InsP_3$-sensitive stores transiently accelerates Na/Ca exchange activity, perhaps through activation by increased cytosolic Ca.

M-Pos308

Na/Ca EXCHANGE PLAYS A KEY ROLE IN Ca^{2+} REMOVAL FROM THE CYTOSOL DURING MEMBRANE DEPOLARIZATION IN RAT CEREBELLAR PURKINJE NEURONES. ((L. Fierro, I. Llano and R. DiPolo.)) AG Zelluläre Neurobiologie, Max Planck Institut für biophysikalische Chemie, D37077 Göttingen, FRG. (Spon. by L. Beaugé)

The role of Na/Ca exchange in removing Ca^{2+} from the cytoplasm under nearly physiological conditions was investigated in Purkinje neurones of rat cerebellar slices using whole-cell voltage clamp and fura-2 microfluorometry. Different Ca^{2+} loads were induced by varying the duration of membrane depolarization. The rate of $[Ca^{2+}]_i$ decline ($\Delta[Ca^{2+}]_i/\Delta t$) was determined from the negative slope of the $[Ca^{2+}]_i$ vs. time record. Contributions of Na-dependent and Na-independent (Na_o replaced by Li_o or NMG_o) process to Ca^{2+} removal were determined in the range from 50 to 2000 nM. The time constant of decay of the calcium signal (τ_{Ca}) was estimated by fitting either one or two exponential to the calcium transient. τ_{Ca} decreased with increasing peak $[Ca^{2+}]_i$ both in the absence and presence of Na_o. For high Ca^{2+} loads (1000-2000 nM) τ_{Ca} were 0.46 $\pm$ 0.038 (n = 18) and 0.85 $\pm$ 0.088 (n = 15) in the presence and absence of Na_o respectively. For small Ca^{2+} loads (50-150 nM) the τ_{Ca} were 1.27 $\pm$ 0.08 (n = 11) and 1.77 $\pm$ 0.106 (n = 18) in the absence and presence of Na_o respectively. The contribution of the Na/Ca exchange to the total removal of Ca^{2+} was estimated in the range of 50-2000 nM Ca^{2+} by subtracting $\Delta[Ca^{2+}]_i/\Delta t$ in the presence and absence of Na_o. In the range between 400 -1000 nM, Na/Ca exchange accounts for about 40 % of total Ca^{2+} removal. At high calcium loads (> 1500 nM) the Na-dependent component continues to increase in contrast to the apparent saturation of the Na-independent component. The present results clearly shows that in Purkinje neurones the Na/Ca exchange plays a significant role in the clearance of calcium following a membrane depolarization under physiological Na and Ca conditions. (CONICIT-Venezuela S1-2651).

M-Pos309

Na^+/Ca^{2+} EXCHANGER ACTIVITY IS INCREASED DURING CULTURE OF RAT CORTICAL NEURONS. ((C. Wang, N. Davis and R. A. Colvin, Biological Sciences Dept., Neurobiology Program, Ohio University College of Osteopathic Medicine, Athens, OH 45701)).

The Na^+/Ca^{2+} exchanger is an important plasma membrane protein that helps to maintain intracellular calcium homeostasis. Our recent work has shown that Na^+/Ca^{2+} exchanger activity in rat cortical neurons increases over 12 days in primary culture. Rat cortical neurons from E-18 rats were dissociated and plated on polyethyleneimene coated 6 -well plates. On day 3, 6, 9 and 12 after initial plating, the Na^+/Ca^{2+} exchanger activity of the neurons was determined. The neurons were sodium loaded in buffer containing 132mM NaCl, 1mM ouabain, 25μm nystatin, 2mM $MgCl_2$, and 10mM HEPES on ice for 10 minutes. Na^+/Ca^{2+} exchange was measured by incubating the neurons at 37°C for 15 minutes with buffer containing either 132mM sodium or 132mM choline chloride and ^{45}Ca. The uptake was terminated by addition of 500μM $LaCl_3$. The neurons were washed, then lysed with NaOH and lysate radioactivity determined by liquid scintillation counting. It was observed that Na^+/Ca^{2+} exchange activity (nmol/mg/15 min) was lowest in 3 day cultures and highest after 12 days in culture. The most significant change occurred between day 6 and 9 of culture (3 day: 1.62±0.16, n=15; 6 day: 1.84±0.31, n=12; 9 day: 8.22±1.12, n=15; 12 day: 9.71±1.22, n=12, mean ± S.E.). Anti-peptide antibodies labeled a protein of 130 kDa on Western blots. Densitometric analysis of Western blots showed that Na^+/Ca^{2+} exchanger protein levels increased by 50% after 9 days of culture. Steady state mRNA levels will be determined to demonstrate the temporal relationship between gene expression and increased Na^+/Ca^{2+} exchanger protein and activity levels. The increased Na^+/Ca^{2+} exchanger expression that accompanies maturation of cultured cortical neurons suggests the importance of exchanger function in neuronal development.

M-Pos310

IN DIALYZED SQUID AXONS N-PHOSPHOARGININE STIMULATES Na/Ca EXCHANGE BY A MECHANISM DIFFERENT FROM THAT OF MgATP. R. DiPolo and L. Beaugé*. CBB, IVIC. Caracas Venezuela. *Instituto M. y. M. Ferreyra, Cordoba, Argentina and MBL, Woods Hole MA. USA.

Previous work from our laboratories revealed that in squid axons dialyzed in the complete absence of MgATP and with $(Ca^{2+})_i$ around 1 µM, N-phosphoarginine (PA) reversibly stimulates the Na/Ca exchanger. The PA stimulation was additive to that of ATP, partially dependent on $Mg^{2+}{}_i$ and largely activated by $Ca^{2+}{}_i$. Further experiments on PA regulation showed that the effect cannot be mimicked by arginine, either alone or in combination with inorganic phosphate. In addition, different inhibitors of phosphatases (okadaic acid, microcystin) or kinases (staurosporine, H_7, tyrphostin, genistein, lavendustin) had no influence on PA stimulation. Interestingly, and similar to the MgATP effect, stimulation by PA is higher on the forward (Ca_i-Na_o) than on the reversal exchange modes (Ca_o-Na_i and Ca_o-Ca_i). On the other hand, PA does not affect the apparent affinities for Na_o and Ca_o nor for Li_o acting on the monovalent cation site. This contrasts with a more than two fold increase in the Na_o affinity induced by MgATP. Other experimental evidences showed even more stricking differences between MgATP and PA regulation. i) While MgATP effect is small or even undetected in the absence of Na_i PA stimulation is independent of Na_i. ii) The phosphatase substrate p-nitrophenilphosphate stimulates the exchanger only in the presence of MgATP but does not so in the presence of PA alone. iii) Finally, prolonged dialysis (> 4 hours) without any substrate (ATP and PA) results in the completed disapperance of the MgATP effect without affecting the PA effect. Under these prolonged substrate free dialysis conditions no changes in the V_{max} of the exchanger are observed. Taken together, these results indicate that the PA regulation of the Na/Ca exchanger takes place by pathways different from those of the MgATP regulation. Although likely, phosphorylation as the basis of the PA effect is by no means certain. (Supported by Grants from NSF, USA (BNS9120177), CONICIT-Venezuela (S1-2651) and CONICET -Argentina (PID-BID 1053).+

M-Pos311

CONSTRUCTION OF THE FULL LENGTH Na^+/Ca^{2+} EXCHANGER CLONE FROM FROG HEART SARCOLEMMA.
((T. Iwata, D. Guerini, A. Kraev and E. Carafoli)) Institute of Biochemistry, Swiss Federal Institute of Technology (ETH), 8092 Zurich, Switzerland.

The cardiac sarcolemmal Na/Ca exchanger is essential for the regulation of the heart contraction/relaxation cycle. The Na/Ca exchanger cDNA clones have been isolated from various tissues and species. All isoforms coded for the NCX1 genes are conserved well across species and tissues, except for the variations caused by alternative splicing of the primary transcript at a site in the main intracellular loop. Mammalian heart is known to express predominantly one isoform, utilizing certain exons, not found in other tissue-specific isoforms. Previously, we have reported the cloning of the Na/Ca exchanger cDNA in a lower vertebrate (frog) heart (Biophys.J. 68: A137). The clone was found to be the product of the NCX1 gene, and its sequence was well conserved with respect to other species except the differences found in the intracellular loop, i.e., an extra sequence of 9 amino acids was found in a clone at the site where the alternative splicing occurs in the intracellular loop in other species. Interestingly, it completes a "Walker's A" nucleotide binding motif, which is not present in any other mammalian Na/Ca-exchangers reported so far. Since this portion of the intracellular loop is the site of various regulation aspects, it could be related to the peculiarities of exchanger regulation in the amphibian heart. We have constructed the full length frog clone in order to analyze its activity. In addition, the portions of the intracellular loop with and without the 9 amino acids in the frog clone and the corresponding region of the dog isoform were expressed in E.coli to analyze the ATP-binding property.

M-Pos312

pH DEPENDENCE OF INTRACELLULAR LACTATE CONCENTRATION IN PERFUSED RIF-1 TUMOR CELLS. *G. Bernard Conyers, U. Pilatus, D. Artemov, and J. D. Glickson*; Division of NMR Research, Dept. of Radiology, The Johns Hopkins University School of Medicine, Baltimore MD 21205.

Tumor cells are highly glycolytic producing significant amounts of lactate. Since, lactate transport across the plasma membrane is mediated by a lactate-proton co-transporter [1,2] which couples it to the transmembrane pH gradient, it is anticipated that the reversed pH gradient of tumors (more acidic outside) is related to the intracellular lactate accumulation within tumors.[3] Therefore, lactate transport should play a significant role in pH homeostasis of tumor cells and a profound understanding of this mechanism is crucial for understanding tumor biology. NMR-spectroscopic studies on perfused high density tumor cell cultures grown on microcarriers offer an excellent tool to study pH related transport of metabolites. While intra- and extracellular lactate concentrations are obtained from diffusion-weighted ^1H NMR spectra the respective pH values are deducted from the chemical shift of the inorganic phosphate in ^{31}P spectra. All parameters are obtained from the same sample due to the non-invasive character of the method. Using this method, we looked at intracellular pH and lactate concentration in RIF-1 tumor cells at different extracellular pH and lactate concentrations. Additionally, we measured the lactate production rate by quantifying the lactate increase in the growth medium. Our results indicate that at low extracellular lactate concentrations (~ 20 mg/dL) the intracellular lactate is dominated by the pH dependency of the transporter's capacity, leading to an accumulation with decreasing extracellular pH. If the intracellular pH drops below 7.0, the lactate productions stops due to inhibition of phosphofructokinase [5] and the intracellular lactate concentration drops to the value at high extracellular pH. At high extracellular lactate concentrations (~ 135 mg/dL) the intracellular lactate concentration is coupled to the pH gradient and the cellular lactate production rate causes minor effects.

[1] T. L. Spencer and A. L. Lehniger. (1976) *Biochemistry.* **154**: 450.
[2] U. Schneider, R. C. Poole, and A. P. Halestrap. (1993) *Neuroscience.* **53:** 1153.
[3] J. R. Griffith. (1991) *Br. J. Cancer* **64:** 425.
[4] B. Triveldi and W. H. Danforth. (1966) *J. Biol. Chem.* **241**: 4110.

M-Pos313

COUPLED FLUXES OF H^+, K^+ AND Ca^{++} IONS ACROSS THE LYMPHOCYTE MEMBRANE. ((A.V. Gyulkhandanyan, S.S. Gambarov, K.M. Markosyan and S.S. Harutyunyan)) Institute of Biochemistry, NAS, Yerevan, 375044, ARMENIA.

The protonophore CCCP and ß-blocker propranolol mediated transport of H^+, K^+, and Ca^{++} ions in human blood and tonsilar lymphocytes has been studied. At pH of 6.3–6.8 of lymphocyte suspension CCCP (18μM) induces K^+/H^+ exchange with stoichiometry 1.35–1.45. At pH above 7.5 K^+ efflux is negligible and H^+ influx is practically not observable. At pH of 7.9–8.0 and in the presence of 1mM of Ca^{++} the propranolol (0.4mM) activates Ca^{++}–dependent K^+ efflux from cells. At pH of 7.1–7.3 and in the presence of Ca^{++} CCCP causes small K^+/H^+ exchange; however, the effect of propranolol is insignificant. Under these conditions sharp H^+ influx and K^+ efflux is demonstrated by successive addition of CCCP and propranolol (or vice versa). Trifluoroperazine (TFP, 80μM), while not affecting H^+ influx, suppresses more than 50% of CCCP–evoked K^+ efflux in the absence of La^{+++} (0.1mM). Together TFP and La^{+++} inhibit K^+ efflux (by 60-80%) and H^+ influx (by 30-40%) induced by successive impact of CCCP and propranolol. As follows from our experiments, both Ca^{++}–independent and Ca^{++}–dependent K^+/H^+ exchange may take place in lymphocytes.

GAP JUNCTIONS; INTERCELLULAR COMMUNICATION

M-Pos314

2-D CRYSTALLIZATION AND PROJECTION MAP OF A RECOMBINANT, TRUNCATED FORM OF THE α, CARDIAC GAP JUNCTION CHANNEL.
((V. M. Unger, N. M. Kumar, G. Klier, N. B. Gilula and M. Yeager)) Dept. of Cell Biology, The Scripps Research Institute, La Jolla, 92037. (Spon. by M. Yeager)

Gap junction proteins, termed connexins (Cx), play an important role in direct cell-to-cell communication. Previous analyses of two-dimensional (2-D) crystals of gap junctions at ~15Å resolution delineated the hexameric organization of the cylindrical subunits. A molecular description of the mechanisms responsible for opening and closing of gap junction channels will require structural information at high resolution. For instance, the evaluation of proposed α-helical models for the transmembrane domains will only be possible at a resolution better than 10Å. The resolution of previous crystallographic studies may have been limited by the existence of multiple connexins and different degrees of post-translational modification in gap junctions isolated from heart or liver tissue. To obviate these problems, a truncated form of the cardiac gap junction protein (α_1Cx-T) that lacks most of the large C-terminal domain has been expressed in stably transfected BHK cells. Freeze-fracture and negative stain electron microscopy demonstrated that recombinant α_1Cx-T assembles with the characterstic morphology of gap junctions and forms small 2-D crystals *in vivo*. The crystallinity was improved by extracting an enriched membrane fraction with Tween20. Optical diffraction revealed that the best crystals were coherent over several hundred unit cells, and the hexagonal lattice had parameters a = b = 81.1±1.2Å with γ = 119.8±0.32°. Density maps calculated without imposing any symmetry (i.e. plane group p1) showed that the connexon is formed by a hexameric cluster of α_1Cx-T subunits. Furthermore, to a resolution of 15Å, the projection phases of negatively stained crystals were consistent with p6 plane group symmetry (mean phase error 12.2°) and revealed a connexon diameter of ~63Å. Preliminary images of unstained, frozen-hydrated α_1Cx-T crystals have been recorded by electron cryo-microscopy. Computed diffraction patterns extend to ~7Å resolution, suggesting that a projection map at higher resolution will be forthcoming.

M-Pos315

CALCIUM INCREASES CONNEXON-CONNEXON INTERACTION FORCES IN ISOLATED GAP JUNCTIONS. ((N. P. D'Costa and J. H. Hoh)) Department of Physiology, Johns Hopkins University School of Medicine, Baltimore, MD 21205.

Calcium has been implicated in the regulation of gap junctional communication. However, the effect of calcium on gap junction structure remains poorly understood. We have previously shown that isolated gap junction membranes under physiological conditions (aqueous buffers) can be dissected using the tip of an atomic force microscope (AFM). This process separates the two membranes exposing the extracellular surface of the membrane attached to the substrate. Assuming that the interaction between the two membranes in the gap junction is dominated by the connexon-connexon contacts, the force required to dissect the gap junction provides a measure of the connexon-connexon interaction forces (so called docking forces). Using this approach we have now assessed the effect of calcium on the dissection force. We find that calcium does not effect the frictional forces between tip and membrane. However, the presence of sub millimolar concentrations of calcium increases the force (normal to the surface) required to separate the membranes by more than a factor of two (with field size, feedback and other parameters constant). This suggests that calcium increases the interaction forces between connexons, and may stabilize the cell-cell channel. Further the effect of calcium on dissection force appears to result from a single saturable binding site. These results are consistent with the recent demonstration by Goshroy et al. (J. Membr. Biol., 146, 15-28, 1995) that calcium inhibits splitting of isolated gap junctions in the presence of high concentrations of urea. Finally, the approach used here to assess connexon-connexon interactions provides a general method for investigating factors that control docking forces.

M-Pos316

CELLULAR NITRIC OXIDE RELEASE AS DETECTED BY FLUORESCENCE DIFFERENCE SPECTRA ((P.J. Andrew, M. Auer, I.J.D. Lindley, and A.J. Kungl)) Sandoz Research Institute, Brunnerstr. 59, A-1235 Vienna, Austria.

The reactive free radical nitric oxide (NO) is an important biological messenger, mediating for example blood vessel dilatation and the bactericidal and tumoricidal actions of macrophages, etc. Large amounts of NO are produced by the enzyme inducible nitric oxide synthase (iNOS), which can be induced in certain cell types upon stimulation with lipopolysaccharide (LPS) and/or cytokines. RAW 264.7 murine macrophages were incubated with LPS and interferon-γ for 6-8 hours to induce iNOS expression. The NO secreted into the medium was detected by its reaction with 2,3-diaminonaphthalene (DAN) to yield the corresponding N-nitroso compound, the fluorescence spectra of which differ significantly from that of the precursor. The addition of NaOH at this point, as described in the literature, to obtain the highly fluorescent naphthotriazole could thus be avoided. Fluorescence difference spectra relative to unstimulated cells were recorded with several concentrations of cells and at different incubation times of the cells with DAN to obtain a time course of NO production. For this purpose only the supernatant was taken for the fluorescence studies to avoid contaminating inner filter effects or overlapping emission signals from the intact cells. A comparison of the spectra obtained using the NO-releasing compound S-nitrosoacetylpenicillamine (SNAP) is made.

M-Pos317

CHARACTERIZATION OF THE CARBOXYL TERMINAL REGIONS INVOLVED IN pH REGULATION OF CONNEXIN43. ((J.F. Ek-Vitorin, G.E. Morley, W. Coombs, S.M. Taffet and M. Delmar)) SUNY/Health Science Center. Syracuse, NY 13210. (Spon. by J. Jalife)

We have previously reported that 10-20-amino acid deletions within region 261-300, together with deletion 374-382 prevent normal pH gating of Cx43. Here we report that similar results can be obtained by specific mutations within those regions. Experiments were carried out in antisense-injected *Xenopus laevis* oocyte pairs expressing Cx43 or its mutants. Junctional conductance was determined by the dual voltage clamp technique. Acidification was induced by superfusion of a Na acetate solution at a pH of 6.2. Substitution of prolines 277 and 280 for alanines decreased the pH sensitivity in a manner similar to that of deletion 261-280. Interestingly, these prolines are part of a proline-rich region, with a $(PXX)_4$ repeat (amino acids 274-285). These sequences tend to form left-handed (Type II) alpha-helices, and are commonly involved in protein-protein interactions. Region 374-382 includes two basic residues (arginines) separated by prolines. Substituting either the two prolines for alanines, or the two arginines for glutamines had an effect similar to that obtained by deletion of the entire 374-382 sequence. The latter shows that acidification-induced uncoupling is not directly related to the net balance of charges within the carboxyl end. Preservation of a structure seems to be required. In separate experiments, using CO_2-induced acidification and simultaneous recordings of Gj and pH_i, we confirmed that the carboxyl terminal domain acts as a pH-dependent "gating particle," which requires regions 281-300 and 374-382 to close the channel. Overall, the data support the hypothesis that intramolecular interactions between well-defined structures are required for pH gating of Cx43.

M-Pos318

THE CARBOXYL TERMINAL OF CONNEXIN43 ALTERS pH REGULATION OF CONNEXIN32 CHANNELS. ((G.E. Morley, S.M. Taffet, and M. Delmar)). SUNY Health Science Center. Syracuse, NY 13210.

Previous results have shown that connexin32 (Cx32) is less sensitive to acidification induced uncoupling than connexin43 (Cx43). In addition, the pH sensitivity of Cx43 is significantly decreased by the truncation of the carboxyl terminal at residue 257 (M257). Co-expression of the carboxyl terminal (i.e., residues 259-382) with M257 confers pH sensitivity to this pH insensitive mutant. Accordingly, we propose that pH gating results from an interaction between the carboxyl terminal domain (acting as a gating particle) and a separate region of connexin, acting as a receptor for the particle. Here we show that the carboxyl terminal of connexin43 can enhance the pH sensitivity of Cx32 channels. Cx32 was expressed in anti-sense injected *Xenopus laevis* oocyte pairs. Junctional conductance was measured electrophysiologically. Intracellular pH was simultaneously determined by measuring the fluorescence emission of the proton-sensitive dye SNARF-1. Intracellular acidification was induced by superfusing oocytes with a $NaHCO_3$-buffered solution where the concentration of CO_2 was progressively increased. The pHi at which the junctional conductance of Cx32 decreased to 50% of maximum (pKa) was 6.47±0.03 (mean±sem; n=8). Co-expression of the carboxyl terminal of Cx43 (residues 259-382) with Cx32 significantly ($p<0.05$) enhanced the pH sensitivity of the Cx32 channels (pKa=6.63±0.05; n=5). These results suggest that the region of Cx43 acting as a receptor for the gating particle is conserved, at least in part, among connexins.

M-Pos319

MUTATION OF A SINGLE AMINO ACID (Asp379) PREVENTS pH REGULATION OF CONNEXIN43. ((G.A. Calero, J.F. Ek-Vitorin, S.M. Taffet and M. Delmar)) SUNY Health Science Center. Syracuse, NY 13210.

Acidification of the intracellular space leads to closure of connexin43 (Cx43) channels (i.e., pH gating). We have previously shown that this phenomenon requires the presence of a functional carboxyl terminal (CT) domain. Here we report that specific mutations of acidic (negatively charged) amino acids at the CT end impairs pH gating in a manner similar to that of truncation of the entire carboxyl terminal region. Antisense-injected *Xenopus laevis* oocytes were injected with wild-type or mutant Cx43 mRNA. Junctional conductance was determined by the dual voltage clamp technique. Acidification was induced by superfusion of a sodium acetate solution buffered at a pH of 6.2. Substituting the three acidic residues at the carboxyl end (Asp378, Asp379, Glu381) for their corresponding (uncharged) amide prevented pH gating. A similar result was obtained when only Asp379 was substituted by either Gln or Asn. Interestingly, pH regulation was not affected by substitution of Asp379 for Lys. Individual mutations of residues Asp378 or Glu381, or substituting Asp379 together with Asp378 or with Glu381 had no significant effect on pH regulation. Finally, replacing both Asp378 and Glu381 for their amide while leaving Asp379 intact had the effect of enhancing acidification-induced uncoupling. These results show that the mechanism of pH gating does not depend exclusively on the net balance of charges at the CT end but rather on the preservation of the overall structure. Taken together with studies by other laboratories (see, e.g., Britz-Cunningham et al; N Eng J Med 332:1323-1329, 1995) the data suggest that specific mutations at the CT end of Cx43 may drastically alter the regulation of cell-cell communication in the heart and other structures.

FLUORESCENCE - PHOSPHORESCENCE

M-Pos320

BROMINATED DETERGENTS FOR STRUCTURAL STUDIES OF MEMBRANE PROTEINS. **((B. de Foresta, P. Champeil and M. le Maire.)) SBPM/DBCM, CEA and CNRS URA 1290, CE Saclay, F-91191 Gif-sur-Yvette Cedex France.(Spon. by P. Champeil).**

New brominated detergents [7,8-dibromododecyl-β-maltoside (BrDM) and 11,12-dibromo-2-O-lauroylsucrose (BrLS)] were used to study static and dynamic aspects of protein-detergent interactions. Rayleigh scattering measurements showed that both detergents solubilized sarcoplasmic reticulum vesicles, containing mainly the Ca^{2+}-ATPase, as rapidly as the non-brominated detergents. However, higher brominated detergent concentrations were required, probably because of a circa twofold increase in the cmc of each detergent. Detergent partition was found rather similar for DM and BrDM. Ca^{2+}-ATPase contains 13 Trp, mainly located in the membrane, at the protein-lipid interface. Both BrDM and BrLS quenched the Ca^{2+}-ATPase fluorescence up to 50% when the membrane was saturated with detergent. This reveals the extent of protein-detergent interactions before solubilization. The fluorescence was further quenched up to circa 80% when the protein was solubilized, indicating further delipidation of the protein surface. Both BrDM and BrLS proved to be sensitive tools to test interactions at the hydrophobic surface of the protein and can in addition prove to be useful to test the accessibility of membrane protein helices containing reporter chromophores.

M-Pos321

SELF-QUENCHING OF NITROBENZOXADIAZOLE LABELED PHOSPHOLIPIDS IN LIPID MEMBRANES. ((John D. Brennan[1] R. Stephen Brown[2] and Ulrich J. Krull[3])) [1]Dept. of Chemistry, Brock University, St. Catharines, ON, L2S 3A1, [2]Biotechnology Research Institute, NRC, 6100 Royalmount Ave., Montreal, PQ, H4P 2R2, [3]Chemical Sensors Group, Erindale Campus, University of Toronto, Mississauga, ON, L5L 1C6.

The emission intensity, wavelength and lifetime of the fluorophore nitrobenzoxadiazole dipalmitoylphosphatidylethanolamine (NBD-PE) are sensitive to the local environmental structure when this species is present as a component of an amphiphilic membrane. Alteration of the physical and electrostatic structure of a membrane can result in changes in the fluorescence signal owing to changes in the extent of self-quenching of the probe. To investigate self-quenching, NBD-PE was incorporated into monolayers and vesicles composed of Egg phosphatidylcholine at concentrations of 0.1 to 50 mol%. Monolayer samples were dipcast onto glass slides at a pressure of 35 $mN.m^{-1}$. Both the integrated intensity per fluorophore (quantum yield) from vesicles and dipcast monolayers, and the mean fluorescence lifetime from vesicles decreased as the concentration of fluorophore in the membranes was increased. At all concentrations studied the decay of NBD-PE fluorescence was fitted to two discrete exponential, and both lifetime components were observed to change with concentration. An empirical model of fluorescence self-quenching was developed which could describe the observed alterations in the fluorescence lifetimes and intensity. The model was based on a combination of Perrin quenching and Förster energy transfer. The fluorescence data was fit by a model wherein NBD-PE formed nonemissive traps sites with a critical radius of $R_C = 1.0 \pm 0.1$ nm, (Perrin Quenching) with Förster energy transfer occurring to the trap sites with an R_0 value of 2.55 ± 0.10 nm, as determined from spectral overlap integrals.

M-Pos322

LOCATION OF THE OXONOL DYE BINDING SITE OF THE BAND 3 ANION TRANSPORT PROTEIN BY FLUORESCENCE ENERGY TRANSFER. **((M.A. Wilson and P.A. Knauf)) Dept. of Biophysics, University of Rochester Sch. of Medicine, Rochester, NY 14642.**

Fluorescent oxonol dyes are excellent reversible inhibitors of band 3-mediated Cl^- exchange and at least some of them, such as WW781, are affected by transport-related conformational changes in band 3. We have used diTBA [bis-(1,3-diethylthiobarbituric acid) trimethine oxonol] as a fluorescent label for the oxonol binding site. Red cell ghosts were labeled with N-fluorescein maleimide (NFM), which labels band 3 at SH groups on the cytoplasmic side of the membrane (Rao et al., Biochemistry 18: 4505 (1979)). When NFM-labeled ghosts were titrated with diTBA, fluorescence emission spectra (with excitation at the donor (NFM) wavelength of 491 nm) exhibited both donor quenching and stimulated emission of the acceptor, diTBA. The donor quenching fit well to a model in which diTBA binds to a high-affinity site (K_d = 16 nM), as well as to nonsaturable low-affinity sites. From the transfer efficiency for the high-affinity component of 0.12, we calculated a transfer distance of 83 ± 16 Å. In comparison, the distance from NFM to the stilbene disulfonate binding site is only 34-42 Å (Rao et al., 1979). This suggests that the oxonol binding site is located near the outer portion of band 3 and also that the transport-related conformational changes of band 3, which affect both stilbene and oxonol binding, must involve global conformational alterations in sites at least 25 Å apart. (Supported by NIH (NIDDK) grant DK27495.)

M-Pos323

COUPLING BETWEEN THE INTRAMOLECULAR PROTON TRANSFER, INTRAMOLECULAR TORSION AND INTERMOLECULAR ENERGY TRANSFER IN THE PROTEIN INTERIOR. ((Alexander Sytnik)) Institute of Molecular Biophysics, Florida State University, Tallahassee, FL, 32306-3015. (Spon. by R. Rill)

Coupled in one molecular system, excited-state transformations can dynamically compete and provide time-resolved information about the molecules possessing these transformations, the excited-state transformations by themselves, and the medium where the coupling takes place. The present work is focused on the pairing among three excited-state events: Förster intermolecular energy transfer, intramolecular proton transfer, and intramolecular torsion. A molecule, 3-hydroxy-2-(2-phenylethenyl)-chromone (HPC), which was synthesized by Dr. Feng Gao (Chemistry Department, Florida State University) simultaneously exhibits excited-state proton transfer, torsion and efficiently accepts energy from excited tryptophan. Steady-state and time-resolved data on HPC - human serum albumin (HSA) complexes suggest the location of HPC binding sites, and also demonstrate the influence of HSA dynamics on HPC torsion. Proton transfer (PT) tautomer fluorescence does not appear at all for the HPC - HSA complexes. Another fluorescence probe, 3-hydroxyflavone (3-HF), which does not possess the intramolecular torsion, shows the green PT fluorescence and efficiently accepts the energy of excited Trp-214 for the 3-HF - HSA complexes.

M-Pos324

Fluorescence spectroscopic study of sapintoxin D binding to protein kinase C ((Cojen Ho, Simon J. Slater and Christopher D. Stubbs)) Thomas Jefferson University, Dept. of Pathology & Cell Biology, Philadelphia, PA 19107

Sapintoxin D (SAPD) is a fluorescent phorbol ester that binds and activates protein kinase C (PKC). The structural similarity between sapintoxin and 12-0-tetradecanoylphorbol-13-0-acetate (TPA) implies that these two molecules may bind and activate PKC in a like manner, as confirmed in this study. The fluorescence properties of SAPD were examined and its potential in the study of PKC activation explored. SAPD, bound to membrane lipid-associated PKCα, exhibited a blue-shifted emission maximum compared to that in buffer or with lipid alone. From a plot of dielectric constants (ε) of different solvents with SAPD emission maximum, ε for SAPD bound to PKCα was found to be ~2, indicating that part of the binding site is highly hydrophobic. Fluorescence energy transfer between PKCα tryptophans and SAPD was used to measure the strength of association between SAPD and PKCα and binding constants were derived. The steady state anisotropy of PKC-associated SAPD increased due to its motional restriction within the binding pocket and decreased with the addition of TPA. When SAPD bound to PKCα, time-resolved fluorescence anisotropy analysis gave two rotational correlation times (ϕ) and fractional intensities (f), corresponding to free and bound SAPD, respectively. Fractional intensity of the long rotational component (bound) decreased with the addition of TPA, again indicating binding competition. Thus the fluorescence properties of SAPD renders an efficient method in the study of phorbol ester -PKC binding.

M-Pos325

FLUORESCENCE MONITORING OF THE REVERSIBLE UNFOLDING OF F102W AND F102(7AW) RAT PARVALBUMIN IN AQUEOUS SOLUTION. ((B. Rajendran[1] J.D. Brennan[2], S. Cyr[1], D. Duforc[1], C.W.V. Hogue[3], and A.G. Szabo[1].)) [1]Dept. of Chemistry and Biochemistry, University of Windsor, Windsor, ON, N9B 3P4, [2]Dept. of Chemistry, Brock University, St. Catharines, ON, L2S 3A1, [3]NCBI-National Institutes of Health, 9600 Rockville Pike, Bethesda, MD 20894.

A potentially powerful method by which protein structure may be studied is through the measurement of intrinsic fluorescence from tryptophan and tyrosine residues. Alternatively, non-natural aromatic amino acids such as 7-azatryptophan (7AW) may be biosynthetically incorporated into proteins in place of tryptophan. The spectroscopic characteristics of this probe are different from those of tryptophan, and therefore new information on protein structure and dynamics may be attained. In the present study rat parvalbumin was prepared with the naturally occurring phenylalanine residue replaced either by a tryptohan, resulting in F102W rat parvalbumin, or by 7AW, resulting in F102(7AW) rat parvalbumin. The fluorescence spectra, intensity, steady-state anisotropy and decay behaviour of the two mutant proteins was examined in solution at different temperatures and guanidine hydrochloride (GdHCl) concentrations. Complementary investigations were done using circular dichroism measurements. Several interesting results were observed. Firstly, it was found that the stablility of the protein was not affected by the addition of 7AW in place of Trp. Secondly, it was determined that both GdHCl and thermal unfolding was fully reversible, as measured by both fluorescence and CD. Lastly, it was found that the changes in the 7AW intensity, wavelength and lifetime were much greater than was found for Trp when the protein unfolded, indicating that 7AW is more sensitive to its local environment. These results suggest that 7AW is a superior probe for investigation of structural transitions in proteins.

M-Pos326

FLUORESCENCE AND NMR OF THIOREDOXIN TRYPTOPHANS: A UNIFIED MODEL OF PROTEIN STRUCTURE AND DYNAMICS ((Christopher Haydock[1], Norberto D. Silva, Jr.[1], Marvin D. Kemple[2] and Franklyn G. Prendergast[1])) [1]Department of Biochemistry and Molecular Biology, Mayo Foundation, Rochester, MN 55905. [2]Department of Physics, IUPUI, Indianapolis, IN 46202-3273.

Multiple experimental probes of one system can offer a more rigorous test of both the underlying model of protein structure and dynamics and of the method specific features of the model. A nonassociated Lipari and Szabo type model for the dynamics of the tryptophans in *Escherichia coli* thioredoxin apparently gives a consistent picture of overall and internal motion of thioredoxin when fit to both NMR and fluorescence data. In this work we compare this model with an associated minimum perturbation map model for the same system and data. This associated model allows excited state reactions between rotational isomers of tryptophan and of neighboring side chains. The model provides estimates of the rate constants of these excited state reactions and of the order parameters for the excited states as well as the order parameters for interconversion between excited states. The model provides detailed estimates of the variability in the apparent zero time fluorescence anisotropy due to excited state reactions. Rotational isomerization of side chains neighboring tryptophan provides a mechanism by which the fluorescence anisotropy can decay on the nanosecond time scale without producing nanosecond components in the NMR spectral density. This work is supported in part by GM 34847.

M-Pos327

TRYPTOPHAN FLUORESCENCE SPECTROSCOPY ON THE MEMBRANE-EMBEDDED MANNITOL TRANSPORT ENZYME (EII^{mtl}) of E. COLI. ((J. Broos, D Swaving Dijkstra, and G. T Robillard)) GBB, University of Groningen, Nyenborgh 4 9747 AG Groningen, The Netherlands.

Using a specially constructed tryptophan-minus mutant (EII^{mtl}(Trp-)) of the mannitol transport enzyme, EII^{mtl}, we have optimized the isolation procedure in order to eliminate fluorescent impurities which cannot be spectroscopically distinguished from tryptophan. Fluorescent impurities, present in detergents used during the isolation procedure, accumulate in enzyme solutions to levels far above the background in buffers containing detergent alone. A procedure has been developed to completely remove all fluorescent impurities from the nonionic PEG-based detergent $C_{10}E_5$. By using this detergent during the isolation procedure, EII^{mtl}(Trp-) and single tryptophan mutants could be isolated, in which the impurities no longer seriously interfere with the tryptophan emission signal.

Based on the corrected emission maximum of EII^{mtl} wild type (331 nm), tryptophan positions 42, 109 and 117 with maxima ranging from 337 to 340 nm can be marked relatively polar, position 384 with a maximum at 346 nm is highly polar, whereas position 30 is highly apolar with a maximum at 324 nm. The highly apolar environment of tryptophan 30 is confirmed by the lack of quenching by I^-, suggesting a non-accessible location for this tryptophan.

When mannitol is bound to EII^{mtl} an increase in fluorescence emission intensity is observed. Analysis of the single tryptophan mutants revealed that this increase in the wild type EII^{mtl} can be attributed to increased fluorescence intensities of the tryptophan residues at positions 30 and 42.

M-Pos328

THE LOCATION OF THE ^1L_a ORIGIN FOR INDOLES IN AR MATRICES AT 20K WITH ACCOMPANYING ^1L_a AND ^1L_b FLUORESCENCE. ((Bruce J. Fender and Patrik Callis*)) Department of Chemistry and Biochemistry, Montana State University, Bozeman, Mt 59717.

Indole is the chromophore of the amino acid tryptophan. We have recently reported the identification of the true ^1L_a origin in Ar at 20K [B. Fender et al.; *Chem. Phys. Letters* 239 (1995)]. We have extended such experiments to include 3-methylindole, 5-methylindole, and 2,3-dimethylindole (2,3-DMI), locating their respective ^1L_a origins in solid Ar. For 2,3-DMI the ^1L_a origin was 200 cm-1 below the ^1L_b origin - giving ^1L_a fluorescence. This gave relatively sharp ^1L_a spectra, which can be distinguished from its ^1L_b counterpart by its Franck-Condon activity. The sharpness of the fluorescence spectra in the Ar matrices has allowed us to identify signature Franck-condon activity which distinguishes ^1L_a and ^1L_b fluorescence. There is also good agreement between calculated ^1L_a fluorescence done from this laboratory and the experimental ^1L_a fluorescence.

M-Pos329

PROBING PROTEIN UNFOLDING REACTIONS USING NON-NATURAL AMINO ACIDS: AN EXAMINATION OF WILD TYPE AND W92(7AW) TRYPTOPHANYL *t*RNA SYNTHETASE USING FLUORESCENCE TECHNIQUES. ((A.G. Szabo[1], J.D. Brennan[2], C.W.V. Hogue[3] and B. Rajendran[1])) [1]Dept. of Chemistry and Biochemistry, University of Windsor, Windsor, ON, N9B 3P4, [2]Dept. of Chemistry, Brock University, St. Catharines, ON, L2S 3A1, [3]NCBI-National Institutes of Health, 9600 Rockville Pike, Bethesda, MD 20894.

There have been a number of studies in which the fluorescence of intrinsic tryptophan residues was monitored in order to observe the unfolding of proteins in solution (M.R. Eftink, *Biophys. J.* **66** (1994) 482). In this presentation, a new approach to the fluorescence monitoring of protein unfolding is introduced. This approach involves the biosynthetic incorporation of the non-natural aromatic amino acid 7-azatryptophan into proteins. The spectroscopic characteristics of this probe are different from those of tryptophan, and therefore new information on protein structure and dynamics can be attained. 7AW was incorporated into the enzyme tryptophanyl-*t*RNA synthetase (TrpRS) to produce W92(7AW) TrpRS. This is a homodimeric protein, and thus contains two Trp or 7AW residues which are located at the subunit interface. The fluorescence spectra, intensity, steady-state anisotropy and decay behaviour of Wild Type and W92(7AW) TrpRS was examined in solution at different temperatures and guanidine hydrochloride (GdHCl) concentrations. It was found that the incorporation of 7AW reduced the thermal stablility of the protein. In addition, it was determined that both GdHCl and thermal unfolding occurred as a two step process involving dissociation of the dimers, followed by irreversible unfolding of the monomers. Furthermore, it was found that the changes in the 7AW intensity, wavelength and lifetime were much greater than was found for Trp when the protein unfolded, indicating that 7AW is more sensitive to its local environment. In fact, the 7AW probe was able to indicate a structural transition which was not observable in the Wild Type protein. These results suggest that 7AW is a superior probe for investigation of structural transitions in proteins.

M-Pos330

SPECTRAL ENHANCEMENT OF PROTEINS: IN VITRO AND IN VIVO INCORPORATION OF TRYPTOPHAN ANALOGS ((J.E. Carlson, L.E. Steward, R. Rusinova, A.R. Chamberlin, J.B.A. Ross)) Mt. Sinai School of Medicine, New York, NY 10029 and University of California, Irvine, Irvine CA 92717

Intrinsic protein absorbance and fluorescence from Trp residues are limited as observables for investigation of protein-protein and protein-nucleic acid interactions. Trp is not generally suitable as an intrinsic probe since most proteins contain Trp, and the absorption spectra of nucleic acids completely overlap that of Trp. The alternate choice, labeling with extrinsic probes such as dansyl or fluorescein, risks altering protein structure or function. To overcome these limitations, we are developing *in vivo* and *in vitro* methods to alter the spectral properties of proteins. Our approach is to replace Trp with Trp analogs whose absorption spectra are red-shifted from that of Trp. These analogs provide a spectral window that can highlight a particular protein in a heteromeric assembly. Analogs suitable for this purpose include 5-hydroxy-Trp or 7-aza-Trp.

We and others have shown that Trp analogs can be incorporated into proteins expressed *in vivo* by using bacterial Trp auxotrophs. This results in uniform replacement of all Trp residues. Uniform replacement, however, may alter protein structure or function. To replace a specific Trp (or other residue of interest), we use *in vitro* transcription/translation with analog-charged, nonsense suppressor tRNAs. Thus, we can probe a single site while residues essential for maintaining structure or function can be left in place. We are using both approaches to study macromolecular interactions involved in blood coagulation and transcription.

Supported by NIH USPHS grants GM-39750 (JBAR), HL-29019 (JBAR), and GM-42708 (ARC). L.E. Steward was supported by NIH NRSA predoctoral training grant GM-07311.

M-Pos331

MULTIPHOTON EXCITATION OF AMINO ACIDS AND NEUROTRANSMITTERS: A PROGNOSIS FOR *IN SITU* DETECTION ((Sudipta Maiti, Jason B. Shear, and Watt W. Webb)) Dept. of Applied Physics, Cornell University, Ithaca, New York 14853.

Multiphoton fluorescence cross sections of the amino acid tryptophan and neurotransmitters serotonin and dopamine have been measured as a function of wavelength in the near infrared using a mode-locked Ti:sapphire laser. The measured three-photon fluorescence excitation spectra differ from the corresponding one-photon fluorescence excitation spectra. For the three-photon processes, the detected fluorescence is observed to be proportional to the cube of the applied power at low power levels. At the highest intensities the fluorescence deviates above or below the cubic values, depending on the excitation wavelength. These deviations reflect four-photon excitation, photobleaching, and other photochemical pathways currently being investigated. The magnitudes of the fluorescence signals predict detectable two- and three-photon fluorescence from large neurotransmitter vesicles. Combined with the inherent three-dimensional resolution of multiphoton excitation using highly focused femtosecond laser pulses and the relative transparency of biological materials to these longer wavelengths, these results suggest new imaging possibilities utilizing the native UV-excitable fluorescence of cellular materials.

Supported by NIH (RR04224, RR07719) and NSF (BIR8800278) at the Developmental Resourse for Biophysical Imaging and Opto-electronics. J. S. is an NSF Postdoctoral Fellow supported by grant CHE-9403174.

M-Pos332

LONG-RANGE DISTANCE MEASUREMENTS USING LUMINESCENCE ENERGY TRANSFER EMPLOYING EUROPIUM CHELATE. **((E. Heyduk and T. Heyduk)) St. Louis University, School of Medicine, St. Louis, MO 63104.**

Selvin et al. (1994)[1,2] have recently showed that bifunctional lanthanide chelates could be potentially extremely useful fluorescence probes for distance measurements using fluorescence energy transfer. These probes have very long, easily measurable lifetimes, and the problems associated with uncertainty of an orientation factor value are eliminated. Also, it is possible to take advantage of their unusually long lifetimes, and using gated data acquisition practically eliminate the background originating from light scattering and fluorescence which decays with nanosecond lifetimes. This, together with large R_0 values possible with this probes[1,2], should permit measurements of much longer distances than with classical probes. We have thus tested some practical aspects of long-range distance measurements employing europium chelates using a model system of 26 bp DNA containing a consensus binding site for cAMP receptor protein (CAP). The opposite ends of this DNA fragment were labeled with CY5 (acceptor) and bifunctional europium chelate (donor). A simple two-step methodology (which employs commercially available reagents) for covalent attachment of bifunctional europium chelate to 5'-end of an oligonucleotide derivatized with an amino group was developed. The donor-acceptor distance in this DNA molecule is expected to be about 100 Å. Additionally, upon binding of CAP the DNA fragment is substantially bent resulting in approx. 15 Å decrease in end-to-end distance. Thus, the effects of small changes in distance could be tested as well. The results showed that using sensitized emission resonance energy transfer at about 100 Å distance could be readily detected (40% increase of signal over the background). Binding of CAP resulted in 2.1 times increase in sensitized emission showing a great potential and sensitivity (about 15% distance change resulted in more than two fold change in signal) for measuring changes of long distances. Additional results of experiments designed to increase the measurable distance range and potential experimental artifacts will be presented.

[1]Selvin, P.R., Rana, T.M., and Hearst, J.E. *J. Am. Chem. Soc.* 116, 6029-6030, 1994
[2]Selvin, P.R., and Hearst, J.E. *Proc. Natl. Acad. Sci. USA* 91, 10024-10028, 1994.

M-Pos333

MAG-FURA-2 -2 EXHIBITS BOTH LOW (μM) AND HIGH (nM) AFFINITY Ca^{2+} BINDING SITES. ((R. Martínez-Zaguilán[1], J. Parnami[2], and R.M. Lynch[2])). Departments of Physiology, [1]Texas Tech Univ., H.S.C., 79430 Lubbock, TX ; and [2]Univ. Arizona, Tucson, AZ 85724.

Based on studies using high affinity Ca^{2+} probes (dissociation constant (Kd; = 0.15-0.3 μM), steady-state $[Ca^{2+}]^{in}$ is believed to be in the nanomolar range in most cells. However, probes with lower affinity indicate that $[Ca^{2+}]^{in}$ may increase to micromolar levels during activation of specific cell functions; e.g contraction. These conclusions rely on accurate knowledge of the Kd of the dyes for Ca^{2+}. Mag-Fura-2 is a low affinity Ca^{2+} indicator (Kd ca. 50 μM) which has been used for such studies. In the present work, Mag-Fura-2 is shown to respond to changes in cytosolic Ca^{2+} in the submicromolar range. In vitro, and in situ titration of Mag-Fura-2 in A7R5 cells, demonstrate the presence of a high affinity Ca^{2+} binding site in addition to the known low affinity site. Moreover, both high and low affinity Ca^{2+} binding sites are sensitive to pH with the dynamic range of the low affinity site maximal at low pH. Since Mag-Fura-2 has been used to study Ca^{2+} within specific subcellular compartments, the present observations indicate that knowledge of factors such as ambient pH of these compartments is required to accurately interpret Ca^{2+} responses. Furthermore, the relative dynamic range of the high affinity site must be considered for accurate determination of Ca^{2+} in specific compartments.

M-Pos334

TWO-PHOTON EXCITED PHOTORELEASE OF CAGED CALCIUM ((J. B. Shear[1], E. B. Brown[1], S. R. Adams[2], R. Y. Tsien[2], W. W. Webb[1])) [1]Dept. of Applied Physics, Cornell University, Ithaca, NY 14853 and [2]Dept. of Chemistry, University of California, San Diego, La Jolla, CA 92093

Photolysis of photolabile caged calcium compounds provides an ability to modify cellular chemistry with high spatial and temporal resolution for the study of the dynamics of fundamental cellular processes, including neurosecretion and second messenger signalling. However, Ca^{2+} release that relies on conventional UV excitation cannot confine photolysis to highly localized three-dimensional volumes. In contrast, two-photon excitation with strongly focused near-IR radiation provides inherent three-dimensional resolution as a result of the square-law intensity dependence of the uncaging process. We present the two-photon action cross sections for several caged-calcium compounds excited with a mode-locked Ti:sapphire laser in the wavelength range 690 nm to 800 nm, using changes in the fluorescence of a calcium indicator as a measure of uncaging cross section. Two commonly used Ca^{2+} cages, NP-EGTA and DM-nitrophen, were evaluated, with both species demonstrating fast uncaging kinetics but relatively low action cross sections at 700 nm. The two-photon action cross section of a novel Ca^{2+} cage, Azid-1, was ten- to 100-fold greater at 700 nm ($\sim 10^{-50}$ cm^4s), providing release of approximately 10% of the total caged Ca^{2+} within 50 µs. Issues in utilization of the three cages for two-photon excited calcium release within cells are discussed.

Supported by DRBIO and grants from NSF (BIR8800278) and NIH (RR04224 and R07719). J. S. is an NSF Postdoctoral Fellow supported by grant CHE-9403174.

M-Pos335

THREE-PHOTON INDUCED FLUORESCENCE OF THE CALCIUM PROBE INDO-1. ((I. Gryczynski, H. Szmacinski and J.R. Lakowicz)) University of Maryland, Center for Fluorescence Spectroscopy, School of Medicine, Dept. Biological Chemistry, Baltimore, MD 21201. (Spon. by J.R. Lakowicz).

We report the calcium-dependent emission spectral properties of the calcium probe Indo-1 using three-photon excitation. We found that Indo-1 could be readily excited with the femtosecond pulses from a mode-locked Ti-Sapphire lasers at 885 nm. This wavelength is too long for two-photon excitation, which is expected to occur for wavelengths no longer than twice the longest single photon absorption wavlength. For excitation at 885 nm the emission intensity was found to depend on the cube of the laser power, as expected for simultaneous interaction with three photons. At wavelengths below 840 nm the emission intensity depends on the square of the laser power, indicating two-photon excitation at shorter wavelengths.

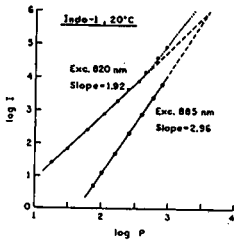

The intensity decays of Indo-1 were found to be dependent on Ca^{2+}, and essentially identical for one- and three-photon excitation. The emission anisotropy of Indo-1 was higher for three-photon than for one-photon excitation, consistent with $\cos^8\theta$ photoselection, as compared with $\cos^2\theta$ for one-photon excitation. The high anisotropy is in agreement with a three-photon process. Calcium-dependent emission spectra were observed for Indo-1 with-three photon excitation, demonstrating that three-photon excitation of Indo-1 can be used for calcium imaging.

M-Pos336

TIME-RESOLVED TERBIUM LUMINESCENCE STUDIES OF THE CALCIUM RECEPTOR BINDING OF CISPLATIN IN HUMAN OVARIAN CANCER CELLS. ((R.G. Canada and D.N. Paltoo)) Howard Univ. Col. Medicine, Dept. Physiology and Biophysics, Washington, D.C. 20059.

Terbium (Tb) has been shown to increase the cellular accumulation of cisplatin (DDP) in DDP-resistant human ovarian cancer cells (C13*). The objective of this investigation was to determine whether DDP interacts with a specific calcium receptor in the plasma membrane of these cells, i.e., the Tb binding protein. The intensity and lifetime of the Tb/C13* complex were quenched in the presence of DDP. According to Stern-Volmer analysis, the quenching of Tb/C13* luminescence was mainly via a static process whereas the quenching of free Tb was dominated by a collisional mechanism. The quenching of Tb/C13* luminescence by DDP was due to a direct electron-exchange interaction and an indirect dipole-dipole resonant energy transfer mechanism. Our results suggest that the Tb binding sites of C13* cells are similar to the Tb binding protein found in other tumorigenic cells. Further, preliminary studies have shown that Tb can increase the cytotoxicity of DDP in these cells. The IC50 value for DDP in C13* cells was reduced in the presence of Tb. A positive correlation was found between the receptor binding of Tb and the cellular accumulation of DDP. It is suggested that the Tb binding protein is involved in the transport of DDP.

M-Pos337

LANTHANIDE LUMINESCENCE STUDIES OF THE METAL BINDING SITES OF S100β PROTEIN. ((D. Chaudhuri†, W. D. Horrocks, Jr.†, J. C. Amburgey‡, and D. J. Weber‡)) †Dept. of Chemistry, Pennsylvania State University, University Park, PA 16802 and ‡Dept. of Biological Chemistry, University of Maryland School of Medicine, 108 N. Greene Street, Baltimore, MD 21201

S100β is a member of a group of low molecular weight acidic calcium-binding proteins widely distributed in the vertebrate nervous system. S100β contains two helix-loop-helix calcium binding motifs (Sites I and II). Lanthanide luminescence spectroscopy using Eu^{3+} and Tb^{3+} as spectroscopic probes for Ca^{2+} is used to characterize the Ca^{2+} binding sites of this protein. The excitation spectrum of Eu^{3+}-bound S100β can be curve resolved into two peaks. Furthermore, the existence of two distinct Eu^{3+} binding environments is conclusively established from Eu^{3+}-excited state lifetime measurements that show lifetime components of 208 µs and 445 µs in H_2O solution. The 445 µs-component is assigned to Site II (EF hand) and the 208 µs component is assigned to Site I (pseudo-EF hand). These lifetimes in conjunction with the corresponding lifetimes measured in D_2O solution lead to the finding that there are 5 Eu^{+3}-coordinated water molecules at site I and 2 at site II. Similar experiments have been conducted with Zn-loaded S100β (it has two independent Zn sites) to characterize the influence of Zn binding on the calcium sites. The single Tyr-17 near the N-terminal Ca^{2+} site is being used for Tb^{3+} luminescence sensitization experiments for distance measurements. Additionally, inter-metal ion Forster-type nonradiative energy transfer (Eu^{3+} to Nd^{3+}) experiments are being carried out to determine the distance between the sites. (Supported by NIH grants GM-23599 to WDH and R29GM5207101 to DJW.)

M-Pos338

SOLVATOCHROMIC/THERMOCHROMIC STUDIES OF THE FLUOROPHORES PRODAN AND METHYLENE VIOLET (BERNTHSEN) ((Jenny Margherio, Lynn Thompson and Brian Wesley Williams)) Chem. Dept., Bucknell University,Lewisburg, PA 17837

A characteristic property of several neutral, solvent-sensitive fluorescent probes (e.g. Nile Red, Prodan) is their ability to support charge-transfer in the excited electronic state. To better understand the behavior and response of such probes, with an eye towards the eventual synthesis of long-wavelength probes, we have undertaken investigation of the solvatochromic and thermochromic properties of several different compounds. In the following, we report on the solvatochromic and thermochromic response of Prodan and the compound Methylene Violet (Bernthsen) (see below). The thermochromic data obtained also permits comparison of two alternative descriptions of thermal "blue shifts" in emission. (Supported by ACS-PRF #27003-B4 and Bucknell University).

METHYLENE VIOLET (BERNTHSEN)

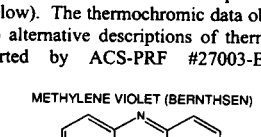

M-Pos339

BINDING OF TRIARYLMETHANE DYES TO PROTEINS: ENHANCED FLUORESCENCE QUANTUM YIELD AND PHOTOREACTIVITY. ((Gary B. Anderson, Monika V. de Arruda,* and Guilherme L. Indig)) School of Pharmacy, University of Wisconsin, Madison, WI 53706, *McArdle Laboratory for Cancer Research, University of Wisconsin, Madison, WI 53706.

We are currently investigating the association of triarylmethane dyes (TAM) with bovine serum albumin (BSA) and low-density lipoproteins (LDL). Crystal violet (CV), ethyl violet (EV), and malachite green (MG) show poor photoreactivity in low viscosity madia due to fast relaxation processes that occur via rotational motions of their phenyl rings. Accordingly, in aqueous solutions the fluorescence lifetime of TAM dyes are very short, typically in the picosecond range (fluorescence quantum yields ~ 10^{-4}). However, in restricted reaction spaces, such as those typically experienced by a ligand bound to a biopolymer matrix, rotational relaxation processes are severely hindered, and the loss of rotational degrees of freedom may lead to substantial increases in fluorescence quantum yield and/or photoreactivity. Indeed, a 50-100 fold increase in the fluorescence quantum yield of CV, EV, and MG was observed upon binding to BSA or LDL (CV). The binding had only minor effects on the respective absorption spectra. In addition, upon laser excitation at 532 nm, the bleaching of the corresponding BSA-dye complexes leads to the appearance of spectral signatures that are characteristic of the formation of leuco derivatives of the triarylmethane dyes as major reaction photoproducts. These observations indicate that an electron or hydrogen atom transfer from the protein to the dye moiety is the first step of the photobleaching process. Since the availability of dissolved molecular oxygen was not a limiting factor for the main phototransformations to occur, the above TAM dyes can be seen as potential phototherapeutic agents for use in hypoxic areas of tumors. Supported by the The Burroughs Wellcome Fund and American Foundation for Pharmaceutical Education (AACP Grant Program for New Investigators).

M-Pos340

CALIBRATION OF FIBER OPTIC BIOSENSOR RESPONSE USING SIMULTANEOUS EVANESCENT WAVE EXCITATION OF CYANINE LABELED CAPTURE ANTIBODIES AND ANTIGENS. ((R.M. Wadkins, J.P. Golden and F.S. Ligler)) Center for Bio/Molecular Science & Engineering, Naval Research Laboratory, Code 6900, Washington, DC 20375 (Spon. by G.P. Anderson)

Fiber optic biosensors have proven their ability to rapidly detect antigens in a variety of environmental and clinical samples. These biosensors are based on the technique of covalently linking antibodies to the core of an optical fiber and detecting antigen binding via measurement of fluorescence induced in the evanescent wave. One problem associated with these biosensors is the fiber-to-fiber variability in measured signal. We have addressed this problem by labeling a portion of the immobilized capture antibody with the fluorescent cyanine derivative Cy5.5 (emission λ_{max} = 696 nm). The antigen was then labeled with fluorescent Cy5 (emission λ_{max} = 668 nm). Both fluorophores were excited by 635 nm light, and their emission was collected using both a fiber optic spectrometer and a biosensor optimized to collect fluorescence at two wavelengths. The fluorescence from the Cy5.5 labeled capture antibody served as a calibration signal for each fiber, and corrected for differences in optics, fiber defects, and varying amounts of capture antibody present on the fiber. Our data show that ratioing the signal measured from Cy5-labeled antigen binding to the Cy5.5 signal provides a standardization process for greatly reducing signal variance between individual fibers.

M-Pos341

MASS TRANSPORT AND KINETIC ANALYSIS OF LIGAND-RECEPTOR INTERACTIONS AS DETECTED WITH AN EVANESCENT WAVE BIOSENSOR. ((P. Schuck)), LBP, NIDDK, NIH, Bethesda, MD 20892. (Spon. by H. A. Saroff)

Evanescent wave (surface plasmon resonance) biosensors have become increasingly popular for determining the affinity and kinetics of ligand binding to a receptor, which is usually covalently bound to a polymer matrix attached to the sensor surface. However, most of the published experimental binding progress curves do not follow the expected ideal pseudo-first order kinetics. To investigate the role of mass transport in this instrument, computer simulations were performed for the combined ligand transport in the buffer flow, partitioning into the polymer matrix and diffusion/pseudo-first-order-reaction within the matrix, as measured with a sensitivity that exponentially decays with increasing distance from the biosensor surface. The influence of diffusion coefficient, partition coeffient, spatial distribution of the immobilized receptor, buffer flow, sensitivity distribution, and thickness of the matrix were investigated. It was found that for fast reactions spatial inhomogeneities of the bound ligand develop and that parameters other than the chemical reaction rate constants dominate the measured binding progress curves. Several types of artifacts resemble those commonly found in published experimental data, e.g. apparently multiphasic binding. At low ligand concentrations apparently ideal binding progress curves are observed which can lead to estimates of rate constants orders of magnitudes lower than the intrinsic chemical rate constants.
A method for the analysis of mass transport-influenced biosensor data is introduced that is based upon a two compartment model, making use only of the approach to binding equilibrium (therefore independent of the details of the transport). In the limit of slow reactions, this method converges to the ideal pseudo-first order expressions, whereas in the limit of infinite fast reactions only the equilibrium constant and the transport rate can be determined. This method can extract reliable kinetic information from data influenced by transport, potentially extending the dynamic range of the instruments by 1-2 orders of magnitude, and can prevent certain transport-related misinterpretations of the data.

M-Pos342

FLUORESCENCE LIFETIME MEASUREMENTS AND SENSING IN HIGHLY SCATTERING MEDIA ((H. Szmacinski and J.R. Lakowicz)) University of Maryland, Center for Fluorescence Spectroscopy, School of Medicine, Dept. Biological Chemistry, Baltimore, MD 21201. (Spon. by M.L. Johnson).

We describe frequency-domain lifetime measurements in an intralipid suspension, and two a reliable techniques which allow phase-modulation lifetime measurements of fluorophores dispersed within or localized within intralipid. Lifetimes can be determined using an intensity decay law which accounts for the time delay, decay time, and pulse broadening effects due to multiple light scattering events occuring in the intralipid suspension. Alternatively, the phase and modulation measurements can be performed relative to a reference fluorophore of known lifetime. This approach provided reliable lifetime data for fluorophore with double-exponential intensity decay and localized up to 4 mm under the surface of an intralipid suspension. Using either method we were able to determine the pH or $[Ca^{2+}]$ from phase and modulation of carboxy SNARF-6 or Calcium Crimson. These results suggest the possibility of minimally noninvasive sensing through skin using probes immobilized on appropriate biocompatible sensor.

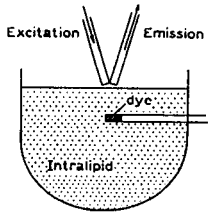

M-Pos343

FAR-RED FLUORESCENCE-BASED HIGH SPECIFICITY TUMOR IMAGING *IN VIVO* ((G. Fisher, B. Ballou, M. Srivastava* and D. L. Farkas)) Center for Light Microscope Imaging and Biotechnology, Carnegie Mellon University, Pittsburgh, PA and *NIDDK, NIH, Bethesda, MD.

Since light scattering decreases sharply with wavelength, new cyanine dyes fluorescing far into the red open new possibilities for tumor detection *in vivo*. To explore this potential we targeted tumors in nude mice using monoclonal antibodies coupled to Cy3 (ex550/em565), Cy5 (650/667), Cy5.5 (674/694), or Cy7 (750/777) cyanines and imaged using a cooled CCD camera. Tumor targeting was studied using a genetically engineered mouse renal cell carcinoma that expresses nucleolin on its cell surfaces; by expressing human nucleolin in the cells and using a human-specific monoclonal antibody, we could avoid any chance of cross-reactivity with other mouse nuclear proteins. We showed that human nucleolin was expressed on the surface of transfected cells. A human melanoma and a mouse teratocarcinoma were also studied, each using an appropriate monoclonal antibody. Particular attention was paid to the following: spatial resolution, sizes and depths of imaged tumors, overall brightness, and the clearing capacity of the liver and kidney with respect to dye/antibody ratios. Specificity was confirmed using isotype-matched monoclonal antibodies conjugated to different cyanine dyes than those used for the tumor-targeting antibodies, co-injected with the targeting antibodies, and imaged in appropriate spectral windows. Confirmation of specific probe fluorescence in the animal was obtained using an imaging spectrometer. Cy5, Cy5.5 and Cy7 were all effective in imaging tumors; Cy3, emitting in the orange, was not. The longer wavelength dyes were more effective for deep tumors. We conclude that fluorescence is as practical for tumor location as radioactivity, but allows higher resolution.

M-Pos344

PHOTOACOUSTIC ANALYSIS OF FLUORESCENT PROTEINS: IMPACT OF NONTHERMAL VOLUMETRIC SIGNALS ON FLUORESCENT QUANTUM YIELD MEASUREMENTS.
((E. Kurian, F.G. Prendergast, and J.R. Small)) Mayo Clinic and Foundation, Rochester, MN 55905; Eastern Washington University, Cheney, WA 99004 (kurian@mayo.edu, jsmall@ewu.edu).

A series of proteins containing either an intrinsic or extrinsic fluorophore has been examined using the time-resolved, pulsed-laser volumetric photoacoustic technique. The proteins studied include the Green Fluorescent Protein (GFP); intestinal fatty acid binding protein (I-FABP), and adipocyte lipid binding protein (ALBP), each labeled noncovalently with 1,8-ANS, and covalently with acrylodan; and acrylodan-labeled I-FABP and ALBP with added oleic acid. Of this group of proteins, only the ALBP labeled with 1,8-ANS showed significant nonthermal volume changes at the β=0 temperature (~3.8 °C) for the buffer (10 mM Tris-HCl, pH 7.5). The nonthermal volume changes for this fluorescent protein involved a rapid (≤1 ns), large contraction, followed by an equal-but-opposite expansion at about 35 ns following photoexcitation with 366.6 nm light. Photoacoustic data from 7 to 35 °C were consistent with the rapid contraction/expansion nonthermal processes occurring in addition to heat release. For all the proteins except for acrylodan-labeled I-FABP, the fluorescent quantum yield calculated assuming simple energy conservation was anomalously high; i.e., the apparent heat signals were lower than those predicted from independent fluorescence measurements. The data are discussed in terms of possible ultrasonic absorption occurring in solutions of proteins with buried fluorescent chromophores.

Supported by GM-34847 (FGP) and DMI-9362206 (JRS).

M-Pos345

REVERSIBLE PHOTOBLEACHING OF FLUORESCEIN CONJUGATES IN AIR-SATURATED VISCOUS SOLUTIONS: SINGLET AND TRIPLET STATE QUENCHING BY TRYPTOPHAN. ((N. Periasamy, S. Bicknese and A.S. Verkman)) Cardiovascular Research Institute, U.C.S.F, CA 94143-0521.

Fluorescence recovery after photobleaching (FRAP) measurements on air-saturated aqueous solutions of fluorescein made viscous with glycerol or sucrose revealed a rapid component of fluorescence recovery with exponential time constants of 30-120 μs at viscosities of 15-300 cP. The rapid recovery process was not related to fluorophore translational diffusion, and was insensitive to fluorophore concentration and the additive used to increase solution viscosity. At constant viscosity, the rate of reversible photobleaching recovery increased 2.5-fold in an O_2 vs. N_2 saturated solution. The relative efficiency of reversible-to-irreversible photobleaching decreased with increasing photobleaching time and/or beam intensity. Reversible photobleaching was also detected for conjugates of fluorescein with dextrans and proteins in viscous media. In screening triplet state quenchers which might influence the reversible recovery, it was found that tryptophan enhanced the rate of reversible photobleaching recovery (2-fold increase at 8 mM) and quenched the fluorescein singlet state (Stern-Volmer constant, 12 M^{-1}). Analysis of fluorescein lifetimes and photobleaching parameters for a series of fluorescein-labeled proteins with different numbers of tryptophans were also carried. The results provide evidence for an oxygen-dependent, reversible photobleaching mechanism for the fluorescein chromophore involving triplet state relaxation. The identification of reversible fluorescein photobleaching has important implications for FRAP measurements of rapid solute diffusion in biological systems.

M-Pos346

DIFUSSIONAL-TYPE MOTIONS DISTORT PHOSPHORESCENCE SPECTRA. **(W.C. Galley and J. Dracopoulos) Department of Chemistry, McGill University, Montreal , Quebec, Canada.**

It has been proposed that vibrational amplitudes become compressed when a chromophore jumps to a neighbouring site in a "diffusional-type step". This enhances the F-C factors involved in radiationless decay producing a dependence of excited triplet-state lifetimes on local viscosity. Observations of a reduction in phosphorescence decay times for: a) globular proteins in solution subjected to fluctuating perturbations under hydrodynamic shear, and b) chromophores in rigid media under high pressure, are consistent with this picture. The steric restrictions encountered in the "jump process" are anticipated to particulary influence the high-amplitude anharmonic motions involved in the non-radiative decay process, but perturbations to the amplitude of lower quantum number ground electronic-state vibrations are also expected. The resulting influence on the latter state is predicted to manifest itself in the distribution of vibronic intensities observed in emission spectra of chromopores subject to compression. Phosphorescence spectra of chromopores whose lifetimes have been significantly reduced either by diffusion in solution or in rigid media under high pressure, provide support for the model.

M-Pos347

TIME-RESOLVED PHOSPHORESCENCE ANISOTROPY OF ERYTHROSIN-EGF IN THE PRESENCE OF MEMBRANES CONTAINING THE EGF RECEPTOR: IS ERYTHROSIN-EGF A GOOD REPORTER OF RECEPTOR DYNAMICS? ((Richard A. Stein, Albert H. Beth, Cheryl A. Guyer, and James V. Staros)) Dept. of Molecular Biology and Dept. of Molecular Physiology and Biophysics, Vanderbilt University, Nashville, TN 37235.

The rotational dynamics of the EGF receptor in membrane preparations has been previously investigated using time-resolved phosphorescence anisotropy (TPA) (Zidovetzki *et al.*, 1986, 1991) and ST-EPR (Rousseau *et al.*, 1993) without agreement in the values of the rotational correlation time for receptor-bound EGF. We have reinvestigated the TPA measurements of erythrosin-EGF (Er-EGF) bound to the EGF receptor in A431 membrane vesicles. Er-EG, prepared from recombinant H22Y-mEGF, was equilibrated with the receptor in vesicles, which were then washed to remove free Er-EGF. At high [Er-EGF] a rising anisotropy was observed, comparable to previously published TPA measurements, indicative of microsecond rotational motion; however, the anisotropy for low [Er-EGF] was flat, indicating that there was no microsecond rotational motion. When samples were not washed after incubation with Er-EGF, the TPA for low [Er-EGF] was also found to be flat; however, a rising anisotropy was observed for high [Er-EGF], but the entire anisotropy decay was shifted to a lower value, reflecting the presence of free Er-EGF. To assess the effect of the free Er-EGF on unwashed samples, the TPA of Er-EGF in the absence of vesicles was measured and found to be flat and equal to zero, as expected for free isotropically tumbling EGF. Further, EGF receptors that were preblocked with unlabeled EGF prior to incubation with Er-EGF had a positive, non-zero anisotropy value indicating that the Er-EGF did not behave like free Er-EGF. Though Er-EGF binds preferentially to the EGF receptor, non-specific binding of the Er-EGF to the vesicles complicates the interpretation of the phosphorescence anisotropy decays. Taking this non-specific binding into account should allow for a less ambiguous analysis of the rotational dynamics of the Er-EGF/EGF receptor complex. (Supported by NIH grants: P01 CA43720, T32 CA09582)

M-Pos348

HIGH RESOLUTION OPTICAL STUDIES OF HEME PROTEINS. ((K. S. Reddy, P. J. Angiolillo, W. W. Wright and J. M. Vanderkooi)) Biochem. & Biophys., School of Medicine, Univ. of Penn. Philadelphia PA 19104

Optical spectra of chromophoric protein prosthetic groups contain unique information about protein motions, relaxation processes, and also about electric fields and configurational interactions. We obtained absorption and fluorescence spectra of myoglobin and cytochrome-c(cyt-c) and their Zn derivatives in the temperature range of 10K to 310K by high resolution interferometry. Zn porphyrins were used because, unlike iron porphyrins, they have long lifetimes and narrow intrinsic linewidths, and their spectra are sensitive to the surrounding protein. Fig 1. shows the absorption spectrum of Zncyt-c. Its spectrum changes dramatically from essentially two bands at 270K to fourteen bands at 10K. The origin is split into two transitions separated by ~110 cm^{-1}. This separation is invarient with temperature, suggesting that the two configurational forms remain distinct, but that at higher temperature the line width is broadened by phonons. Details of the resolved spectra were dependent upon the pocket structure. In contrast to Zn Cyt c, no vibrational structure of the optical transitions were observed for Znporphyrin in polymer films. We interpret the spectra as an indication that the protein holds the porphyrin in various distinct configurations. (Supported by PO1 GM48140).

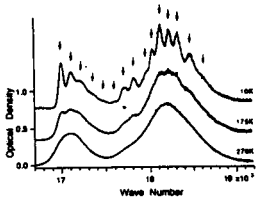

M-Pos349

DISTANCE MEASUREMENTS OF A FLUORESCENT INHIBITOR AS IT TRAVELS UP THE CHANNEL OF CYCLOXYGENASE: A FLUORESCENCE ENERGY-TRANSFER STUDY TO THE HEME ((C. A. Lanzo[1], L. J. Marnett[1], J. M. Beechem[2])) [1]A.B. Hancock Jr. Lab., Center. in Molecular Toxicology, Dept. of Biochem., [2]Dept. of Mol. Phys. and Biophysics, Vanderbilt University, Nashville, TN 37232.

Cycloxygenase (COX) is a 70kDa bifunctional heme containing enzyme with a unique ½ integral membrane insertion motif and an extended ligand access channel. This enzyme is the site of action of COX inhibitors such as aspirin and ibuprofen. We have used fluorescence spectroscopy to study the interaction of a COX-1 selective inhibitor, S8076, with enzyme purified from ovine seminal vesicles. The fluorescence emission spectrum of S8076 overlaps the large heme absorption in COX-1 with an R_0 of approximately 26Å. Steady-state and time-resolved fluorescence titrations of S8076 with COX-1 produces a dramatic quench in the fluorescence, with transfer efficiencies (all dynamic) approaching 90%. Time-resolved heme titrations into apo COX-1 (with bound S8076) firmly establish that the heme prosthetic group is responsible for the observed quenching. Analysis (which is not yet complete) indicate that the distance of the bound inhibitor to the heme in the channel of COX is ≈18Å . The kinetics of S8076 moving up the COX-1 channel are being examined using stopped-flow fluorescence techniques. These data should allow us to construct a millisecond "distance-movie" of S8076 traveling up the ligand channel of COX. (Supported by NIH CA47479. CAL suported by the NIEHS TG ES07028.)

MODEL PROTEINS

M-Pos350

PROBING PROTEIN HYDRATION AND CONFORMATIONAL STATES IN SOLUTION ((C. Reid, N. Fuller, R.P.Rand)) Biological Sciences, Brock University, St. Catharines, Ontario, Canada

We have measured, from its sensitivity to water activity, the decrease in number of water molecules, Δn_w, associated with the reaction of glucose binding to hexokinase. Using polyethyleneglycol (PEG) to control water activity, Δn_w increases from 50 to a maximum of 250 with increasing PEG MW from 300 to 1500: i.e. over this range, larger PEG's are excluded from larger aqueous compartments around the protein. For PEG's of 8000>MW> 1000, Δn_w falls from 250 to 25 with increasing osmotic pressure or decreasing water activity. Remarkably, the osmotic work to make this change is of the order of 1 kT per hexokinase. We conclude that under thermal fluctuations, unbound hexokinase in solution explores all conformations that include this full size range of PEG-excluding aqueous compartments.

M-Pos351

LIGAND BINDING STUDIES OF HEMES IN SYNTHETIC FOUR HELIX BUNDLE: K. S. Reddy, B. R. Gibney, Y. Isogai, F. Rabanal, C. C. Moser and P. L. Dutton, Johnson Research Foundation, Department of Biochemistry and Biophysics; University of Pennsylvania, Philadelphia PA 19104.

The multi functional heme protein chemistry from oxygen transport to oxygen reduction is defined by the heme and its surrounding amino acids. Recent[1] work on water soluble 62 residue synthetic heme protein forms the basis for the designing of functional heme proteins with minimal peptide architecture. The maquettes studies described here focus on the chemical and spectroscopic investigations on similar α-helical peptide with four hemes with a glycine loop instead of cysteine bridges. The four helix bundle heme peptide with His-Fe-His as basic structural unit has been found to be stable and undergoes ligand exchange reactions and peroxide activation reactions with organic substrates. In reduced state it binds with CO and NO. This external ligand binding process has been observed to be kinetically competitive in the ferric state where as facile in ferrous state. The infrared spectra of with hemoglobin and myoglobin is shown in fig1. The νC-O is blue shifted and the half band is broader than that of heme proteins suggesting multiple CO conformations. The Heme-CO of this peptide is reversibly photolabile similar to heme proteins. The detail study of CO, NO binding and reactions of peroxide activation in presence of substrate will be presented.

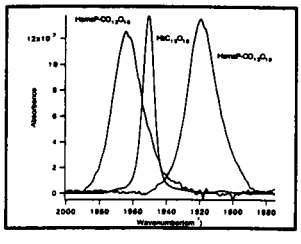

1. D. E. Robertson, R. S. Farid, C. C. Moser, J. L. Urbauer, S. E. Mulholland, R. Pidikit, J. D. Lear, A. J. Wand, W. F. DeGrado and P. L. Dutton; Nature., 368, 425-432 (1994)

M-Pos352

A HEMEPROTEIN MODEL FOR THE SUBSTRATE-BOUND FIVE-COORDINATE FERRIC CYTOCHROME P-450CAM ACTIVE SITE

((Mark P. Roach[1], Stefan Franzen[2], Phillip S. H. Pang[3], Steven G. Boxer[3], William H. Woodruff[2], John H. Dawson[1]))
1. Dept. of Chemistry and Biochemistry, University of South Carolina, Columbia, SC 29208
2. Biosciences and Biotechnology Group, CST-4 MS J586, Los Alamos Natl. Laboratory Los Alamos, NM 87545 3. Dept. of Chemistry, Stanford University, Stanford, CA 94305

A model for the ferric five-coordinate camphor-bound cytochrome P-450 active site has been created using the H93G mutant of sperm whale myoglobin (Mb) in which the proximal histidine has been replaced by glycine [1], leaving a cavity that can be filled by exogenous ligands to iron [2]. When the ligand ethanethiol (EtSH) is dialyzed into the H93G Mb, it ligates to the heme iron as a thiolate resulting in a high spin ferric complex. Magnetic circular dichroism (MCD) spectroscopy (see Figure) demonstrates the similarity of the iron coordination in the model and camphor-bound P-450cam. The recently reported H93C/H64V double mutant of horse heart Mb exhibits a similar ferric MCD spectrum [3]. The model does not extend to ferrous P-450. We present evidence that, upon reduction, the thiolate ligand is replaced by the distal histidine. Preliminary data indicate that the oxoferryl complex, Fe(IV)=O, can be observed by adding H_2O_2 to ferric H93G(EtSH), although it is not stable for more than a few minutes at 4°C. The convenience of proximal ligand exchange will enable fine-tuning of the electronic effects leading to observation of increasingly reactive oxoferryl species approaching the postulated high-valent intermediate involved in P-450 catalysis.

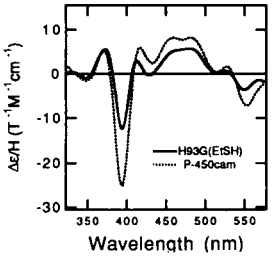

1. Barrick, D. Biochem. (1994) 33: 6546
2. DePillis et al. JACS (1994) 116: 6981
3. Hildebrand et al. Biochem. (1995) 34: 11598

M-Pos353

ANALYSIS OF ATOMIC PACKING IN PROTEIN STRUCTURES

((B. Mao)) Upjohn Research Labs, Kalamazoo, MI 49001.

The packing of atoms in the polypeptide backbone and amino acid residue side-chains of a protein molecule into the three-dimensional molecular structure is analyzed for protein structures deposited in the Brookhaven Protein DataBank. Although structural domains of these proteins are not entirely smoothly and regularly shaped objects, they can be described as combination of a central core and a peripheral shell; such a characterization could be useful for further structural analysis of protein conformation. Characteristics of atomic packing in these structural regions, such as atomic density and shape deviation from ideality will be presented.

M-Pos354

PRESENCE OF A CATALYTIC BASE WITHIN NBF1 OF CFTR IS PREDICTED BY COMPUTER MODELING OF 3-DIMENSIONAL STRUCTURES OF THE NUCLEOTIDE BINDING DOMAINS. (M. A. Bianchet, Y. H. Ko, L. M. Amzel and P. L. Pedersen) Departments of Biophysics and Chemistry, Johns Hopkins University School of Medicine, Baltimore, MD 21205. (Sponsored by P. L. Pedersen)

Many of the mutations that cause cystic (CF) reside in or near the two nucleotide binding domains (NBF1 and NBF2) of CFTR. The most severe mutation (ΔF508), responsible for 70% or more of all cases of CF, lies within NBF1. In order to obtain insight into the structure and functional importance of this and deletions of other amino acids which cause CF, 3-D models of the two nucleotide binding domains would be invaluable. In recent work using the "homology modeling" approach, we have obtained 3-D models for both NBFs of CFTR. This model clearly indicate where the Walker's A and B motifs, and the "C" consensus signature for ABC transporters are located, and where the major disease causing mutations reside. These models also indicate NBF1 may be an ATPase because the catalytic base found in the β subunit of ATP synthase is conserved and located near the terminal phosphate of ATP. (E504 in NBF1) Significantly, in wild type CFTR the F508 is located in an α helical region within the bonding distance of ATP. When the two nucleotide binding domains of CFTR are positioned as in the α and β subunits of ATP synthase, the phenylalanine in the second nucleotide binding domain, comparable to F508 in NBF1, is seen to reside at the domain interface.

M-Pos355

FT-RAMAN SPECTROSCOPY OF HUMAN HAIR

((C. Pande)) *Clairol Inc. Stamford, CT. 06922.*

Human hair is primarily composed of keratin proteins. There are at least two distinct structural components of hair. The shingle-like cuticle scales form the protective exterior, and determine the surface properties of a fiber. Each cuticle cell is ~ 0.5 μ thick and 45 μ long. Typically the cuticle layer is 8 scales thick. The fiber interior is composed of cortical cells; each cell is ~ 8 μ thick and 100 μ long. The cortical cells, packed with α-helical protein in a fibrillar arrangement, provide the fiber its tensile strength.

We are developing *in situ* spectroscopic probes to fingerprint functional groups in hair to better characterize hair damage. This, we feel, is the essential first step in reducing damage. We have previously shown the potential of FT-Raman technique in this regard[1,2]. Using Raman microprobe we have now obtained the Raman spectra from the cortex and the cuticles of unpigmented human hair. Differences in the observed spectra are being analyzed to relate them to the differences in the composition of the cortical cells and the cuticle cells.

[1)] Pande, C. *Biophys J.* 64, 2, A276, 1993; [2)] Pande, C. *J. Soc. Cosmet. Chem.* 1994; 45, 257-268.

ENZYMES

M-Pos356

HIV-1 REVERSE TRANSCRIPTASE RESISTANCE TO NON-NUCLEOSIDE INHIBITORS. ((R. A. Spence and K. A. Johnson)) Pennsylvania State University, University Park, PA, 16802.

Rapid Chemical quench techniques were used to determine the parameters governing the polymerization mechanism of the mutant reverse transcriptase, Y181C. The alteration of tyrosine to cysteine at position 181 is one of the most common point mutations found after prolonged use of the non-nucleoside inhibitor, Nevirapine. The pathway for single nucleotide incorporation catalyzed by Y181C is similar to that determined for the wild-type RT (Spence, *et al.*, 1995, *Science* 267, 988), where a rate-limiting conformational change precedes fast chemistry and is followed by slow steady-state release of the primer/template. The Y181C mutant enzyme binds a 25/45-mer duplex DNA tightly; however, the mutation weakens the nucleotide affinity three-fold relative to the wild-type complex. We also determined the parameters governing the mechanism of non-nucleoside inhibitor resistance with Y181C. The K_d value of Nevirapine with the mutant E• DNA complex increased ~500-fold. The decreased affinity of Nevirapine for the mutant enzyme is a consequence of a faster inhibitor dissociation rate from the enzyme complex. The E• DNA complex of Y181C may be saturated with Nevirapine, and the I•E• DNA complex is capable of a maximum incorporation rate of 0.1 s^{-1}. (Supported by NIH grant GM 44613).

M-Pos357

VICINAL SULFHYDRYL GROUPS INVOLVED IN NEUTROPHIL NADPH OXIDASE ACTIVATION ((Jian-Rong Li and Richard J. Guillory)) Dept. of Biochemistry & Biophysics, Univ. of Hawaii, Honolulu, HI 96822

Phenylarsine oxide (PAO), a vicinal SH-specific reagent, inhibits phorbol 12-myristate 13-acetate activated O_2^- generation of intact bovine neutrophils. PAO also inhibits the O_2^- generation of a cell-free system in which signal transduction is bypassed and in a partially purified cytochrome b558 preparation. Our experimental results indicate that PAO reacts directly with a component of the NADPH oxidase rather than with the signaling system. The fully assembled and activated oxidase is not inhibited by PAO. This suggests that the SH-modifying reagent does not affect enzymatic turnover but rather the enzyme's assembly and/or activation. The essential group modified by PAO is located on the membrane since preincubation of the membrane with PAO completely abolished its ability to generate O_2^-. Inhibition by PAO is readily reversed by the vicinal dithiol 2,3-dimercaptopropanol but not by cysteine, 2-mercaptoethanol or 1,4-dithiothreitol. We have attempted to identify the PAO reacting vicinal SH group involved in NADPH oxidase activation. The labeling of PAO complexed vicinal SH groups reveals a broad radioactive band at 80-100KDa on SDS-PAGE, consistent with the labeling of the diffuse band of cytochrome b558. Further support for cytochrome b558 labeling by PAO comes from the fact that the radioactive band shifts to a lower molecular weight region following deglycosylation. We speculate that cytochrome b558 is a site of PAO reaction and that this site may be involved in the activation of the NADPH oxidase. The question as to whether the vicinal SH group reactivity is a result of three dimensional proximity of SH groups or a characteristic of the primary sequence is being examined.

M-Pos358

Evolution of the Na^+ Binding Loop of Thrombin.

Quoc D. Dang and Enrico Di Cera. Dept of Biochem & Mol Biophys, Washington Univ Med School, St. Louis, MO 63110.

The Na^+ binding loop of thrombin contains the sequence (residues 220-226) CDRDGKYG, which is highly conserved in 11 species and is similar to that found in other blood clotting proteases (e.g., factor Xa). The carbonyl O atoms of R221a and K224 participate in the coordination shell of the Na^+ ion. Structural comparison with homologous loops in trypsin and chymotrypsin reveals a molecular strategy through which the Na^+ binding site might have been introduced in blood clotting proteases. The sequence in chymotrypsin (CS-TSSPG) lacks R221a and makes the loop too short for proper coordination of the Na^+ ion. Trypsin (CAQKNKPG) has a loop of proper length, but the presence of P225 orients the carbonyl O atom of K224 in a way that is incompatible with Na^+ binding. The Na^+ binding site of thrombin might have evolved from chymotrypsin through the pathway: chymotrypsin→trypsin→thrombin. Factor Xa (CARKGKYG) might have evolved from thrombin itself. This factor has a loop of proper length and conformation, but has lower Na^+ affinity compared to thrombin due to the replacements D221A and D222K that affect the negative electrostatic potential at the Na^+ site. These hypotheses are supported by site-directed mutagenesis studies of the Na^+ binding loop of thrombin.

M-Pos359

PERTURBATION OF THE YEAST 3-PHOSPHOGLYCERATE KINASE (PGK) PATHWAY BY CRYOSOLVENTS.

((A. Geerlof, F. Travers and T. Barman)) INSERM U128, CNRS, BP 5051, 34033 Montpellier Cedex, France. (Spon. by D. Mornet)

PGK catalyzes the reversible transfer of phosphate between ATP and 3-phosphoglycerate (PG): ATP + PG $\rightleftharpoons$ ADP + 1,3-bis-P-glycerate (bPG). Despite extensive structural studies, there is little information on the kinetics of PGK. There are several reasons for this: PGK has a high turnover, its pathway is complex (two substrates, two products), the reaction is reversible and its affinities for ATP and PG are poor. In previous work [Schmidt *et al.* (1995) *Biochemistry 34*, 824-832] we showed that intermediates containing bPG accumulate on the PGK pathway but their kinetics of formation were too rapid to be measured. These kinetics were reduced by including 40% ethylene glycol in the buffer but because of the low concentration of the bPG intermediates they remained difficult to exploit. Here we searched for a better cryosolvent and after testing several (DMSO, methanol, ammonium acetate) we choose 30% methanol. This cryosolvent has the important effect of increasing significantly the affinities of PGK for its substrates and of decreasing the kinetics of formation of bPG intermediates to measurable levels. Further, it increased the equilibrium constant for the central ternary complexes 20 times *i.e.* towards Enzyme•bPG•ADP. As a consequence, in methanol the concentration of enzyme-bound bPG in the steady state is about 65% of the total enzyme. These favourable conditions allowed for a wide range of transient kinetic experiments, from which we obtained rate constants for several of the steps on the PGK pathway.

A.G. was supported by an INSERM fellowship.

M-Pos360

ACTIVE-SITE MUTATIONS OF EXOTOXIN A.

((B.K. Beattie & A.R. Merrill)), Guelph-Waterloo Centre for Graduate Work in Chemistry, Dept. of Chem. and Biochem., Univ. of Guelph, Guelph, ON, Canada, N1G 2W1.

The extracellular 66-kDa protein, exotoxin A (ETA), is the most potent of the many virulence factors produced by the bacterium *Pseudomonas aeruginosa*. Based on the crystal structure of ETA, the protein is proposed to consist of three distinct structural domains. Domain III contains an extended cleft postulated to be the active site of the enzyme. The active site catalyzes the transfer of the ADP-ribose portion of NAD^+ to the eukaryotic protein elongation factor-2 (eEF-2). The transfer inactivates eEF-2, inhibiting protein synthesis, and killing the host cell. From the crystal structure data, computer modeling results, and chemical modification studies, Trp-466 and Trp-558 in domain III were proposed to be important for catalysis. The role of these tryptophans was studied using an enzymatically active, truncated form of the toxin, PE40, that contains domains II and III. The three catalytic domain tryptophans were individually or jointly replaced with phenylalanine by site-directed mutagenesis. The W466F mutation decreased the ADP-ribosyltransferase and NAD-glycohydrolase activities by nearly 100-fold and 3-fold, respectively. The W558F mutation had a less dramatic effect as the activites were both decreased only 2-fold. The enzyme's NAD-affinity was also measured by observing the quenching of intrinsic protein fluorescence which correlated well with the reductions in enzyme activity. There were no major alterations in stability of the mutant proteins as evidenced by proteolytic digestion and circular dichroism. The results indicate Trp-466 is a major determinant of NAD affinity. Also, they implicate this residue as a candidate for modification in the development of inactive forms of the toxin for use in vaccine development. [supported by the Medical Research Council of Canada (A.R.M.)]

M-Pos361

EPR INVESTIGATION OF CARBON MONOXIDE-INHIBITED MO-NITROGENASE.

((L.M.Cameron and B.J.Hales)) Dept. of Chemistry, Louisiana State University, Baton Rouge, LA 70803. (Spon. by B.J.Hales)

Nitrogenase catalyzes the reduction of dinitrogen to ammonia. This reaction, nitrogen fixation, is essential for life on this planet. Reduction of small molecule substrates, including N_2 and C_2H_2, and inhibition by carbon monoxide (CO), occurs at the nitrogenase MoFe protein (one of two component proteins) and involves the protein's two metal clusters. To date, the mechanism of electron transfer is unknown and the binding sites of substrates and inhibitors have not been identified. The first reduction step of enzymatic turnover is readily observed by EPR spectroscopy, while higher reduction states of the enzyme are not as well characterized. Here we report that CO-induced EPR signals (called hi-CO and lo-CO) from Mo-nitrogenase undergoing turnover can serve as spectroscopic probes of turnover states of the MoFe protein. The delay and time-dependent formation of the CO signal during low electron flux suggest that CO binds to and stabilizes a high reduction state of the enzyme. The hi- and lo-CO signals generated during moderate flux are interconvertible and show enhanced stability in ethylene glycol (EG). CO can add to the EG-quenched state, despite the cessation of turnover, provided that the enzyme is initially exposed to CO ("pulse") prior to EG treatment. ENDOR spectra show that one or two CO's can bind to the same metal cluster (1). Pulse-chase studies such as these of a substrate or inhibitor "chase" may yield additional evidence of substrate/inhibitor-metal cluster interactions.

(1) Pollock, R. C., Lee, H-I., Cameron, L. M., DeRose, V. J., Hales, B. J.,Orme-Johnson, W. H., and Hoffman, B.M. *J. Am. Chem. Soc.* **1995**, *117*, 8686-8687.

M-Pos362

LIGAND ACTIVE SITE MOTIONS IN CARBOXYPEPTIDASE A.

((Huiming Zhang and Robert G. Bryant)) Department of Chemistry, University of Virginia, Charlottesville, VA 22901

We have measured deuterium NMR spectra of small labeled aromatic molecules in polycrystalline samples of carboxypeptidase A. The lack of protein rotational averaging of the deuterium nuclear electric quadrupole interaction provides a direct means for characterization of the active site motions in the hydrated crystals. The deuterium NMR lineshape is sensitive to the exchange rate of the ligand between the active site and the dynamically isotropic spaces between protein molecules in the crystal as well as the bound site motions. We report rates and amplitudes of local bound site motions as well as exchange rates for L-phenylalanine, D-phenylalanine, phenyl propionic acid, and phenyl acetic acid.

M-Pos363

DIRECT ENZYMATIC MODIFICATION OF A PEPTIDE SURFACE WITH COVALENTLY IMMOBILIZED α-CHYMOTRYPSIN.

((M. A. Testoff, D. C. Turner, and B. P. Gaber)) Laboratory for Molecular Interfacial Interactions, Code 6930, Naval Research Laboratory, Washington, DC 20375-5348.

We have demonstrated that covalently bound α-chymotrypsin (ACHT) can modify a peptide which has been covalently coupled to a separate solid surface. The fluorescent chymotrypsin substrate suc-ala-ala-phe-AMC (SAAP-AMC; Novabiochem) was coupled to a butyl-amine silane modified fused-silica slide via amide bond formation in the presence of EDC (1-ethyl-3-(3-dimethylaminopropyl) carbodiimide hydrochloride) and sulfo-NHS (Pierce Chemical). When ACHT cleaves the AMC group from SAAP-AMC a spectral shift occurs in the fluorescence providing a standard marker for enzymatic activity. Immobilized SAAP-AMC surfaces were characterized with using water wettability, fluorescence spectroscopy and x-ray photoelectron spectroscopy. Results indicate sub-monolayer coverage of the peptide with a fluorescence intensity signal to noise at peak maximum (325nm ex, 395nm em) of over 10:1. ACHT was immobilized onto butyl-amine silane modified 250 nm solid silica spheres. ACHT coupling to the spheres was carried out using gluteraldehyde and EGS (ethylene glycolbis(succinimidyl-succinate)) followed by a 2X rinse with 0.5% TWEEN 20 in phosphate buffer to remove any physisorbed ACHT. Activity of ACHT-beads was measured using a fluorescent kinetics experiment using SAAP-AMC in solution. It was verified that no free ACHT in solution was contributing to the measured activity. Treatment of the SAAP-AMC fused silica surfaces with ACHT-beads showed a reduction of the fluorescence to background in less than 24 hours indicating strong activity of the immobilized ACHT to the immobilized peptide. Applications in surface chemistry and patterning will be discussed. Supported by the Naval Research Laboratory Core program.

M-Pos364

HUMAN ORNITHINE TRANSCARBAMYLASE: MODELLING, EXPRESSION, PURIFICATION, AND CHARACTERIZATION. ((H. Morizono, C.D. Listrom, X. Yuan, M. Tuchman[1] B.S. Rajagopal[1]and N.M. Allewell)) Department of Biochemistry, University of Minnesota, St. Paul MN 55108. [1]Department of Pediatrics, University of Minnesota Medical School, Minneapolis, MN 55455.

Mutations in ornithine transcarbamylase (OTCase) are the most common cause of inherited defects in the urea cycle. They produce hyperammonemia ranging from less severe, "late-onset" cases to fatal neonatal hyperammonemic coma. We have modelled the structure of human OTCase using the catalytic subunit coordinates from the crystal structure of *E. coli* aspartate transcarbamylase (PDB:8ATC), and have shown that many of the mutations that produce clinical symptoms are located at the active site. The human cDNA encoding "mature" OTCase was cloned into a pET21a(+) expression plasmid. The vector has been transformed into *E. coli* HMS 174(DE3) cells and induced with IPTG, resulting in abundant expression.. Purification to single band homogeneity on SDS PAGE has been achieved by affinity chromatography with the bisubstrate analog ∂-N-(phosphonacetyl)-L-ornithine attached to an epoxy-activated Sepharose 6B column. Both carbamyl phosphate and ornithine show slight substrate inhibition at pH 8.3. Fitting to a rate equation that includes substrate inhibition yields K_m values of 0.055 mM and 0.32 mM for carbamyl phosphate and ornithine, respectively. Further characterization of the pH dependence of substrate binding and catalysis, crystallization and electrostatic modelling are underway.

Supported by NIH grant DK47870-01A1

M-Pos365

NMR STUDIES OF PROTON DONATION AND METAL ION SPECIFICITY IN SUPEROXIDE DISMUTASE. ((D. L. Sorkin, C. K. Vance, A.-F. Miller)) Johns Hopkins University, Baltimore MD 21218.

We are exploiting NMR as a probe of function as well as structure to better understand fundamental aspects of redox catalysis in Superoxide Dismutase (SOD). We are directly observing the active site amino acids that are proposed to determine SOD's specificity for Fe or Mn. To this end, we have exploited the low gyromagnetic ratio of ^{15}N to circumvent severe paramagnetic relaxation due to high spin Fe^{3+} and observe Gln 69, even though it is the non-ligand amino acid sidechain closest to Fe. We have achieved highly selective isotopic labeling of the Gln sidechains and have tentatively identified the ^{15}N resonances of each of the Gln sidechains in FeSOD. SOD's unique ability to alternately reduce and oxidize the same substrate rests on its ability to provide at least one proton to the reaction. Thus, the pK_A of the proton donor is a key determinant of the reaction energetics. A pK near 9 was predicted for reduced FeSOD in 1985 (Bull & Fee, 1985, *J. Am. Chem. Soc. 107*, 3295-3304) and was tentatively ascribed to a proton donor. We report the first direct measurement of a pK consistent with the prediction, and ascribable to a group in the active site of reduced FeSOD. We measure a pK of 8.6 ±.1 with a Hill coefficient of 0.8 ± .1 at 30 °C. Supported by ACS-PRF 28379-G4 & N.S.F. MCB-9418181.

M-Pos366

CRYSTALLIZATION OF THE MONOOXYGENASE DOMAIN OF PEPTIDYLGLYCINE α-AMIDATING MONOOXYGENASE. (S. T. Prigge, A. S. Kolhekar, B. A. Eipper and L. M. Amzel) Departments of Biophysics and Neuroscience, Johns Hopkins University School of Medicine, Baltimore, MD 21205. (Sponsored by L. M. Amzel)

Approximately 50% of mammalian bioactive hormones, neurotransmitters, and growth factors are peptides with a COOH-terminal carboxamide, generated by N-oxidative cleavage of a glycine-extended prohormone. A single bifunctional enzyme is responsible for catalyzing the α-amidation of these physiological regulators, many of which are inactive without α-amidation. Peptidylglycine α-amidating monooxygenase (PAM) (EC 1.14.17.3) catalyzes two reactions at two separable catalytic domains: the first domain, peptidylglycine α-hydroxylating monooxygenase (PHM), catalyzes the copper, ascorbate, and molecular oxygen dependent α-hydroxylation of peptidylglycine substrates; the second domain, peptidyl-α-hydroxyglycine α-amidating lyase (PAL), is required to generate α-amidated peptide product and glyoxylate. The catalytic core of the PHM domain (residues 42-356 of rat PAM) has been over-expressed in Chinese Hamster Ovary cells, purified to > 95% purity through Fast Protein Liquid Chromatography, and crystallized in the orthorhombic space group P212121 with cell dimensions a=68Å, b=70Å, c=81Å, and α=β=γ=90°. Single crystals of dimensions of .4 x .1 x .1 cubic millimeters diffract to 2.5Å resolution using a rotating anode generator.

HEME PROTEINS AND PORPHYRINS I

(See also Su-Pos464, Su-Pos465, and Su-Pos466)

M-Pos367

STRUCTURE OF CHEMICALLY MODIFIED HEMOGLOBIN PROBED BY UV RESONANCE RAMAN SPECTROSCOPY. ((D. Wang, V. Jayaraman, G. Heibel & T. G. Spiro)) Department of Chemistry , Princeton University, Princeton, NJ 08544.

The structure of chemically modified desArg α-141hemoglobin (Hb) has been studied at various pH conditions using UV resonance Raman spectroscopy. At pH 6.5 and in the presence of inositol-hexaphosphate, deoxy desArg α-141Hb has been found to be in a T like quaternary structure. However, the spectra indicate weaker contacts at the α1β2 interface relative to deoxyHb. Furthermore, there is a marked perturbation in the environment of the Trp β37 which can be attributed to the absence of the H-bond between Val β35 and Arg α141, which is present in deoxyHb. The structure of the ligated carbonmonoxy form of desArg α-141Hb exhibits the same Trp and Tyr environment relative to HbCO indicating no perturbation in this structure due to the modification. At pH 9 deoxy desArg α-141 Hb exists in an R quaternary structure with a tertiary perturbation close to the deoxy heme. These large perturbations at the α1β2 interface can account for the large change observed in the dimer tetramer association free energy for deoxy desArg α-141Hb relative to deoxyHb[1]. These structures indicate the intricate network in the structure of Hb wherein a deletion of one residue causes a perturbation in the structure far from the modification.

1. LiCata *et al* (1993) Proteins 17, 279.

M-Pos368

Non - Boltzmann Vibrational Energy Distribution in Deoxyhemoglobin on a 30 Picosecond Timescale ((M. C. Simpson[1,2], E. Peterson[3], C. Shannon[3], D. Eads[3], J. Friedman[3], C. M. Cheatum[1], M. R. Ondrias[1],)). [1]University of New Mexico, Department of Chemistry, Albuquerque, NM 87131. [2]Current Address: Sandia National Laboratories, Fuel Sciences Div., Albuquerque, NM 87185. [3]Albert Einstein School of Medicine, Department of Physiology and Biophysics, Bronx, NY.

Intramolecular vibrational energy redistribution (IVR) and vibrational energy relaxation to the solvent (VR) may plan important roles in directing reactivity at biological catalytic centers. We have previously demonstrated the ability to generate, maintain, and detect a non-Boltzmann vibrational energy distribution in the heme active site of deoxyhemoglobin and in protein free model compound in a steady state manner using nanosecond pulses (M. C. Schneebeck et al., (1993) Chem. Phys. Lett., 215:251. C. M. Cheatum et al., (1995) 7th International Time Resolved Vibrational Spectroscopy Meeting). Here we demonstrate that a non-Boltzmann vibrational energy distribution can be observed in pulses of ~30 picoseconds in duration as well. these results are discussed in terms of the electronic and vibrational structures and dynamics of these biologically important molecules.

This research was funded by the National Institutes of Health (GM33330) (MRO) and a D.O.E. Distinguished Postdoctoral Fellowship (MCS). M. C. Simpson was previously M. C. Schneebeck.

M-Pos369

PHOTOINDUCED ELECTRON TRANSFER IN PORPHYRIN-QUINONE DONOR ACCEPTOR PAIRS: pH MODULATION OF CHARGE SEPARATION YIELD

((T. Buranda[1], N. Soice S. Niu[2], R. Larsen[2] and M. R. Ondrias[1])) [1]Chemistry Department University of New Mexico, Albuquerque, NM. 87131. [2]Department of Chemistry, University of Hawaii, Honolulu, Hawaii 96822.

The central role of quinones in electron and hydrogen transfer systems is widely known. The versatility of quinone reactivity in these processes has been attributed to the sensitivity of quinone redox properties to structural and environmental influences. The protonation of 2,3-Dimethoxy-5-methyl-1,4-benzoquinone (Q_0) has been determined to improve the quantum efficiency of charge separation between a zinc-meso-tetra (4-sulfonatophenyl) porphine (MP) donor and Q_0 (QH^+ upon protonation) acceptor system. Transient absorption data show a >4-fold increase in free ion product yields upon Q_0 protonation in absolute ethanol. Cyclic voltammetry has been used to determine the reaction driving forces at different pH. The effect of protonation is manifested in the back electron transfer (BET) process rather than the primary ET step. The importance of these results for understanding trends in the rates of BET is discussed. **This research is funded by the National Institutes of Health (GM33330 (to MRO).**

M-Pos370

NANOSECOND TIME-RESOLVED CIRCULAR DICHROISM MEASUREMENTS USING AN UPCONVERTED Ti:Sapphire LASER

((Youxian Wen, Eefei Chen, James W. Lewis and David S. Kliger)) *Dept. of Chemistry and Biochemistry, University of California, Santa Cruz, California 95064*

Several years ago, measurements of time-resolved circular dichroism in the far-uv region (Far-UV-TRCD) with sub-microsecond (10^{-7} sec) time-resolution were achieved in this laboratory which used a Xenon flash lamp to probe CD signals. With application of Ti:sapphire lasers and the ability to frequency convert their output to produce SHG, THG & 4HG pulses, a single wavelength circular dichroism measurement technique has been developed in this laboratory with nanosecond (10^{-9} sec) time-resolution over a broad range of probe wavelengths (from 205 ~ 900 nm). This should provide a powerful technique to study fast biophysical phenomena such as protein folding processes. In this poster, the application of this new technique will be presented. *This work is supported by NIH grant # GM 35158.*

M-Pos371

OXIDATIVE REACTIONS OF SPERM WHALE MYOGLOBIN AND ITS DISTAL POCKET MUTANTS WITH HYDROGEN PEROXIDE

((A.I. Alayash[1], B.A. Brockner Ryan[1], Y. Osawa[2], R.E. Cashon[3], R. Eich[4] and J.S. Olson[4])) [1]Center for Biologics Evaluation and Research, FDA, [2]NHLBI, NIH, Bethesda, MD 20892, [3]University of Maine, Orono, ME 04469, and [4]Rice University, Houston, TX 77251

The effects of key amino acid substitutions on the redox reactivity of a series of distal pocket mutants of sperm whale myoglobin are under study. These studies are relevant to the design of a simple prototype for hemoglobin-based blood substitutes. Myoglobins were oxidized with bolus addition of HOOH in increasing ratios of HOOH to heme in phosphate buffer, pH 7.0 at 37°C. Analysis of the kinetic data suggests a simple model composed of three distinct steps: initial oxidation, peroxidative loop, and heme degradation. Decreasing the space adjacent to ligands by replacing leucine 29 with larger aromatic phenylalanine (L29F) markedly decreases the initial oxidation step, and the rate of reversion of ferryl heme back to the ferric form (peroxidative activity). However, decreasing the volume of the back portion of the distal pocket by substitution of valine 68 with phenylalanine (V68F) has the opposite effect of accelerating both of these activities. Combining the two mutations (L29F/V68F) results in a protein that exhibits an intermediate peroxidation profile. This double substitution represents a good approach for increasing the resistance of blood substitutes to auto-oxidation and peroxidative reactions.

M-Pos372

EXPLAINING NON-EXPONENTIAL STRUCTURAL RELAXATION IN PROTEINS.

((S. J. Hagen and W.A. Eaton)) Laboratory of Chemical Physics, NIDDK, NIH, Bethesda, MD 20892-0520 (Spon. by G. Felsenfeld).

Conformational changes in proteins have been observed to exhibit a non-exponential time course. Like relaxations in glasses they may be described by the "stretched" exponential function, $\exp(-(\kappa t)^{\beta})$, where $0<\beta<1$. In myoglobin the conformational relaxation that follows photodissociation of the heme ligand is a single, continuous process that extends ($\beta \sim 0.1$) from less than 1 picosecond to nearly 1 microsecond (Jackson et al., *Chemical Physics* **180**, 131, 1994). We explain these kinetics with a model in which the initial protein conformational substates are connected to the final substates and to each other via transition states of a single energy. Single molecule experiments might distinguish between possibilities for the kinetic connectivity among substates.

M-Pos373

THE PROBLEM OF COOPERATIVITY AND THE INEQUIVALENCE OF α AND β SUBUNITS IN T STATE HEMOGLOBIN

(S. Bettati[‡], A. Mozzarelli[‡], G. L. Rossi[‡], A. Tsuneshige[¶], T. Yonetani[¶], W. A. Eaton[§] and E. R. Henry [§]) [‡]University of Parma, 43100, Parma, Italy; [¶]Unversity of Pennsylvania School of Medicine, Philadelphia, PA 19104; [§]NIDDK, NIH Bethesda, MD 20892-0520.

Oxygen binding by the Hb tetramer in the *T* quaternary structure is apparently non-cooperative in the crystalline state, in keeping with the two-state MWC allosteric model. However, analysis of the binding curves for light polarized along two different crystal directions, for which the projections of the α and β hemes are slightly different, revealed that a small amount of cooperativity is exactly compensated by inequivalence in the intrinsic oxygen affinity of the α and β subunits to give a Hill $n = 1.0$ ($p50(\alpha) \approx 80$ torr, $p50(\beta) \approx 370$ torr at 15°C) (Rivetti et al., *Biochemistry 32*, 2888, 1993). To further investigate this problem, we have measured oxygen binding curves of single crystals of Hb (in a different lattice) in which the iron in the α subunits has been replaced by the non-oxygen binding nickel(II). The Hill n is 0.90 ± 0.06, and the average $p50$ for the β subunits is about 110 ± 20 torr at 15°C, close to the $p50$ of 80 torr observed in solution, but about three-fold less than the $p50$ calculated by Rivetti et al. for the β subunits of the unsubstituted tetramer. These results suggest that Rivetti et al. did not underestimate the α/β inequivalence. They also, therefore, did not underestimate the cooperativity within the *T* quaternary structure, when they concluded that it represents a small deviation from the perfectly non-cooperative binding of an MWC allosteric model. Our conclusion of nearly perfect MWC behavior for binding to the *T* state of unmodified Hb raises the question of the relevance of the highly exaggerated *T*-state cooperativity inferred for cyanide binding to oxidized Hb (Ackers et al., *Science 255*, 54, 1992).

M-Pos374

ALLOSTERIC EFFECT IN AUTOOXIDATION OF HEMOGLOBIN

((J. Horsky and J. Rifkind)) NIA, NIH, Baltimore, MD 21224 (Sponsored by J. Rifkind)

Autooxidation of hemoglobin (Hb) involves production of oxyradicals and thus it is a potential source of cell damage. Autooxidation is enhanced at intermediate oxygen pressures (pO_2) which may be expected if the oxidation of deoxygenated subunits is also involved. Recent detailed analysis of the dependence of the Hb autooxidation rate on pO_2 revealed that the rate of oxidation is influenced by the oxygenation state of other subunits in Hb tetramers (allosteric effect). The validity of this conclusion can, however, be challenged by subsequent experiments at atmospheric pressure which showed that the rate of autooxidation also depends on the concentration of hemoglobin. Therefore, we measured the dependence of the autooxidation of Hb A_0 on pO_2 at three Hb concentrations (90, 180, 450 μM heme). Catalase and superoxide dismutase were added in order to suppress secondary reactions of oxyradicals formed during autooxidation with Hb. Although oxygenation curves were indistinguishable and less than 10% of Hb might be expected to dissociate into dimers there were distinct differences in oxidation rates especially at intermediate oxygenation. The model disregarding the allosteric effect was not able to produce an adequate fit to experimental data at finite concentrations or to the curve obtained by tentative extrapolation to infinite Hb concentration which eliminates the possibility that the failure of such model previously observed was because of dissociation of tetramers. The model allowing different rate constants of autooxidation for subunits in Hb tetramers with different degree of oxygenation reproduced oxidation curves well. Thus, the allosteric effect in Hb oxidation was confirmed. Paradoxically, if the allosteric effect is operative the oxidation of deoxygenated subunits need not be invoked in order to explain the bell shaped curve for Hb oxidation.

M-Pos375

2-D DISTRIBUTIONS OF ACTIVATION ENTHALPY AND ENTROPY FROM KINETICS BY THE MAXIMUM ENTROPY METHOD ((Peter J. Steinbach)) DCRT, NIH, Bethesda, MD 20892

The Maximum Entropy Method (MEM) was used to numerically invert the kinetics of ligand rebinding at low temperatures to obtain the underlying two-dimensional distribution of activation enthalpies and entropies, $g(H,S)$. A global analyisis of the rebinding of carbon monoxide (CO) to myoglobin (Mb), monitored in the Soret band at temperatures from 60 to 150 K (1), was performed. The MEM approach describes the data much better than traditional least-squares analyses, reducing chi-square by an order of magnitude. The MEM resolves two barrier distributions suggestive of rebinding to different bound conformations of MbCO, the so-called A1 and A3 substates, whose activation barriers have been independently estimated from kinetics monitored in the infrared (2,3). The distribution corresponding to A3 possesses higher activation entropies, also consistent with infrared measurements. Within an A substate, correlations of S and H are recovered qualitatively from simulated data but can be difficult to obtain from experimental data. When the rebinding measured at 60 K is excluded from the inversion, two peaks are no longer clearly resolved. Thus, data of very high quality are required to unambiguously determine the kinetic resolvability of subpopulations and the shape of the barrier distribution for a single A substate.

1. Steinbach et al., *Biochemistry 30* (1991) 3988.
2. Ansari et al., *Biophys. Chem. 26* (1987) 337.
3. Berendzen and Braunstein, *Proc. Natl. Acad. Sci. USA 87* (1990) 1.

M-Pos376

HEME STABILITY OF PARTIALLY OXIDIZED HEMOGLOBINS. ((M.D. Chávez, B.E. Shrader, H.S. Zahwa, and V.W. Macdonald)) Blood Research Detachment, Walter Reed Army Institute of Research, Washington, D.C. 20307

A continuing issue raised with acellular hemoglobin-based blood substitutes concerns the toxic effects it produces upon clinical application. Among several parameters, the loss of the heme prosthetic group is known to cause several undesired consequences. Hemoglobin no longer binds oxygen and denatures irreversibly without the heme group present. In addition, the free heme and iron can catalyze reactions to produce toxic free-radical oxygen species. Therefore, optimizing the stability of the heme within hemoglobin-based blood substitutes is a desired goal. Rates of hemin loss (Fe(III)PPIX) have previously been measured for several varieties of hemoglobin (1,2), revealing that heme loss can be affected in either direction depending on the modified hemoglobin. Our studies focus on heme loss within partially oxidized hemoglobins. Without a reduction pathway available, hemoglobin can become substantially oxidized in an acellular environment. Our results show that under partially oxidized conditions, heme loss does occur but at a somewhat lower rate than fully oxidized hemoglobin. This observation was noted in both HbA_0 and $\alpha\alpha$-cross-linked HbA. The presence of Fe(II)-His linkage(s) within a partially oxidized hemoglobin tetramer appears to inhibit heme loss in neighboring Fe(III) sites.

1. Benesch, R.E. and Kwong, S. J. Biol. Chem. 265 (1990), 14881
2. Vandegriff, K.D., and Le Tellier, Y.C. Artif. Cells, Blood Subst., Immob. Biotech. 22 (1994), 443.

M-Pos377

FURTHER STUDIES OF HORSE CYTOCHROME C IN DIMETHYL SULFOXIDE. ((E.W. Findsen[1] B.S. Wicks[1]; J.D. Satterlee[2]; S. Sukits[2];))
[1]Department of Chemistry, University of Toledo, Toledo, Ohio 43606.
[2]Department of Chemistry, Washington State University, Pullman, Washington 99163.

We previously reported that results of optical absorption studies of ferric horse heart cytochrome *c* (HHC) in DMSO/TRIS indicated that the protein appeared to be unfolded and that its optical properties were similar to those reported by Drew and Dickerson for the acid/methanol denatured intermediate II of the protein. Recent NMR studies confirm that ferric HHC lyophilized from TRIS buffer (pH 7) and dissolved in DMSO is partially unfolded. Room temperature and variable temperature studies of the NMR spectrum of HHC in DMSO/TRIS suggest that at least two conformations exist and that interconversion between these forms may be taking place. The dominant form of the protein is high spin. The Met resonance at ~-23 ppm is not observed indicating that the Met ligand has been displaced from the heme.

Results will be presented which demonstrate that the solubilization of the protein in DMSO/TRIS is due to specific charge interactions rather than by nonspecific solvation effects.

M-Pos378

LIGAND MOTIONS FOLLOWING FLASH PHOTOLYSIS IN MYOGLOBIN ((Ben McMahon, J. Bruce Johnson*, Don Lamb#, Joachim D. Müller, & G. Ulrich Nienhaus)) Department of Physics, University of Illinois at Urbana-Champaign, IL 61801, (*)Arkansas State University, & (#)TU München

We follow the dynamics of CO and sperm whale myoglobin after flash photolysis by monitoring the infrared absorbance bands of bound CO (A states near 1940 cm^{-1}) and the much weaker absorbance band of photolyzed CO (B states near 2130 cm^{-1}). We present kinetics of A and B states from 2 μs to 3 s in 10 K intervals from 180 K to 300 K. At the lowest temperatures and earliest times, CO recombines directly from B → A, so the B state kinetics mirror the A state kinetics. At higher temperatures and longer times, additional loss of B state signal occurs, reflecting changes in the equilibrium protein structure, nonequilibrium relaxation of the heme pocket and possibly motions of the CO to different sites within the heme pocket. Further broadening of the spectrum is seen at later times as the CO leaves the pocket and equilibrates with the solvent. Finally, we observe disappearance of the B state absorbance as CO rebinds to the iron. We relate these data to experiments on band III and models of ligand motions and recombination in myoglobin.

M-Pos379

THE ROLE OF HIS97 AND HIS64 IN CO-LIGATED SPERM WHALE MYOGLOBIN **((Joachim D. Müller, Ellen Y.T. Chien, Ben McMahon, Stephen G. Sligar & G. Ulrich Nienhaus)) Department of Physics, Biophysics, Biochemistry & Chemistry, University of Illinois at Urbana-Champaign, IL 61801.**
(Sponsored by H. Frauenfelder)

We combine site-directed mutagenesis with pH-titrations to study the influence of histidines on the active site. Our investigation relates spectroscopic markers to the physiologically important ligand binding function of myoglobin. The pH dependent changes of the α band, the CO stretch band and the association rate coefficient of CO for wild type, a distal mutant (H64V) and a proximal mutant (H97F) were characterized using global analysis methods. We were able to isolate the influence of both histidines on the association rate coefficient of myoglobin and determined the pK's unequivocally. Histidine 97 titrates with a pK close to 6 in all our experiments. Histidine 64 titrates with a pK around 4.7 for the spectroscopic titration and a pK of 4.2 for the kinetic experiments, reflecting the destabilising influence of bound CO on distal histidine in the pocket. We will discuss and connect the changes of the spectroscopic markers to the function of myoglobin. (Supported by NIH PHS 2 R01 GM18051 and GM31756).

M-Pos380

KINETIC AND STRUCTURAL CHANGES IN LIGAND BINDING TO MYOGLOBIN AT HIGH PRESSURE OBSERVED BY RAMAN AND TRANSIENT ABSORPTION SPECTROSCOPY ((A. Schulte, O. Galkin, A. Tabirian Murazian)) Department of Physics and Center for Research and Education in Optics and Lasers, University of Central Florida, Orlando, FL 32817.

The pressure dependence of the CO binding kinetics to (horse) Mb following flashphotolysis has been studied in the time range $5 \cdot 10^{-8}$ to 10^{2} s at temperatures from 80 to 295 K employing absorption spectroscopy. The multistep kinetics at intermediate temperatures speeds up with pressure. To probe structural changes and connect them with the activation volume we measure the Raman spectrum as a function of pressure. In particular, the peak position of the iron-proximal histidine vibration shifts to higher frequency with pressure ($\approx 1.6\ cm^{-1}$ / 100 MPa in Mb/H_2O at 295 K). The observed shift is interpreted as a conformational change, which alters the tilt angle between the heme plane and the proximal histidine and the out-of-plane iron position. Absorption studies of band III near 760 nm provide additional support for iron movement.
(Supported by NSF, Grant No. MCB-9305711).

M-Pos381

L-EDGE X-RAY ABSORPTION SPECTROSCOPY OF LIGAND-BOUND AND PHOTOPRODUCT STATES OF MYOGLOBIN. ((L. M. Miller,[1] E. Scheuring,[1] H. Wang,[2] G. Peng,[2] S. P. Cramer,[2] and M. R. Chance[1])) [1]Department of Physiology and Biophysics, Albert Einstein College of Medicine, Bronx, NY 10461 and [2]Division of Energy and Environment, Lawrence Berkeley Laboratory, Berkeley, CA 94720

We demonstrate the first application of L-edge x-ray absorption spectroscopy (XAS) in conjunction with a biochemical photoreaction, and illustrate the power of the method for understanding electronic transitions coupled to photolysis-induced structural changes. L-edge XAS measurements, which probe $2p \rightarrow 3d$ transitions, provide a direct probe of the Fe 3d orbital configurations of the intermediate conformational states involved in the process of ligand-binding to myoglobin. Thus, the detailed electronic information attainable from L-edge XAS complements the structural information obtained through K-edge EXAFS and x-ray crystallography. The L-edge XAS spectra for the ligand-bound species, MbCO and MbO_2, have been compared to their corresponding photoproducts, Mb*CO and Mb*O_2, and to the unligated state, deoxy Mb. These spectra have also been simulated using a ligand field multiplet calculation so that similarities and differences in the 3d orbital configurations for these species can be elucidated. In addition, the analytical results, compared with the available structural information about the myoglobin species, provide an excellent test system for this technique, so that L-edge experimental data can be used for a wider range of metalloprotein systems. This work is supported by NIH grants GM-48381 (to S. P. C.) and HL-45892 (to M. R. C.).

M-Pos382

IDENTIFICATION OF CONFORMATIONAL SUBSTATES INVOLVED IN NITRIC OXIDE BINDING TO MYOGLOBIN THROUGH DIFFERENCE FOURIER TRANSFORM INFRARED SPECTROSCOPY. ((M.P. Patel, L. M. Miller, A.J. Pedraza, and M. R. Chance)) Department of Physiology and Biophysics, Albert Einstein College of Medicine, Bronx, NY 10461

Nitric oxide (NO) is of widespread importance in mammalian physiology. Among its functions, it serves as a neurotransmitter, vasodilator, and cytotoxic agent. Nitric oxide synthase is a hemeprotein that catalyzes the conversion of L-arginine and O_2 to L-citrulline and NO. The binding of O_2 and CO to hemeproteins has been extensively studied; however, far less is known about the mechanism of NO binding. In myoglobin, several protein conformational substates have been identified with respect to the CO stretching frequency in both the ligand-bound (*A states*) and photoproduct (*B states*) states. These substates have unique rebinding kinetics which is evidence that they are involved in regulating ligand binding. Therefore, as a stepping stone for studying NO binding to NO synthase, we have identified the conformational substates in MbNO. Earlier attempts to assign the bound NO stretching frequency in myoglobin have proven to be difficult because the NO stretching frequency falls in a region (~1600 cm^{-1}) which contains intense contributions from the porphyrin ring and the protein amide I band. In order to identify both the A and B states of MbNO, we have generated photolyzed / unphotolyzed difference FTIR spectra of MbNO at 10 K. At pH 7, MbNO has 2 A states (1584 and 1612 cm^{-1}) and 3 B states (1819, 1852, and 1856 cm^{-1}) In addition, the pH dependence of these states and their rebinding rates are also being investigated.

M-Pos383

OPTICAL PUMPING OF MYOGLOBIN-LIGAND COMPLEXES AT LOW LIGHT LEVELS. ((A. J. Pedraza, L. M. Miller, and M. R. Chance)) Department of Physiology and Biophysics, Albert Einstein College of Medicine, Bronx, NY 10461

Optical pumping of hemeprotein-ligand complexes has, for a long time, been correctly associated with an increase in the ligand binding barrier (Powers et al. *Biochemistry*; **26**, p.4785, Srajer et al., 1991, *ibid*, **30**, p.4886, Nienhaus, et al., 1994 *ibid*, **33**, p.13413). These high barrier states are created by a forced relaxation of the photoproduct structure towards the deoxy state based on continuing illumination. We have taken an alternative approach to optical pumping studies by examining the creation of photolyzed states as a consequence of interrogation with defined pulses of low light levels, following the reaction from the unphotolyzed state to the maximum extent of photolysis that can be achieved at cryogenic temperatures, in these cases, 10 K. Upon photolysis of the horse Mb (Fe^{+2})-nitric oxide complex at pH 7.0, we achieved virtually 100% photolysis at 10 K based on examination of Soret band spectra. Rebinding studies demonstrated that this MbNO photoproduct has a very low barrier to rebinding. When we followed the appearance of photoproduct as a function of illumination, we observed very different photolysis rates for the horse Mb samples bound to CO, O_2, and NO. The MbCO samples had a single rate of photolysis, consistent with each absorbed photon leading to a stable photoproduct. The MbO_2 and MbNO samples had distributed rates of photolysis. We connect these results to the presence of distal pocket hydrogen bonding and multiple distal substates in the MbNO and MbO_2 complexes. This research was supported by a grant from NIH HL-45892.

M-Pos384

STUDIES OF THE ELECTRON TRANSFER PROCESS BY FLUORESCENCE SPECTROSCOPY. ((M.K.K. Nakaema, N.L.L. Sales and R. Sanches)) Instituto de Física de São Carlos, Universidade de São Paulo, São Carlos, SP, Brazil.

It is an old idea to try to simulate the photosynthetic reaction center and, in the last few years, a lot of new molecules were synthesized for this purpose. We used as our model system organic molecules usually found in nature (as porphyrins and quinones) and, to study the electron transfer process, we imposed restrictions in the donor-acceptor distance by distributing the molecules in a polymeric matrix. The films made were then analyzed by fluorescence spectroscopy. It is known that the electron transfer causes the fluorescence quenching of the donor molecule, therefore, this is an indirect way of observing this process.

We used tetraphenylporphyrin (TPP and Zn-TPP) as donor molecules, duroquinone and tetrachloroquinone as acceptor molecules, and polystyrene as the matrix. The data were analyzed taking into account the random distribution of donor and acceptor molecules, and the rate of electron transfer could be obtained.

Supported by FAPESP, FINEP and CNPq

M-Pos385

COMPARISON OF THE GILL AND IMAI METHODS FOR EQUILIBRIUM HEMOGLOBIN OXYGEN BINDING MEASUREMENTS ((L. Kiger, A.L. Klinger and G.K. Ackers)) *Department of Biochemistry and Molecular Biophysics, Washington University School of Medicine, St. Louis MO 63110.*

Two major instrumentation methods have been developed for measuring hemoglobin (Hb) O_2 binding isotherms in a UV-vis spectrophotometer. These methods differ mainly in the concentration of sample used and in the manner of varying and determining O_2 partial pressure. The method of Gill[1] utilizes a cell in which a thin-layer of a high concentration sample is covered by a transparent gas-permeable membrane and contained in a reaction chamber. The O_2 partial pressure inside the reaction chamber is changed in discreet dilution steps and is calculated from the known volume of gas in the dilution valve. This method has been used especially for studies of sickle cell Hb where O_2 binding is coupled to polymerization[2]. In contrast, the method of Imai[3] utilizes a stirred cell which contains a low concentration solution of sample. The oxygen partial pressure is changed by flowing N_2 over the surface of the solution and is measured with an O_2 electrode. This method has been used extensively for studies where subunit dissociation is linked to O_2 binding[4]. We compare results obtained from both methods on Hb systems with a range in affinity and cooperativity properties, in particular, HbA_0, several crosslinked Hbs and a series of recombinant Hbs (βW37A,G,Y and N). We find that the results obtained from the different methods are consistent, and we discuss the positive and negative points of each of these methods for studies of Hb binding isotherms.

[1] Dolman & Gill (1978) *Analyl. Biochem. 87*:127-134.
[2] Gill *et al.* (1979) *J. Mol. Biol. 130*:175-189
[3] Imai *et al.* (1970) *Biochim. Biophys. Acta 200:189-196.*
[4] Chu *et al.* (1984) *Biochem 23*:604-617.

M-Pos386

TRANSFORMATION OF COOPERATIVE FREE ENERGIES BETWEEN LIGATION SYSTEMS OF HEMOGLOBIN: RESOLUTION OF THE CARBON MONOXIDE BINDING INTERMEDIATES. ((Yingwen Huang and Gary K. Ackers)) Department of Biochemistry and Molecular Biophysics, Washington University School of Medicine, St. Louis, MO 63110.

A method has been developed for quantitatively translating cooperative free energies of all ligation intermediates between Co/FeX (X= CO or CN) and Fe/FeX systems. Using hybridized combinations of normal and cobalt-substituted Hb, ligation systems Co/FeX were constructed and experimentally studied. Energetics of Co-induced structural perturbation were determined for all species of both the "mixed metal" Co/Fe system and also the ligated Co/FeCN system. Major energetic perturbations of the Co/Fe hybrid species were found to originate from a Co-substitution effect on the α-subunit. These perturbations are transduced to the β-subunit within the same dimeric half-tetramer, resulting in alternation of the free energies for binding at the non-substituted (Fe) sites. Using the linkage strategy developed in this study along with the determined energetics of these couplings, the experimental assembly free energies for the Co/FeCO species [Speros et al. (1991) Biochemistry 30, 7254-7262] were transformed into cooperative free energies of the 10 Fe/FeCO species. The resulting values were found to distribute according to predictions of a Symmetry Rule Mechanism proposed previously [Ackers et al. (1992) Science 255, 54-63] and are consistent with accurate CO binding data [Perrella et al. (1990) Biophys. Chem. 37, 211-223] and O_2 binding data [Chu et al. (1984) Biochemistry 23, 604-617] of normal Hb.

M-Pos387

HYDROPATHIC ANALYSIS OF INTERACTIONS IN THE DIMER-DIMER INTERFACE OF HUMAN HEMOGLOBIN. ((Donald J. Abraham, Glen E. Kellogg, Jo M. Holt* and Gary K. Ackers*)) Department of Medicinal Chemistry, Virginia Commonwealth University, Richmond VA 23298-0540 and *Department of Biochemistry and Molecular Biophysics, Washington University School of Medicine, St. Louis, MO 63110

The strengths of the individual non-covalent subunit interface bonds in the hemoglobin $\alpha1\beta2$ (dimer-dimer) interface can be estimated by analysis of hydropathic character of the bonds in a new software program HINT (Hydropathic INTeractions). The HINT analysis provides a quantitative value for the nonpolar-nonpolar, polar-polar and nonpolar-polar character of each interaction in the interface of both oxy and deoxy hemoglobin. These HINT values have been compared with experimentally measured energies (Turner et al., PROTEINS 14, 333-350, 1992), specifically, the free energy changes which occur upon single-site mutagenesis within the dimer-dimer interface as determined from the measured free energies of dimer-tetramer assembly. The correlation observed between the calculated HINT hydropathies and the measured free energies provides a quantitative characterization of subunit interactions based upon individual atomic contacts in the $\alpha1\beta2$ interface.

M-Pos388

THE CO TILTING AND BENDING POTENTIAL ENERGY SURFACE OF CARBONMONOXYHEMES. ((Abhik Ghosh and David F. Bocian)) Department of Chemistry, University of California, Riverside, CA 92521.

The geometry of the Fe-C-O unit in carbonmonoxy hemes and heme proteins is controversial. On the one hand, there are crystallographic data favoring significantly bent Fe-C-O units. On the other hand, recent spectroscopic experiments favor almost perfectly linear Fe-C-O units. To address this controversy, we used density functional calculations with extended basis sets to construct the CO tilting and bending potential energy surface of carbonmonoxyhemes. The results modify our present understanding of this surface and demystify the controversy associated with it.

M-Pos389

HEMOGLOBIN OXIDATION, HEME DESTRUCTION AND IRON RELEASE IN HEMOGLOBIN-LIPID MIXTURES UNDER PHYSIOLOGICAL AND NON-PHYSIOLOGICAL CONDITIONS. ((Merita N. Dias, and L. W.-M. Fung)) Department of Chemistry, Loyola University of Chicago, Chicago, IL, 60626.

We have studied hemoglobin (Hb) oxidation, heme destruction and iron release in Hb-lipid mixtures under physiological buffer condition (110 mM NaCl, 35 mM phosphate, pH 7.4) and non- physiological buffer conditions (10 mM Tris, 5 mM KCl, pH 6.5). Lipid peroxidation in these mixtures were also monitored. Results for systems using normal Hb (HbA) and sickle Hb (HbS) were compared. Our studies done under non-physiological buffer conditions show a difference in rates of oxidation between HbA and HbS and no differences were observed for the rates of heme destruction and the extent of iron release. The experiments performed under physiological buffer conditions did not show any difference between HbA and HbS. We also monitored the heme partitioning to the lipid phase under both buffer conditions. (Supported by Loyola University of Chicago.)

M-Pos390

CALIBRATED IMAGES OF THE EARTHWORM HEMOGLOBIN IN SOLUTION ((Shaohua Xu and Morton F. Arnsdorf)) University of Chicago, Chicago,Il 60637. shxu@medicine.bsd.uchicago.edu. (Spon. by Z. Zhou)

Untreated extracellular hemoglobin molecules of the common North American earthworm, *Lumbricus terrestis*, were imaged in NH_4Ac solution (5 mM NH_4Ac, 1mM $MgCl_2$, pH 7.0) using calibrated scanning (atomic) force microscopy (SFM). Individual molecules were clearly identified. A central depression, the presumed mouth of the hole, was detected. We analyzed sixty two molecules one by one for their lateral dimensions. The amount of compression, presumably due to the variation of the interaction between the SFM tip and the protein, differs for each protein and for different portions of the same protein molecule. Two effective heights were identified for each protein (between 4.09 and 16.2 nm for h_1 and 1.23 nm and 7.99 nm for h_2), which corresponds to the heights of the points of the hemoglobin molecule first and last touched by the tip. The apparent diameter measured ranged from 44.9 nm to 74.2 nm (58.6nm $\pm$ 7.1, n=62) which is about twice the size of the diameter of the molecule reported by EM for the top view orientation. So the tip convolution effect varies for different molecules. The higher the measured effective heights, the worse was the tip convolution effect. We imaged some spherical gold particles to determine the tip parameters (semivertical angle, curvature of radius and the cut-off height) and to calibrate images of earthworm hemoglobin molecules (Shaohua Xu and Morton F. Arnsdorf, J. of Microscopy, 173(3), 199-210, 1994.). We subtracted the tip sectional radii at distances of h_1 and h_2 above the tip apex from the apparent diameter of the protein. The calibrated lateral dimension was 27.4nm $\pm$ 3.36, which is close to the reported EM data 30nm $\pm$ 0.8. Calibrated SFM image is generalizable to the study of other bio-macromolecules.

M-Pos391

FUCTIONAL STUDIES OF THE INTERACTION OF HEMOGLOBIN (HbA) WITH NO AND O_2. BINDING OF NITRIC OXIDE TO α-SUBUNITS OF HbA CONVERTS HbA TO A LOW-AFFINITY, ALLOSTERIC O_2-CARRIER. THUS NO IS A NEGATIVE ALLOSTERIC EFFECTOR OF HbA TO FACILITATE EFFECTIVE OXYGEN DELIVERY ((Antonio Tsuneshige & Takashi Yonetani)), Department of Biochemistry & Biophysics, School of Medicine, University of Pennsylvania, Philadelphia, PA 19104-6089, USA.

Nitric Oxide (NO) in the blood acts a regulator of various cellular functions. Furthermore, NO diffuses into erythocytes to rapidly bind to HbA, as HbA has an extremely high affinity for NO. It has been reported that NO in the blood converts HbA preferentially to α-*nitrosyl* HbAs [α(Fe-NO)$_2\beta$(Fe)$_2$ and α(Fe-NO)α(Fe)β(Fe)$_2$] (Kosaka et al.[1994] *J. Am. Physiol. 266*, C1400-C1404). We have prepared α-*dinitrosyl* HbA [α(Fe-NO)$_2\beta$(Fe)$_2$] and examined its oxygenation properties in the presence and absence of BPG or IHP. *Alpha-dinitrosyl* HbA, [α(Fe-NO)$_2\beta$(Fe)$_2$] in the presence of IHP is a non-cooperative, low-affinity O_2 carrier in accordance to its ***Super-T*** structure (an extreme low-affinity, non-allosteric state having no Fe-His(F8) bonds in the α subunits) as exemplified by HbM_{Iwate} [α(Fe[III] ^{87}His$\rightarrow$Tyr)$_2\beta$(Fe)$_2$], HbM_{Boston} [α(Fe[III] ^{58}His$\rightarrow$Tyr)$_2\beta$(Fe)$_2$], and α(protoporphyrin)$_2\beta$(Fe)$_2$ (Fujii et al. [1995] *J. Biol. Chem. 268*, 15386-15393). In the absence of IHP, [α(Fe-NO)$_2\beta$(Fe)$_2$] is in a predominantly ***Super-T***-state in the *deoxy* form, and in the ***R***-state in the *oxy* form, [α(Fe-NO)$_2\beta$(Fe-O$_2$)$_2$], as reported in the accompanying abstract (Yonetani & Tsuneshige, 1996). Therefore, [α(Fe-NO)$_2\beta$(Fe)$_2$] behaves as an allosteric, low-affinity O_2-carrier. Thus, it is likely that NO facilitates effective oxygen delivery *in vivo* via vasodilation and formation of α-nitrosyl HbA. Supported by NIH grants, HL14508 and GM 48120.

M-Pos392

NITRIC OXIDE (NO) IN THE BLOOD: EPR, NMR, AND FUCTIONAL STUDIES OF THE INTERACTION OF HEMOGLOBIN (HbA) WITH NO, SHOW THAT NO IS A NEGATIVE ALLOSTERIC EFFECTOR OF HbA TO FACILITATE EFFECTIVE OXYGEN DELIVERY ((Takashi Yonetani & Antonio Tsuneshige)), Department of Biochemistry & Biophysics, School of Medicine, University of Pennsylvania, Philadelphia, PA 19104-6089, USA.

Nitric oxide (NO) acts as a regulator of a variety of vital physiological and biochemical reactions. Nitric oxide in the blood rapidly diffuses into erythrocytes and binds to HbA, because HbA has a more than 10^4-fold higher affinity for NO than O_2. Unlike CO, however, a limited supply of NO in the blood ([NO] $\approx$ several μM) causes no apparent NO poisoning. The NO in the blood converts HbA preferentially to α-*nitrosyl* HbAs [α(Fe-NO)α(Fe)β(Fe)$_2$ or α(Fe-NO)$_2\beta$(Fe)$_2$](Kosaka et al [1994] *J. Am. Physiol. 266*, C1400-C1404) which we found to be an allosteric, low-affinity O_2-carrier under physiological conditions to facilitate more efficient delivery of O_2 to peripheral tissues, as described in the accompanying abstract (Tsuneshige & Yonetani, 1996). EPR and NMR measurements indicate that the Fe-His(F8) bonds in the α-subunits of HbA(NO)$_4$ are broken at lower pH or in the presence of IHP as well as those of *deoxy* α-*nitrosyl* HbA [α(Fe-NO)$_2\beta$(Fe)$_2$] in the presence and absence of IHP, causing their quaternary structural transition to ***Super-T*** states having non-allosteric, extremely low O_2-affinity, as observed in other known ***Super-T*** HbAs such as HbM_{Iwate} [α(Fe[III] ^{87}His->Tyr)$_2\beta$(Fe)$_2$], HbM_{Boston} [α(Fe[III] ^{58}His->Tyr)$_2\beta$(Fe)$_2$ and α(protoporphyrin)$_2\beta$(Fe)$_2$] (Fujii et al [1995] *J. Biol. Chem.268*, 15386-15393). In the absence of IHP, α(Fe-NO)$_2\beta$(Fe)$_2$, which is in a ***predominantly Super-T*** state, reversibly forms the α Fe-His(F8) bonds upon oxygenation and shifts its quaternary structure toward ***R***-states, so that α(Fe-NO)$_2\beta$(Fe)$_2$ becomes an allosterically-sensitive, low-affinity O_2-carrier. Thus, NO facilitates increased oxygen delivery to tissues through the vasodilation as well as the formation of an allosteric, low-affinity HbA, α-*nitrosyl* HbA or α(Fe-NO)$_2\beta$(Fe)$_2$. Supported by NIH grants, HL14508 and GM 48120.

M-Pos393

PHYSICAL PARAMETERS OF FcγRII-IgG INTERACTIONS IN THE ABSENCE AND PRESENCE OF A PROTEIN ANTIGEN

((Lixin Chen, Erin D. Sheets and Nancy L. Thompson)) Department of Chemistry, University of North Carolina, Chapel Hill, NC, 27599-3290

Total internal reflection fluorescence microscopy has been used to examine the interaction of a mouse monoclonal IgG2b with mouse FcγRII in substrate-supported planar membranes. Equilibrium and kinetic dissociation constants were measured for the antibody S6-34.11, which is specific for bovine prothrombin fragment 1, in the presence and absence of the antigen. The measured IgG2b-FcγRII dissociation constants were not significantly different in the absence or presence of saturating concentrations of fragment 1. These results demonstrate that the effects of possible conformational changes in IgG which occur upon antigen binding do not appreciably affect subsequent interaction with FcγRII. Supported by NIH GM-37145 and NSF GER-9024028.

M-Pos394

FLUORESCENCE MICROSCOPIC STUDIES FOR DETERMINATION OF Fcγ RECEPTOR CLUSTERING.

((F.Y.S.Chuang*†, J.Unkeless†, J.J.Macklin‡, J.K.Trautman‡, L.E.Brus‡, J.Eisinger* and M.Sassaroli*)) *Dept of Physiology and Biophysics, †Dept of Biochemistry, Mount Sinai School of Medicine, New York, NY 10029; and ‡AT&T Bell Laboratories, Murray Hill, NJ 07974.

We are exploring biological applications for new methods of near and far-field microscopy developed for the fluorescence imaging and spectroscopy of individual molecules. Specifically, we are investigating the hypothesis that crosslinking of the human neutrophil glycan phosphatidylinositol (GPI) anchored huFcγRIIIb results in the co-localization of huFcγRIIa, and the induction of the tyrosine kinase cell activation cascade. In T cells, it is clear that signaling via GPI-anchored proteins requires the T cell antigen receptor. We suggest that huFcγRIIIb and huFcγRIIa, which has a cytoplasmic tyrosine activation motif, may similarly interact. In previous studies we have used conventional immunofluorescence to show clustering of huFcγRIIa and capping of huFcγRIIIb upon direct crosslinking by monoclonal antibodies. However, in order to show that the separation between adjacent receptor molecules is less than the diffraction-limited optical resolution of 250nm, we label the two receptor isotypes with monoclonal F(ab) conjugated to fluorophores which constitute an appropriate donor-acceptor pair for resonance energy transfer (FRET). The development of an experimental arrangement which allows concurrent measurement of fluorescence lifetimes and spectra of individual clusters, enables us to identify groups of labeled cell surface receptors, whose separation approximates the Förster distance for energy transfer.

M-Pos395

CRYSTAL STRUCTURE OF TWO SALMETEROL SALTS AND THEIR RELATION TO THE PUTATIVE BINDING SITE ON THE β_2 RECEPTOR

((David G. Rhodes[1,*], Chang Fan[1], Shou Dao Wang[2], and Roger Newton[3])) (1) Dept. Pharmaceutical Sciences, School of Pharmacy, U.Conn. Storrs, CT (2) U.Conn. Health Center, Farmington, CT, (3) Chemical Research Div., GLAXO Group Research, Ltd., Greenford, Middlesex, UK

Small molecule crystal structures are often used to attempt to identify properties and features of receptor sites, but these data can be misleading. Salmeterol (Serevent) is a long-acting sympathomimetic amine used as the hydroxynaphthoate salt in asthma therapy. We have determined the crystal structure of this compound in the form of the hydroxynaphthoate and sulphate salts. The crystal structures are quite distinct. The hydroxynaphthoate (1) is a monoclinic unit cell with space group P 21 (a=8.380Å, b=45.06Å, c=9.370Å, β=108.72). The molecules are in two conformations, an essentially all-*trans* configuration and another with a *gauche* kink near the ether O. For the sulphate (2), a monoclinic unit cell with space group C_c (a=27.956Å, b=5.9213Å, c=30.604Å, β=94.458) was found. In this crystal, the molecules are "C"-shaped, quite unlike those in the crystal structure of 1, but MMP2 calculations indicated minor differences between experimental and minimized conformations, and small energy differences among all conformations. The difference in the salmeterol conformations is apparently due to packing constraints imposed, in part, by the difference in the size and valence of the counterions. The result is discussed in terms of the likely binding site in a β_2-receptor model, and the need for caution in using crystal structures to develop structure/activity relationships.

M-Pos396

FLUORESCEIN-EGF PHOTOBLEACHING CORRECTION FOR BINDING KINETICS AT THE SINGLE CELL LEVEL.

((J. C. Chung and D. J. Gross)) Program in Molecular and Cellular Biology and Department of Biochemistry and Molecular Biology, Box 34505, University of Massachusetts, Amherst, MA 01003-4505.

We have reported previously on EGF binding kinetics at the single cell level.* Fast and slow binding and debinding rate constants were found for fluorescein-EGF (f-EGF) association with A431 cells at 4°C. Here, similar data are presented with analysis of and correction for the contribution of photobleaching to the measured kinetic rate constants. Images were collected in time lapse with periodic fluorescence excitation leading to cyclic photobleaching and recovery. One-site and two-site first order binding models, with the addition of a first order photobleaching pathway, were solved for this pulse illumination acquisition procedure and fitted to the data by an iterative procedure. Applications of this analysis technique to more complicated models of the EGF/EGF-receptor interaction on intact cells are discussed.

Supported by NSF

*J. Chung, N. Sciaky, and D. J. Gross. 1993. *Biophys. J.* 64:A83.

M-Pos397

THREE-DIMENSIONAL MODELS OF NON-NMDA GLUTAMATE RECEPTORS

((M.J. Sutcliffe†, Z.G. Wo§ and R.E. Oswald§)) †Department of Chemistry, University of Leicester, Leicester, LE1 7RH, UK, and §Department of Pharmacology, Cornell University, Ithaca, NY 14853, USA.

We will discuss the three-dimensional models which we have produced for three types of non-NMDA ionotropic glutamate receptors: (1) an AMPA receptor, GluR1; (2) a kainate receptor, GluR6; and (3) a low molecular weight kainate receptor from goldfish brain, GFKARα. Our modeling was restricted to two domains of the proteins: (1) the extracellular domain which binds the neurotransmitter, glutamate, and (2) the transmembrane domain. This model building combined the methodologies of homology modeling, distance geometry, molecular mechanics, and interactive modeling. The resulting models were consistent with known constraints—particularly the requirement for glycosylation sites to be exposed on the surface of the extracellular domain. The models indicate new potential interactions in the extracellular domain between protein and agonists, and suggest that the transition from the "closed" to the "open" state involves the movement of a conserved positive residue (K683 in GluR1) away from, and two conserved negative residues (E651 and D652 in GluR1) into, the extracellular entrance to the pore upon agonist binding. As a first approximation, the transmembrane domain was modeled with a structure comprising a central antiparallel β-barrel (TMII) which partially crosses the membrane, and against which two α-helices (TMI and TMIII) from each subunit are packed; a third α-helix (TMIV) packs against these two helices in each subunit. Much, but not all, of the available data were consistent with this structure. Modifying the β-barrel to a loop-like topology for TMII produced a model consistent with available data.

M-Pos398

SOLID STATE NUCLEAR MAGNETIC RESONANCE (ss-NMR) OF LIGAND PROTEIN INTERACTIONS IN THE NICOTINIC ACETYLCHOLINE RECEPTOR (nAChR)

((P. Williamson, G. Gröbner, #K. Miller, A. Watts)) Biochemistry Dept., University of Oxford, South Parks Road, Oxford, OX1 3QU and #Dept. of Anesthesia, Harvard Medical School, MGH, BOSTON, MA 02114.

Although low resolution electron diffraction structures are available for the nAChR, very little is known at an atomic level about ligand binding. We have applied ss-NMR techniques to achieve two goals: 1). to probe the local environment around the ligand binding site, and 2). to deduce the conformation of bound acetylcholine(ACh). Due to motional restriction associated with ligand binding, we have been able to apply cross polarization magic angle spinning (CP-MAS) NMR methods to observe selectively carbon-13 enriched acetylcholine at the binding site which has been confirmed through the use of specific inhibitors such as α-bungarotoxin. The ring current effects expected, if the binding site has homologous characteristics (bounded by three aromatic residues) to the acetylcholine esterase, have not been observed suggesting that the nature of binding of ACh is either different, or the ligand is more distant (>4Å) from such residues in the receptor than in the esterase. Dynamic studies show that the ligand is mobile in the binding site. Rotational resonance (RR) NMR experiments are being performed between dilute homonuclear spin pairs within carbon-13 acetylcholine perchlorate giving distances which, in the solid are in agreement with those obtained by X-ray crystallography, and are being determined in the membrane bound receptor.

M-Pos399

THE STRUCTURAL ROLE OF THE PRO-X-PRO MOTIF IN DOMAIN 4 OF A MODEL HUMAN SEROTONIN 5HT2A RECEPTOR. ((J.A. Weinstein, F. Guarnieri, H. Weinstein)) Dept. of Physiology and Biophysics, Mt. Sinai School of Medicine, New York, NY 10029.

In a model of the transmembrane domains of the human serotonin 5HT2a receptor (5HT2aR), a member of the family of G-protein coupled receptors (GPCRs), transmembrane domain 4 (TM4) includes a Pro-Ile-Pro sequence that appeared incompatible with helical structure. Most models of GPCRs predict TM4 to be a 21 residue long helix ending before Pro-X-Pro or Pro-Pro motifs found in many neurotransmitter receptors. The Pro-Ile/Val-Pro sequence located in 5HT2 receptors may play a role in ligand specificity and affinity. In addition, the inherent flexibility of this region may be indirectly involved in receptor activation. Consequently, this sequence has been included in a 29 residue long TM4 domain of the 5HT2aR model. A structural database search suggested that the helix would be distorted at the Met position before the first Pro, and that the Pro-Ile-Pro starts a second helix. In the model, TM4 ends four residues after Pro-Ile-Pro based on the polarity of residues in this region. The feasibility of the distorted helix model was tested with energy minimization using ECEPP/3 [Némethy, G. et al, *J. Phys. Chem.*, **96**: 6472, 1992] from multiple starting points which had different combinations of *phi* and *psi* dihedral angles for the Met residue. An exploration of the conformational space was carried out with a simulated annealing Monte Carlo method (Conformational memories: Guarnieri, F. and Wilson, S.R., *J. Comp. Chem*, **16**: 648,1995] in which all dihedrals were allowed to rotate for the Pro-X-Pro and the four residues before the motif. The analysis yielded a finite number of feasible structures for the TM4 domain. Selection of the TM4 domain suitable for incorporation in the helix bundle of the 5HT2aR model is undertaken on the basis of optimization of hydrogen bonding patterns, and minimization of the solvent accessibility of the backbone carboxyl groups of the turn preceding the Pro-X-Pro. *Supported by NIH grants DA09083 and K05 DA00060.*

M-Pos400

QUANTIFICATION OF INTERCONVERTING RECEPTOR STATES FOR THE N-FORMYL PEPTIDE RECEPTOR IN HUMAN NEUTROPHILS AT 4°C ((J.F. Hoffman, G.M. Omann, and J.J. Linderman)) Depts. of Biological Chemistry, Surgery, and Chemical Eng., Univ. Michigan, and VA Medical Center, Ann Arbor, MI (Spon. by R. Neubig)

With the aid of high time resolution kinetic data extracted from a flow cytometer and mathematical modeling, we examined binding to the N-formyl peptide receptor on human neutrophils at 4°C. We show that a G-protein independent conversion from a low to a high affinity receptor state occurs at 4°C and, by correlating model simulations with response data in the literature, we show that the low affinity receptor state is consistent with an active, signaling form.

We further examined the competitive binding of different ligands (3 peptides and one antagonist) to the N-formyl peptide receptor at 4°C and determined that both the rate constant for ligand dissociation from the low affinity receptor and the rate constant for the conversion of the receptor from low to high affinity are ligand-dependent. The different rate constants for ligand dissociation (ranging from 10^{-2} to 1 s^{-1}) and for ligand-induced receptor affinity conversion (ranging from 10^{-4} to 10^{-2} s^{-1}) may contribute to differences in ligand efficacy.

M-Pos401

NEUTROPHIL N-FORMYL PEPTIDE RECEPTOR DYNAMICS AT 37°C ((J.F. Hoffman, J.J. Linderman, and G.M. Omann)) Depts. of Biological Chemistry, Surgery, and Chemical Eng., Univ. Michigan, and VA Medical Center, Ann Arbor, MI

High resolution kinetic data obtained by flow cytometry of the binding of the fluorescent peptide N-formyl-Nle-Leu-Phe-Nle-Tyr-Lys-fluorescein to the N-formyl peptide receptor of neutrophils at 37°C allowed for the development of a ligand binding model that accounts for ligand association and dissociation, receptor upregulation, ligand-receptor complex internalization, interconverting receptor states, and the quenching of internalized fluorescent ligand. Receptor upregulation was both agonist- and temperature-induced. Model fits of data on ligand association to phenylarsine oxide-treated cells suggested not only an inhibition of receptor upregulation and internalization but also a decreased rate of receptor affinity conversion. Model fits of data on ligand association to pertussis toxin-treated cells showed that while receptor upregulation was inhibited, rate constants for ligand binding, receptor affinity conversion, and internalization of ligand-receptor complexes were unaffected. This result suggested G-protein-mediated receptor upregulation and G-protein-independent receptor affinity conversion. The new model predicts statistically larger binding rate constants for the low affinity form of the receptor (k_f=8.4±1.9x10^7 $M^{-1}s^{-1}$, k_r=3.7±1.0x10^{-1} s^{-1}) than those previously reported for intact neutrophils.

M-Pos402

BIOACTIVE CONFORMATION OF TRH. ((L. Laakkonen, W.Li, J.H. Perlman, F. Guarnieri, K.D. Moeller, M.C. Gershengorn, R. Osman)) Mt Sinai School of Medicine, New York, NY10128, Washington University, St. Louis, MI 63130, Cornell Medical College, New York, NY 10021

Thyrotropin-releasing hormone TRH (pGlu-His-ProNH_2) acts through specific TRH receptors, TRHR, that belong to the superfamily of seven helix, G-protein coupled receptors. To study the action of TRH/TRHR, in the absence of experimental structures, we have combined data from computational and biological work to develop a molecular model of the complex, concentrating on the binding site. Mixed mode Monte Carlo / stochastic dynamics simulations show TRH in a helix-like conformation inside the receptor, which is very different from the extended conformation found in solution by NMR. As an independent way to study the binding conformation of TRH, two new covalently constrained analogs, that differ from each other only in the streochemistry of one carbon, were synthesized with a novel electrochemical method. The affinity and potency of the analogs were determined: K_d of (B) is 10^2 higher than that of TRH, whereas that of (A) is >10^4 times higher. Conformations accessible to TRH and (A) and (B) were studied with an importance sampling Monte Carlo method. The analogs show very little flexibility, and differ from each other only in one backbone angle. Interestingly, the major conformation of the analog B overlaps favorably with the simulated conformation of TRH inside the receptor, adding credibility both to the proposed bioactive conformation and the design of the binding pocket. *Supported by US PHS Grant DK43036*

M-Pos403

A MODEL OF THE THYROTROPIN RELEASING HORMONE RECEPTOR EXTRACELLULAR LOOPS. ((Anny-Odile Colson, Alex Smolyar, Liisa Laakkonen, Roman Osman)) Mount Sinai School of Medicine of the City University of New York, Department of Physiology and Biophysics, New York, NY 10029.

Previous mutational and computational studies of the thyrotropin-releasing hormone receptor (TRH-R) performed in our laboratory resulted in a proposed model of the binding pocket of TRH (pyroGlu-His-ProNH_2). To study the process of TRH entry into the transmembrane domain, we have constructed a receptor model with extracellular loops. Energy minimizations were performed for initial construction of the 3 interhelical loops. Subsequently, 14 MD simulated annealings from 1500K to 300K over 60ps followed by 60ps constant temperature simulations at 300K were performed on the model. The environment of the loops was represented by a distance dependent dielectric (ε=4r) and the helices were kept frozen. Analysis of 8400 structures from the constant temperature simulations reveals flexible and rigid segments in individual loops. Loop 1 is rigid at the amino and carboxy termini, whereas loop 3 has a 6 residue long rigid segment at its center, and is flexible at the termini. The first segment of loop 2 from F161 to C179 is mostly rigid while the remainder of the loop consisting of 10 residues is flexible. Analysis of the correlated motions of the loops may provide a description of the formation of a path for TRH entry.
Supported by US PHS Grant DK43036

M-Pos404

COEXISTENCE OF ENDOTHELIN ETA1, ETA2, ETB1 AND ETB2 RECEPTORS IN SMOOTH MUSCLE. ((H. Karaki, S. A. Sudjarwo, T. Yoneyama, M. Hori and H. Ozaki)) Dept of Vet Pharmacol, Univ of Tokyo, Tokyo 113, Japan.

In the rat aorta (with ETA), endothelin-1 (ET-1) and ET-3, but not sarafotoxin S6c (STX) and IRL 1620 (IRL), induced contraction which was inhibited by BQ-123, BQ-788 and [Thr^{18}, γ$MeLeu^{19}$]-ET-1 (TM). In the rat aorta with endothelium (with ETB), ET-1, ET-3, STX and IRL induced endothelium-dependent relaxation which was inhibited by RES-701-1 (RES), BQ-788, TM and ETB-desensitization. In the rabbit saphenous vein, all the agonists induced contraction. RES inhibited the effects of IRL. BQ-788 and ETB-desensitization inhibited the effects of ET-3, STX and IRL. TM inhibited the effects of all the agonists. In the rabbit trachea, all the agonists induced contraction. RES inhibited the effects of ET-3 and IRL. BQ-788 and ETB-desensitization inhibited the effects of ET-3, STX and IRL. TM inhibited the effect of all the agonists. In the vein and trachea, BQ-123 was ineffective, and BQ-123 with ETB-desensitization only partially inhibited the ET-1-induced contraction. These results suggest the existence of contractile ETA1 in rat aorta,, relaxing ETB1 in endothelium, and two subtypes of contractile ETA (ETA1, ETA2) and two subtypes of contractile ETB (ETB1 and ETB2) in rabbit saphenous vein and trachea.

M-Pos405

EVIDENCE FOR ACCELERATED TRANSBILAYER MOVEMENT OF PHOSPHATIDYLCHOLINE MOLECULES IN GIANT VESICLES UNDER DEFORMATION. ((Robert M. Raphael and Richard E. Waugh)) Dept. of Biophysics, University of Rochester School of Medicine and Dentistry, Rochester, NY 14642.

Numerous biological phenomena involve bending of the bilayer membrane. Thus, the response of membranes to mechanical deformation is important for many cellular processes. We imposed deformation in model membranes by pulling a tubular string out of the membrane (a tether) under a known force. Tether formation involves an expansion of the outer leaflet of the bilayer and a compression of the inner leaflet. This differential dilation can be dissipated by slip between the leaflets of the bilayer to equilibrate the area per molecule over the surface and by movement of molecules from the compressed leaflet to the expanded leaflet. Slip between the leaflets of the bilayer is opposed by viscous drag at the interface, and the time course of tether formation enables a measurement of the coefficient of intra-bilayer viscosity (~3.4 x 10^8 N-s/m^3) and the magnitude of the nonlocal bending stiffness (3.0 x 10^{-19} J). We have extended a theoretical model for dissipation of differential dilation originally described by Evans and Yeung (*Chem.Phys.Lipids.*73:39-56,1994) to account for transbilayer movement. The extended model enables the rate constant for dissipation of differential area to be measured from the time course of tether formation. The rate constant is measured to be .009 s^{-1}, which corresponds to a half-time for transbilayer movement on the order of 8 minutes. This accelerated rate is thought to be due to the formation of mechanically-induced defects in the structure of the membrane. This ability of membranes to move molecules rapidly across the bilayer under situations of high curvature may be important in membrane biogenesis, exocytosis and cell division. (Supported by NIH grant. no. HL-31524.)

M-Pos406

DETECTING SHAPE TRANSFORMATIONS IN MIXED PHOSPHOLIPID VESICLES USING LIGHT SCATTERING TECHNIQUES. ((D.G. Hunter and B.J. Frisken)) Department of Physics, Simon Fraser University, Burnaby, BC CANADA V5A 1S6.

Shape transformations in lipid vesicles have been predicted by the spontaneous curvature , bilayer coupling and area-difference elasticity theories, and phase diagrams for these various shapes have been computed. Recent electron microscopy experiments (Mui et al., Biophys. J. 69:930-941, 1995) have suggested that it is possible to cause mixed, charged phospholipid vesicles to changes their shapes by creating a pH gradient between the interior and the exterior of the vesicle. Using static and dynamic light scattering techniques, we have confirmed the existence of these shape transformations in mixed vesicles composed of phosphatidylcholine and phosphatidylglycerol. We compare the hydrodynamic radii and radii of gyration of spherical and non-spherical vesicles as a means of estimating the mean shape. (Supported by NSERC of Canada.)

M-Pos407

BRUSH-LIKE BEHAVIOR OF THE POLYMERIC COAT OF STERICALLY STABILIZED LIPOSOMES. ((Joel A. Cohen[1], Valentina Khorosheva[1] and Martin C. Woodle[2])) [1]University of the Pacific, San Francisco, CA 94115 and [2]Sequus Pharmaceuticals Inc., Menlo Park, CA 94025. (MCW's present address: Genta Inc., San Diego, CA 92121.)

The pharmacologic utility of sterically-stabilized liposomes as intravenous drug carriers is based on their ability to circulate in the bloodstream for extended periods of time. This longevity is conferred by the presence of grafted neutral hydrophilic polymer, typically polyethylene glycol (PEG), on the liposome surface. The polymeric coat presumably shields the liposome surface from protein and macrophage binding, although the precise protective mechanism is unknown. By use of particle electrophoresis, we have determined hydrodynamic thicknesses of grafted PEG polymer coats on PEG-DSPE/POPG/POPC multilamellar liposomes as a function of polymer length and grafting density. PEG molecular weights ranged from 120 to 5000 daltons (2 to 115 monomers), and the PEG-PE mole fractions ranged from 0.005 to 0.10. In all cases the mole fraction of $PEG\text{-}PE^- + PG^-$ was held constant at 0.10 to ensure a constant surface-charge density. Except in the low-density mushroom regime, the measured hydrodynamic thicknesses scaled approximately linearly with polymer MW and as the 1/3 power of the grafting density, in accordance with Alexander-de Gennes theory for surface-grafted brushes. Plasma longevity appears to require a brush-like configuration of the PEG polymer layer.

M-Pos408

OSMOTICALLY INDUCED OPTICAL CHANGES IN UNILAMELLAR VESICLES: EXPERIMENT AND THEORY. ((J.S. Pencer*, G. White*, J. Wood#, F.R. Hallett*)) *Department of Physics and #Department of Microbiology, University of Guelph, Guelph, ON N1G 2W1. (Spon. by J. Wood)

Studies of osmotically stressed vesicles are applicable to areas ranging from the modelling of membrane bilayers under strain to the development of liposome based drug delivery systems. Light scattering studies on unilamellar 100nm diameter DOPG (dioleoylphosphatidylglycerol) vesicles show the unexpected result that there is a decrease in low angle scattered intensity from vesicles swollen by a small (50 to 200 mOsm) osmotic down shift and an increase caused by a small osmotic up shift.

These results are inconsistent with a commonly used model that assumes negligible changes in the optical properties of the bilayer and predicts an increase in scattering with increasing osmotically induced strain. The experimental results are provided together with an interpretation based on an improved Rayleigh-Gans-Debye model for light scattering from vesicles that includes effects due to osmotically induced optical (refractive index) and structural (thickness) changes to the polar headgroup and acyl chain regions of the bilayer.

{Supported by NSERC}

ELECTROSTATICS

M-Pos409

DOMAIN FORMATION INDUCED BY BINDING OF BASIC LIGANDS TO MEMBRANES CONTAINING ACIDIC LIPIDS: AN ELECTROSTATIC MECHANISM. G.Denisov, S.Wanaski†, L.Peng†, M.Glaser† and S.McLaughlin. Dept. of Physiology and Biophysics, HSC, SUNY Stony Brook, NY 11794 and †Dept. of Biochemistry, University of Illinois, Urbana, IL 61801

Direct fluorescent microscope observations demonstrate that a basic peptide corresponding to the effector domain of MARCKS, a major PKC substrate, self-assembles into membrane domains enriched in the acidic phospholipid PS (Yang and Glaser, 1995, *Biochemistry* 34:1500). We present a simple model to describe this phenomenon. Domain formation decreases the electrostatic free energy of the system because binding of MARCKS peptide increases steeply with mole % of acidic lipids in the membrane or domain (Kim et al., 1994, *Biophys. J.* 67:227). For domain formation to occur, the decrease in the electrostatic free energy must overcome the increase in the free energy of mixing of neutral and acidic lipids in the membrane. Our computations, based on a Gouy-Chapman-Stern model of ligand binding, predict that domain formation is favored by low ionic strength, which agrees with experimental results obtained previously with MARCKS peptide. The model also predicts that domains break up at high ligand concentration. Experiments with spermine and pentalysine support this conclusion: the PS enriched domains formed at moderate spermine concentration do break up at higher concentration. Domains formed by MARCKS peptide do not disappear at high concentration, which suggests that additional factors (e.g. entropic repulsion between long charged rods) help domain formation with this peptide. The relevance of domain formation to signal transduction will be discussed.

M-Pos410

VIBRATIONAL STARK EFFECT ON THE CO-STRETCH OF HEME PROTEINS: ELECTROSTATIC FIELD CALCULATIONS AND VIBRATIONAL FREQUENCIES. ((Monique Laberge, Kim Sharp and J.M. Vanderkooi)) Johnson Research Foundation, Department of Biochemistry and Biophysics, University of Pennsylvania- Philadelphia, PA 19104

Several studies performed on carbonyl heme proteins and model compounds show that the carbonyl stretching frequency varies significantly (1940-2002 cm^{-1}) from one species to another. Recent work has recognized the importance of polar interactions on the CO-stretch of heme proteins and several models have been put forward. We propose that the charged amino acid residues of the protein act as an electrostatic field which can produce a vibrational Stark effect on the vibrational frequency of the CO ligand. In this work, we report electric field and electrostatic potentials calculations which show that a vibrational Stark effect can be invoked to explain the 6 cm^{-1} shift observed between the CO-stretch frequencies of horse and yeast cytochrome c-CO. The calculations are performed using the Finite Difference Poisson-Boltzman method: treating the protein as the field applied on the CO-ligand, potentials and electric field components are calculated at the CO with charge first formally distributed on the protein's ionizable groups and then partially on all atoms. Results show that formal charge variations induced by the protein on the CO yield a potential of -16.0 kT/e on the CO's oxygen for yeast cytochrome c and of -2.23 kT/e for the same oxygen in horse cytochrome c. The z-components of the electric field (aligned along CO) are respectively -0.916 and -2.06 kT/e/Å for yeast and horse c respectively. [Supported by NIH Grant PO1 GM48130]

M-Pos411

CONTINUUM APPROACHES TO MEMBRANE ELECTROSTATICS

(M.Wagner, J. Bordner, F. Saied, E. Jakobsson and S. Subramaniam) University of Illinois, National Center for Supercomputing Applications, Beckman Institute, Urbana, IL 61801

Electrostatic interactions play an important role in the structure and function of membranes. The dielectric behavior in the membrane-solvent interface and the charge distribution in the lipid-embedded proteins render the problem of calculating electrostatic potentials difficult. We report here the development of a rapid method based on the multigrid-Newton algorithm developed earlier in our laboratory for solving the nonlinear Poisson-Boltzmann equation that describes the electrostatics of a membrane-solvent system. We compute the electrostatic potentials for a realistic membrane-electrolyte interface and compare our results with the Gouy-Chapman models. We also apply the method for studying the electrostatic behavior of a model ion channel embedded in the lipid bilayer. Of special interest is the region of the interface that comprises the lipid head groups, the protein side chains and the solvent. This method provides a realistic approach for computing electrostatic potential of mean force profiles for ion transport.

Supported by the National Science Foundation and the National Center for Supercomputing Applications

M-Pos412

EFFECTS OF MOLECULAR SHAPE REPRESENTATIONS ON BOUNDARY ELEMENT METHOD FOR PROTEIN ELECTROSTATICS COMPUTATIONS

((Jie Liang[1,2], Herbert Edelsbrunner[2], Shankar Subramaniam[1,3])) [1]NCSA, Beckman Institute, and [2]Dept. of Computer Science, and [3]Dept. of Molecular and Integrative Physiology & Program in Biophysics and Computational Biology, University of Illinois at Urbana-Champaign,Urbana, IL 61801

Continuum models of protein solvation provide a convenient route to obtaining electrostatic potentials in proteins. A good geometric shape representation is critical for obtaining an accurate solution of the PB equation. Boundary element method (BEM) has been employed previously to solve the Poisson-Boltzmann equation for protein electrostatics computations. In this presentation, we report BEM solution of the Poisson-Boltzmann equation using an alpha-shape based surface triangulation scheme. We take the underlying topological structure of the molecule into account and triangulate the surfaces at different levels of resolution. With this representation of the protein surface, we also compare several numerical techniques for solving the dense, nonsymmetric linear equations resulting from the boundary integral formulation. Supported by grants from the National Science Foundation.

M-Pos413

PREDICTION OF PROTEIN PKAS: INFLUENCE OF PARAMETERS UPON ACCURACY FOR FOUR PROTEINS.

((J.Antosiewicz[1], J.A. McCammon[2] and M.K.Gilson[3])) [1] University of Warsaw, Warsaw, Poland. [2] University of California at San Diego, San Diego, CA. [3] Center for Advanced Research in Biotechnology/NIST, Rockville, MD.

Previous calculations of protein pKas based upon the Poisson-Boltzmann model for electrostatics yielded more accurate results when the dielectric constant of the protein was assumed to be 20 than when a more realistic value of 4 was used. The present study demonstrates that the results with a protein dielectric constant of 4 become more accurate when atomic parameters optimized for use with the PB model are employed. The results also improve when solution structures obtained from NMR studies are used in place of the crystal structures of the proteins. Nonetheless, the most accurate cumulative results are still those obtained with a protein dielectric constant of 20.

The accurate results obtained here permit analysis of the causes of the pKa shifts of the protein turkey ovomucoid third domain. The resulting picture differs significantly from that inferred from an analysis of measured chemical shifts. A resolution of the apparent discrepancies is proposed.

M-Pos414

THE ELECTROSTATIC POTENTIAL FROM THE BACKBONE DIPOLES IS PREDOMINANTLY POSITIVE INSIDE ALL PROTEINS

((M.R.Gunner, M. Saleh, E. Cross, A.-U.-Doula, and M. Wise)) Physics Dept. City College of New York., 138th St. and Convent Ave. N. Y., NY. 10031.

The electrostatic potential due to the backbone dipoles was calculated for >300 different proteins with >150 different folds using a dielectric continuum model with the programs GRASP or DelPhi (Nicholls & Honig, Columbia Univ)). The average potential generated by the charges on the backbone amide bonds contributes ≥5 kcal/e to 31±8% and ≤-5 kcal/e to 6.5±2.5% of the protein's interior volume (average >300 proteins). Thus, the neutral backbone makes a significant contribution to the electrostatic potential in all proteins. In addition, in every case the backbone dipoles yield positive rather than negative potentials in a larger portion of the protein. These conclusions hold for all motifs. In particular, the backbone in β-sheet proteins has as large an impact as the backbone in α-helical proteins. The contributions of individual amide groups to the interior potential depend on their orientation. If the O is more exposed to solvent the amide makes the internal potential more positive, while an exposed H lowers the potential. One reason for the positive interior is that the van der Waals radius and partial charge of the amide O is larger than that of the H, so structures that orient the amide carbonyl oxygens further apart and to the protein surface are more prevalent. It is to be noted that the final potentials found in the protein are quite different than those produced by the backbone alone. Thus, acidic sidechains, if buried in regions where the contribution of the backbone is positive yield a protein which can be negative inside. The preponderance of areas where the backbone can stabilize a negative group suggest a reason why there are more buried acidic than basic sidechains in proteins. (supported by N.I.H. GM-42726).

M-Pos415

POISSON-BOLTZMANN CALCULATIONS OF TRIPLE HELICAL DNA FORMATION.

((GEORGE R. PACK, LINDA WONG AND GENE LAMM)) UIC College of Medicine, Rockford, IL 61107

The energetics of formation of a triple helical structure in homopurine·homopyrimidine mixtures have been modeled using Poisson-Boltzmann calculations. Oligomers with the sequence $d(TC)_n$ and $d(AG)_n$ form hydrogen-bonded triple helical structures of the form $d(TC)_n \cdot d(AG)_n \cdot d(TC^+)_n$. The third base, a pyrimidine in this case, forms Hoogsteen-type hydrogen bonds with the purine. This requires that the cytosine residues of the third strand are protonated at N3. The pK_a of cytosine, 4.3 in the isolated molecule, is raised by the strong electrostatic fields in the triple helix. We report calculations of the effective pK_a of this cytosine and compare the results with experimental studies of the extent of triple helix formation as a function of pH. This provides a test of various models of the dielectric constant for nucleic acids and their local environment.

M-Pos416

THE CALCULATION OF DIELECTRIC COEFFICIENTS NEAR POLYELECTROLYTES IN SOLUTION

((GENE LAMM AND GEORGE R. PACK)) UIC College of Medicine, Rockford, IL 61107

The recent application of numerical Poisson-Boltzmann methods to the determination of the electrostatic potential and counterion distribution around polyelectrolytes such as DNA has prompted the determination of accurate solvent dielectric coefficients. The previous assumption for proteins of using a constant of 78.4 for the solvated environment appears inadequate when dealing with the much higher potential gradients of charged polyelectrolytes in solution. Approximations using lower dielectric values of 10 near the surface and increasing with distance to a bulk value of 78.4 have been incorporated into finite difference Poisson-Boltzmann techniques and have led to more reasonable estimates of counterion distributions. Choosing the dielectric coefficient, however, has usually been less than rigorous. To put these techniques on a firmer foundation we present a simple procedure for computing reliable dielectric coefficients near a macromolecular surface. To show the accuracy of the calculation, we compare results for the dielectric coefficient near the surface of DNA with data from recent experiments measuring this quantity in both the major and minor grooves of B-form DNA. This procedure can be useful for proteins as well and may be particularly applicable in solvent pockets where strong potential gradients may lead to the electrostatic guiding of ions or ligands toward specific binding sites.

M-Pos417

ELECTROSTATICS OF PROTEINS: DESCRIPTION IN TERMS OF TWO DIELECTRIC CONSTANTS SIMULTANEOUSLY. ((L.I. Krishtalik, A.M. Kuznetsov, E.L. Mertz)) A.N. Frumkin Institute of Electrochem. Russian Academy of Sciences, Leninskii prosp. 31, 117071 Moscow, Russia. (Spon. by S.E. Ostroy)

There are two components of the energy in the semi-continuum treatment of the energetics of charge formation (or transfer) inside a protein. The energy of interaction of the ion with the pre-existing intraprotein **E** field, and the energy of the medium polarization by the newly-formed charge. The pre-existing field is due to charges (partial or full) of the protein atoms fixed in a definite structure. This field depends only on the electronic polarization of the protein because the polarization due to shifts of heavy atoms has been already accounted for by their equilibrium coordinates. Therefore, the first component should be calculated using the optical dielectric constant, ε_O, for protein and the static constant, ε_{SW}, for aqueous surroundings, as the positions of H_2O molecules are not fixed. The formation of a new charge, absent in the equilibrium X-ray structure, results in electronic polarization and small shifts of all charged atoms, i.e. medium polarization described by the static dielectric constant, ε_S, of the protein, and polarization of water, ε_{SW}. Thus, in calculations of total energy, two different protein dielectric constants are operative. (Supported by grants from the ISF (MD93000) and NIH (Fogarty TW00063)).

M-Pos418

MACROION ATTRACTION BY CORRELATED COUNTERION FLUCTUATIONS: APPLICATION TO CONDENSATION OF DNA ((I.F.Rouzina & V.A.Bloomfield) Biochem, U of Minn,St.Paul MN 55108)

Electrostatic correlation between screening counterions can lead to attraction of highly charged macroions. We present a simple semianalytical method to calculate the attractive free energy. It is based on a 2D picture of correlations, taking into account that the majority of the screening ions reside in a thin surface layer with thickness of order $l_z = q_e/4\pi\sigma z l_b$, where q_e is the electron charge, z the counterion valence, σ the surface charge density and l_b the Bjerrum length. The parameter defining the total interaction is the 2D coupling strength $\Gamma_2 = (zq_e)^2/a_z\varepsilon kT$, where $a_z = (\sigma/zq_e)^{-1/2}$ is the average lateral distance between counterions. A stable bound state of the macroions exists if $\Gamma_2 > \Gamma_{2\,cr} = 1.8$. The theory also permits estimation of equilibrium spacing and binding energy. At small surface separation in low ionic strength both correlation attraction and kinetic repulsion are independent of bulk ionic composition. Universal curves, when rescaled with the appropriate system parameters, reproduce well the results of GCMC and HNC calculations. These ideas are used to interpret the collapse transition of DNA in monovalent salt solution upon addition of multivalent counterions. Most features of the transition, including the change in the short range repulsive decay length coupled to the onset of the collapse, are reproduced simply by the replacement of monovalent by multivalent counterions at the surface, leading to the increase of Γ_2. Calculated values of Γ_2 are consistent with the observation that DNA condensation occurs when about 90% of the DNA charge is neutralized by counterions.

M-Pos419

A SELF-CONSISTENT, FREE ENERGY APPROACH TO CALCULATE pH DEPENDENT PROPERTIES OF PROTEINS. ((E.L. Mehler, F. Guarnieri, & P.T. Morgan)) Dept. of Physiol. & Biophys. Mount Sinai Schl. of Med., CUNY, New York, NY 10029. (Spon. by V. Brezina)

A novel, constrained variational approach is used to derive self-consistent equations for determining the optimal, pH dependent, charge state of all the protonatable groups in a protein. The method uses a screened Coulomb potential (SCP) with a sigmoidal, distance dependent dielectric screening function for calculating the interaction energies between the charges in a protein. In addition, a formula is derived from the integral Born equation, using radially dependent permittivities, for calculating the solvation energy. With this formulation the pK's of the titratable groups, T, can be estimated from the relation

$$pK_T(p) = pK_T^o(s) + (w_T^{int} + \Delta w_T^{sol})/2.303RT$$

where w_T^{int} and Δw_T^{sol} are the interaction and solvation contributions, respectively, and pK^o is the model solvent pK. The method has been applied to calculate the pK's of the titratable groups in bovine pancreatic trypsin inhibitor, hen egg white lysozyme, ribonuclease A and ribonuclease T_1. The results are compared to recent calculations by J. Antosiewics et al., 1994, JMB, **238**, 415-436, who used the finite difference method for solving the Poisson-Boltzmann Equation (FDPB). It is shown that the reliability of the present method is similar to that achieved by the FDPB approach (overall rmsd between calculated and measured pK is about 0.7 for both methods), but that the approach derived here is about 10^2 - 10^3 times faster. The origin of this increase in computational speed is the calculational simplicity inherent in using an SCP, and that the statistical treatment for calculating the charge state of each titratable group is bypassed.

M-Pos419a

BIOLOGICAL EFFECTS OF EXTREMELY-LOW-FREQUENCY (ELF) MAGNETIC FIELDS MAY GO LINEARLY (NOT QUADRATICALLY) WITH FIELD AMPLITUDE. ((Stefan Machlup[1], Carl F. Blackman[2], Janie Page Blanchard[3])), Case Western Reserve University[1], NHEERL, U.S.EPA[2], Bechtel Corporation[3].

There is controversy concerning the mechanism of biological changes caused by exposure to weak ELF magnetic fields[1]. Polk and Wu[2] treat the response of a trapped ion to AC + earth's field by classical electromagnetic theory. Because the natural frequency of the ion oscillating in the trap (intra-red) is at least 10^6 times the Zeeman splitting, the solution of equations of motion can be approximated as a frequency-modulated oscillation, with the difference of the two Zeeman frequencies beating with the ELFrequency (ion parametric resonance). How does this differ from Lednev's approach[3], which focuses on the intensity of the radiation from the ion? We are concerned with biological activity controlled by chemical reactions, whose rate depends on electron- wavefunction overlap that goes linearly (not quadratically as does radiation intensity) with the near (not a radiated) magnetic field. Such an assumption for the mechanism of biological effects of weak ELF magnetic fields overcomes "constraints" enumerated by Adair in ruling out the possibility of power-line-induced biological changes, including cancer.

[1] Robert K. Adair, "Constraints on biological effects of weak extremely-low-frequency electromagnetic fields", Physical Review A43: 1039-1048 (1991) and "Criticism of Lednev's Mechanism for the Influence of Weak Magnetic Fields on Biological Systems", Bioelectromagnetics 13: 231-235 (1992)
[2] C. Polk and S.H. Wu, "AC/DC Magnetic Field Synergism: Comments on the Lednev and IPR Models", The 1994 Annual Review of Research on Biological Effects of Electric and Magnetic Fields from the Generation, Delivery and Use of Electricity, Nov. 6-10, 1994, Albuquerque, NM.
[3] V.V. Lednev, "Possible Mechanisms for the Influence of Weak Magnetic Fields on Biological Systems", Bioelectromagnetics 12: 71-75 (1991)

STATISTICAL THERMODYNAMICS

M-Pos420

HYDROPHOBIC INTERACTIONS: A FLUCTUATION MODEL. ((Gerhard Hummer, Shekhar Garde,[1] Angel E. García, Andrew Pohorille,[2] and Lawrence R. Pratt)) Theoretical Division, Los Alamos National Laboratory, Los Alamos, NM 87545, U.S.A. [1]present address: Department of Chemical Engineering, University of Delaware, Newark, DE 19716, U.S.A. [2]Department of Pharmaceutical Chemistry, UCSF, San Francisco, CA 94143; and NASA-Ames Research Center, MS-239-4, Moffett Field, CA 94035-1000, U.S.A.

Protein folding, lipid-membrane formation, and oil-water separation are tightly associated with hydrophobic interactions. These poorly understood interactions of nonpolar solutes and residues in water are investigated based on concepts of information theory. A model describing hydrophobic effects in terms of density fluctuations is developed. It accounts quantitatively for the central hydrophobic processes of cavity formation, association of hydrophobic solutes, and torsional equilibria in hydrocarbons. The physics underlying hydrophobic effects is clarified. Important biological applications will be discussed such as ligand docking to binding sites and conformational equilibria of amino-acid side chains.

M-Pos421

THE PLANCK-BENZINGER THERMAL WORK FUNCTION: NEW THERMODYNAMIC STUDIES ON THE HYDROGEN BOND ENERGY OF LIQUID WATER. ((P.W. Chun)) Dept. of Biochem. & Mol. Biol., Univ. of Florida, Gainesville, FL 32610-0245

The Planck-Benzinger thermal work function, $\Delta W(T) = \Delta H(T_o) - \Delta G(T)$, represents the heat flux term responsible for the breaking or forming of noncovalent bonds in a chemical reaction, and thus is a more accurate measure of the basic energy level of that process. Based on the Planck-Benzinger thermal work function, the temperature-invariant enthalpy, $\Delta H(T_o)$, for the hydrogen-bonded water cluster in equilibrium with non-hydrogen bonded H_2O molecules was determined to be 3.6 kcal mole^{-1}, while the $\Delta H^1(T_o)$ value for the dielectric relaxation of liquid water, using the transition state theory, was 3.8 kcal mole^{-1}. The temperature-invariant enthalpy, $\Delta H^o(T_o)$, for the dimerization and condensation of water vapor in the standard state were determined to be 0.39 kcal mole^{-1} and 0.044 kcal mole^{-1} respectively. These thermodynamic results indicate that the Frank-Wen flickering cluster model (Frank, H.S., and Wen, W.Y., Discussion Faraday Society, 24, 133-140, 1957) and dielectric relaxation model exhibit a rigid liquid water structure or glass-like crystal state. The fact that the entropy of the system appears to remain independent of temperature suggests that there is no significant reorientation between unbonded and hydrogen-bonded water molecules in equilibrium in this system.

This work was supported by a Faculty Development Award, Division of Sponsored Research, University of Florida.

M-Pos422

EXTRACTING HYDROPHOBIC PARAMETERS: SOLVATION EFFECTS OF MOLECULAR SIZE AND SHAPE. ((Hue Sun Chan, Anton E. Krukowski* and Ken A. Dill)) Department of Pharmaceutical Chemistry and * Graduate Group of Biophysics, University of California at San Francisco, CA 94143-1204.

We present a theoretical framework for resolving the recent debate on the validity of including "volume" or "size" effects in the extraction of contact free energy parameters from transfer experiments. The question is the following: If a solute and its solvent have different molecular sizes, is the configurational entropic part of the chemical potential more appropriately given by "classical" solution theory or by Flory-Huggins theory? We study a general statistical mechanical treatment of solvation, a generalized Flory-Huggins theory, related treatments by Hildebrand and by Sharp et al., and exact lattice models of solvation to determine the physical basis for size-dependent contributions. We find that the extra configurational entropy in the Flory-Huggins theory does not arise from the disparity of sizes of solute and solvent, from free volume, or from artifacts of approximations. Rather, when solutes and solvents have sufficient complexity that they can "interfere" with each other in solution, there is an "entropy of coupling" of translational freedom to excluded volume or internal or rotational degrees of freedom. The coupling effects among molecules that are "articulated," such as flexible polymers for example, are reasonably well approximated by Flory-Huggins theory, but globular molecules are qualitatively and quantitatively different, and are better treated by the classical chemical potential, consistent with experiments of Shinoda and Hildebrand. This study rationalizes several other experimental and simulation studies, and indicates that coupling entropies that depend on molecular size and shape are needed in general to treat complex solvation processes.

M-Pos423

BINDING ENERGETICS: MODEL STUDY OF CYCLIC DIPEPTIDES. ((P. Brady, K. Sharp)) U. of Pennsylvania, Philadelphia, PA 19104.

Bimolecular binding processes are ubiquitous in the biological sciences and the ability to compute absolute binding constants has implications for immunology, pharmacology, and rational drug design. Our calculation strategy involves using surface area hydrophobics, Poisson-Boltzmann electrostatics, and normal mode vibrational analysis to calculate ΔG, ΔH, and ΔS. This procedure was tested on the solvation and crystallization equilibria of cyclic diglycine. The calculated solvation free energy is -16.4 kcal/mol (-16.3 kcal/mol experimental), with electrostatics accounting for -18.6 kcal/mol and hydrophobics for 2.2 kcal/mol. For gas-to-crystal transfer, ΔH_{calc} is -24.4 kcal/mol (-24.8 kcal/mol experimental) and the intrinsic binding free energy is -14.7 kcal/mol (-19.0 kcal/mol). The association entropy, which is the barrier to binding posed by the exchange of high-entropy translational and rotational degrees of freedom for lower-entropy vibrational motions, was -27.6 eu (-8.2 kcal/mol), compared to a total experimental entropy of -19.5 eu (-5.8 kcal/mol).

M-Pos424

OPTIMIZING THE POTENTIAL FUNCTIONS FOR PROTEIN FOLDING ((Ming-Hong Hao and Harold A. Scheraga)) Baker Laboratory of Chemistry, Cornell University, Ithaca, NY 14853 -1301

A correct potential function is the foundation for fundamental theoretical studies of protein folding. In this work, we studied the problem of optimizing potential functions to improve the theoretical perspective for folding a protein correctly to its native structure under realistic conditions. A general procedure is proposed to optimize the energy parameters for proteins based on the conformational distribution of the protein in both folded and unfolded states. The complete density of states of the protein, used in the optimization, is represented by multiple canonical distributions generated by an entropy sampling Monte Carlo simulation. The optimization of the energy parameters is carried out by gradient descent in an iterative process which updates the conformational distributions of the protein with the changed energy parameters. By this optimization approach, the folding temperature and the statistical weight of the native state of the modeled protein can both be increased, the cooperativity of the folding transition is enhanced, and, by a proper choice of the interaction scheme, a two-state folding transition can be realized. A case study of the protein crambin was carried out, in which, by optimizing the energy parameters, the ground state of a lattice model of the protein is defined to less than 1.5 Å rms deviation from the crystal structure of crambin, the native state of the model protein is the lowest-energy structure among all other alternatives, and, most importantly, the model protein has the desired statistical-mechanical characteristics for correct folding. (Supported by NIH grant GM-14312 and NFS grant DMB-90-15815).

M-Pos425

Electrophoresis Of DNA In An Irregular Matrix And Counterion Condensation. ((U. Mohanty)), Department of Chemistry, Boston College, Chestnut Hill, MA 02167

We propose a model to describe the electrophoretic mobility and diffusion of polymer chains through a random matrix like agarose gel. The lifetime of the conformations of the gel as well as the entropic interactions between the matrix and the probe are taken into account by a generalization of the Zimm-Lumpkin model.
We make use of density functional theory of inhomogeneous systems and theories of liquid state to describe counterion condensation in polyelectrolytes and oligoelectrolytes. Our results are compared with Manning's counterion condensation and non-linear Poisson-Boltzmann approaches.

M-Pos426

ANALYSES OF ENZYMIC TRANSDUCTION OF FLUCTUATING ELECTRIC SIGNALS
((Yi-der Chen and T. Y. Tsong)) NIDDK, NIH, Bethesda, MD 20892-0520 and Department of Biochemistry, Hong Kong University of Science and Technology (Spon. by Robert Rubin)

Memebrane enzymes have the ability to transduce a signal or energy from a regularly oscillating potential, such as an electric, acoustic, osmostic, or chemical potential. A previous study (Biophys. J. 67:1247 (1994)) showed that this energy coupling also applies to random telegraph fluctuating electric fields (RTF) consisting of alternating square electric pulses of constant amplitude with random lifetimes. Recently, it has been shown experimentally that a small but significant change in the efficiency of transduction is observed when the amplitude of the applied RTF is not constant but randomly distributed according to a Gaussian distribution function. In this report, we extend the previous stochastic arguments (PNAS 84: 729 (1987)) and show how to calculate or evaluate the fluctuation-induced flux of an arbitrary biochemical cycle in this case. Specifically, we show that the directional flux of an arbitrary biochemical cycle induced by this kind of random telegraph noise can be evaluated by a general iteration procedure. The application of the theory and procedure to a number of amplitude distributions is discussed.

M-Pos427

INTEGRATED FRAMEWORK FOR MODELING, SIMULATION AND VISUALIZATION OF CELL STRUCTURE AND PHYSIOLOGY. ((J.C. Schaff, J.H. Carson[1], L.M. Loew[2])) Center for Biomedical Imaging Technology, Department of Biochemistry[1] and Physiology[2], University of Connecticut Health Center, Farmington, CT 06030.

A method is described for modeling, simulating, and visualizing cell structure and physiology within a single integrated framework. The spatial organization of cellular structure is captured by incorporating geometry derived from volume data sets. Each geometric feature is identified as a specific cellular component and associated with a mathematical model that represents its function in a cell. The phenomena represented by the models fall into two categories, chemical dynamics and mechanical dynamics. The current implementation of the chemical dynamics involves uniformly sampling the model geometry into simulation elements. The dynamics are described as fluxes of molecular species across boundaries separating adjacent elements. These fluxes can be functions of diffusion, ion drift, membrane potential, chemical reaction, or any other relationship involving the spatial distribution of molecular species. Membranes may be represented by element boundaries separating dissimilar elements. The sum of all concentrations of each molecular species within each simulation element constitutes the state variables of the system. The modeling of mechanical dynamics requires a mesh of connected elements where each element interacts with its neighbors through applied forces and each element reacts according to applicable equations of motion. The current implementation describes cell surface movement as tensile, compressive, and viscous forces acting on distributed inertial masses. Geometric models and simulation elements are both displayed within an integrated 3D viewer. The model can be displayed as polygonal surfaces that can be quickly manipulated with accelerated graphics. The simulation elements are then volume rendered into the same scene as the surface model. Simulation results can be directly correlated with experimental time series volume datasets because the simulation is of a model with the same geometric features. This method allows a framework for encapsulating knowledge about the interaction of intercellular components. As a demonstration of chemical dynamics we have modeled the progression of a wave of increased free calcium ion concentration that occurs after a localized intracellular triggering event.

M-Pos428

DEGENERATE RECOGNITION LEADING TO SELF-ORGANIZATION IN COMPUTER SIMULATED SELECTIVE SYSTEMS (S.P. Atamas) University of Maryland School of Medicine, Baltimore, MD 21201. (Sponsored by R.A. Sjodin)

In certain biologic systems, the signal selects functional or numerical expansion of the recognizing elements. Examples of these systems include the immune system, brain cortex, and evolution. One common features of these Darwinian-type systems is degenerate recognition, in which one signal can recognize several different elements, with different affinities and consequences. For example, T cell antigen receptors and antibodies demonstrate relative but not absolute specificity of recognition. Thus, the variables of dose of the signal and affinity of the recognizing element modulate the outcome. Another feature of these systems is the ability to create self-organizational patterns, which do not mirror the incoming signals. The hypothesis of this study is that degenerate recognition with subsequent selection of recognizing elements can explain self organization of these systems. An entirely numerical model was explored, using the cellular automata approach. Three intrinsic features of a common selective system were incorporated into this model: a large number of recognizing elements; degenerative recognition of stimuli by these elements; and subsequent selection. Different numerical patterns of incoming stimuli were tested. The model showed self-organizational dynamics. Usually, the population of recognizing elements demonstrated initial period of equilibrium, then a chaotic transitional state, and, finally, the bifurcational appearance of a stable self-organizational pattern. The final resolution into a stable pattern can be either gradual or quasi-saltational. I conclude that systems with a large number of recognizing elements, degenerative recognition, and selection of recognizing elements can self organize based upon the pattern of the incoming stimuli. This may explain some aspects of negative selection in the immune system.

M-Pos429

MS WINDOWS VERSION OF NEURON SIMULATION PROGRAM

J. W. Moore*, Dept. Neurobiology, Duke Univ. Med Cntr., Durham, NC 27710, M. L. Hines, Dept. Computer Sci., & N. T. Carnevale, Dept. Psychology, Yale Univ., New Haven CT 06520

NEURON is a nerve simulation system designed to solve problems involving complex cell morphology, cell membranes with ion-specific channels, and ion accumulation. In 1993, we demonstrated a graphical interface version of NEURON at several meetings. It employed "InterViews", an X-windows based interface builder, and thus ran only on unix machines - but could be accessed from DOS and Macintosh machines via X-window servers.

Several improvements since then enhance its ease of use and make it readily available to a much wider group of users:

1) Porting NEURON to PCs running Microsoft Windows 3.1.

2) Placing a hypertext User's Manual on-line on the Internet, accessible by Internet browsers.

3) Making NEURON a "viewer" for browsers so that simulations can be run from the User's Manual via hypertext links. Current examples in the Manual range from simulations of (a) current and voltage clamps of patches of membrane with a variety of mechanisms, (b) impulse propagation in both uniform and non-uniform axons, and (c) temporal and spatial integration of synaptic imputs to (d) Ca dynamics in nerve terminals, These "digital neurons" offer the facility for learning neurophysiological function while also learning how to use NEURON.

4) Internet availability of NEURON (both unix and PC versions, including instructions for downloading and installation) along with the User's Manual at http://www.neuro.duke.edu/neuron/home.html

Support: NIH grant NS11613 and Yale Cntr. for Theoret. and App. Neurosci.

M-Pos430

MODELING ACTION POTENTIAL VARIATION IN CANINE VENTRICLE. ((S.S. Demir and R.L. Winslow)) Dept. of Biomedical Engineering, The Johns Hopkins Univ. School of Medicine, Baltimore, MD 21205

A mathematical model was developed to investigate electrophysiological differences between action potentials of epicardial, midmyocardial (M) and endocardial single cells in canine left ventricle. The model depends on both voltage-clamp and action potential data, and has two major components; a membrane model and a fluid compartment. The membrane model describes the known ionic currents, membrane pumps and exchangers in canine ventricular cells. The fluid compartment model formulates mass balance equations for the ions both in the cytoplasm and the extracellular space, as well as Ca^{2+} buffering by the myoplasmic proteins and uptake and release of Ca^{2+} by the sarcoplasmic reticulum. Model results show that the prominent spike, dome, and phase 3 repolarization characteristics experimentally recorded in the action potentials of epicardial and M type cells, but not of endocardial cells, are due to the various contributions of the I_{to}, I_{Ks}, I_{Kr} and I_{CaL} currents in these cell types. These single cell modeling studies therefore contribute to an understanding of ionic basis of action potential variation within the canine ventricle.

M-Pos431

THE INFLUENCE OF SPATIAL INHOMOGENEITY ON CYTOSOLIC CALCIUM WAVES. ((M. S. Jafri)) Dept. of Biomedical Engineering, The Johns Hopkins Univ. School of Medicine, Baltimore, MD 21205

This study investigates some of the effects of spatial inhomogeneity in the cell on Ca^{2+} wave propagation based on a realistic model for agonist induced calcium waves [Jafri and Keizer, *Biophys. J.* 69 (1995)] that includes the activation and inhibition of the IP_3 receptor Ca^{2+} channel (IP_3R) and the ryanodine receptor (RyR) in the ER membrane, diffusion of calcium in the cytosol and the ER, the breakdown and diffusion of IP_3 and the effects of both mobile and stationary buffers. The Ca^{2+} pumps, channels, leaks, IP_3 production sites, and stationary buffers are inhomogeneously distributed in the cell. The Ca^{2+} wave speed increases in regions where there are more channels or pumps and in regions where there is less of a leak from the ER or less stationary buffers. The inhomogeneous distribution of IP_3 can alter wave propagation. We also studied the effects of the separation of clusters of IP_3R Ca^{2+} release sites. The maximum separation between sites that allows Ca^{2+} wave propagation is greater for kinematic waves than for trigger waves. Similar results were obtained for RyR. The effects of a mixed population of ryanodine receptors and IP_3R on wave propagation was also studied. These results are applied to simulate some of the spatially complex patterns of calcium waves seen in various cells such as acinar cells and astrocytes.

M-Pos432

IDEALIZATION OF SINGLE-CHANNEL CURRENTS USING THE SEGMENTAL K-MEANS METHOD. ((Feng Qin, Anthony Auerbach and Frederick Sachs)) Department of Biophysical Sciences, SUNY at Buffalo, Buffalo, NY 14214. (Spon. G. Willsky)

Hidden Markov modeling (HMM) has been emerging as a powerful technique for single-channel data analysis. Although capable of providing both amplitude and kinetic parameters, the HMM technique is slow compared to techniques based on dwell times (Ball and Sansom. 1989. *Proc. R. Soc. Lond. B.* 236:385-416). Thus, idealization of a data record is still an important step in kinetic analysis.

To obtain an idealized record, the standard HMM exploits the Baum-Welch algorithm to find the model parameters and then applies the Viterbi algorithm to detect the underlying state sequence (Chung et al. 1990. *Proc. R. Soc. Lond. B.* 329:265-285). While being a full likelihood method, the Baum-Welch algorithm is computationally expensive. We present here an alternative HMM technique for idealization, namely, the segmental k-means method (Rabiner et al. 1986. *AT & T Tech. J.* 65:21-31). This method employs the joint probability of the data and underlying state sequence as the likelihood function. To maximize the likelihood, the method proceeds in iterations of two fundamental steps. The first step is to segment the data into state sequence for an assumed model. This step is optimally performed by the Viterbi algorithm, which leads to a state sequence with the maximal likelihood for the given model. The second step is to reestimate the model based on the newly idealized state sequence. This is done by calculating the mean and variance of the data points associated with each state. The new mean is subsequently used as the state amplitude and the variance as the noise model. Compared to the Baum-Welch algorithm, this method is much faster and retains comparable accuracy.

Supported by NSF (AA), MDA (FS) and SUNYAB School of Medicine and Biomedical Sciences.

M-Pos433

System Identification of Phycomyces Light-Growth Response; The Box-Jenkins Technique. ((C.H. Trad)) Physics Department, American University of Beirut 850 Third Avenue New York . N.Y. 10022-6297.

The Box-Jenkins model provides a simple representation of the input-output relation of the light-growth response of the zygomycete phycomyces blakesleeanus. The input-output relationship of the growth-response is obtained as a discrete model in the Z-transform domain. The main advantage of the resulting model lies in the fact that representation in the Z-transform domain allows easier conversion to difference equations, differential equations, state-variables models or transfer functions in the Laplace-transform domain. The optimal Z-domain input-output model is found to be a transfer function containing four zeros and five poles together with a delay that reflects the lag of the output with respect to the input. Results are in agreement with earlier work using Wiener kernels as the means of the identification process.

M-Pos434

THE CALCULATION OF pK_aS IN PROTEINS: RESULTS FROM A LARGE-SCALE MOLECULAR DYNAMICS SIMULATION OF LYSOZYME IN AQUEOUS SOLUTION WITHOUT TRUNCATION OF LONG-RANGE FORCES. ((Francisco Figueiridо, Gabriela S. Del Buono and Ronald M. Levy)) Department of Chemistry, Wright-Rieman Laboratories, Rutgers, The State University of New Jersey, Piscataway, NJ 08855-0939. (Spon. by R. Levy)

The calculation of ionization constants (pK_as) in biological macromolecules is still a challenging project. Since they arise from delicate cancellations among large energy terms, they provide a very stringent test of atomistic models. Moreover, they require an accurate treatment of the long-range electrostatic forces, which precludes the use of time-saving cutoffs. We have run a simulation several hundred picoseconds long of lysozyme in a large box of water (14,093 molecules) to minimize the finite-size effects. To do this, a version of the Fast Multipole Method (FMM) that runs in parallel using the Parallel Virtual Machine (PVM) message-passing environment was implemented as a subroutine in the molecular mechanics program impact. Our implementation correctly handles periodic boundary conditions, so that infinite-range correlations can be taken into account. The simulation was run on a 32-processor Cray T3D, a state-of-the-art massively parallel machine and it took an average of 1 hour per picosecond. From this simulation we obtain the distribution of electrostatic potentials at the titratable sites, which allows us to determine the relative pK_as.

M-Pos435

DISSECTING STABILIZING FORCES OF PROTEINS BY SENSITIVITY ANALYSIS. ((Chung F. Wong and Qiang Wang)) Mount Sinai School of Medicine, Department of Physiology and Biophysics, NY, NY 10029-6574

A combined molecular dynamics/sensitivity analysis approach has been used to learn how the secondary and tertiary structural elements of proteins are stabilized. The advantage of this approach is that it allows one to study the role of each amino acid and each interaction in determining the stability of a protein in a systematic and efficient manner. We have learned some useful principles of protein structure and stability from an initial analysis of four proteins: bovine pancreatic trypsin inhibitor (BPTI), α-dendrotoxin, cytochrome c, and cytochrome b562. For example, we have confirmed that the capping box motif, UXXZ where U is a serine or a threonine and Z is a glutamate or an aspartate, is a useful structural motif for stabilizing the N-termini of α-helices. However, in contrast to previous studies, our analysis suggests that the interaction between the side chains of U and Z may play a more significant stabilizing role than the main chain-side chain interactions proposed earlier. It also appears that the N-termini of helices are more likely to be stabilized by interactions among the residues in this region of the helices whereas the C-termini of helices are more often stabilized by interacting with the other parts of their host proteins. In addition, there appears to be a small number of exceptionally strong interactions that help to give a native protein one well-defined structure rather than two or more distinct structures with comparable stability. Although the proteins BPTI and α-dendrotoxin have a similar 3-dimensional fold, the two proteins seem to be stabilized by rather different interactions. Consistent with experimental findings, the N- and C-termini of cytochrome c are found to interact strongly and may form a detectable folding intermediate.

M-Pos436

TECHNIQUES FOR LARGE-SCALE KINETIC MODELING OF SPECTROSCOPIC DATA SETS. ((Eric R. Henry)) NIDDK, NIH Bethesda, MD 20892-0520.

Multichannel detector technology has enabled the rapid accumulation of large sets of optical spectra of molecular systems as a function of one or more experimental variables (time, pH, temperature, etc.). Mathematical models are used to describe the observed variations in these spectra in terms of interconverting populations of molecular species. The goal of such modeling is to determine the model parameters governing the interconversion between species, as well as the spectra of the species themselves. We have developed methods for solving such problems which exploit the formal expression of the complete matrix of measured spectra (for all sets of experimental conditions) as the product of a matrix of species populations and a matrix of species spectra. Matrix methods facilitate the simultaneous determination of both species populations (prescribed by a specified set of model parameters) and the most consistent species spectra, the product of which produces the simulated data matrix. The modeling proceeds by varying the model parameters until the simulated data matrix best approximates the experimental data matrix. The method allows the user to easily incorporate known species spectra into the analysis, enforce simple feature relationships (e.g. relative peak positions) between otherwise unspecified spectra, and constrain the shapes of unknown spectra through the use of parametrized analytical functions. In applying this approach to kinetic modeling of time-resolved spectroscopic data on photolyzed hemoglobin, we have successfully addressed a number of other important issues, including the automatic generation of large (hundreds of states) complex models from simple prescriptions for state connectivity; economical mechanisms for introducing temporally extended behavior (e.g., stretched exponential relaxation) into a modeling scheme; enforcing consistency between equilibrium and kinetic descriptions of the system; and the integration of model systems of differential equations using initial conditions which accurately reflect the photophysics of the experiment.

M-Pos437

Thermodynamic analysis of the interaction of the Grb2 SH2 domain with phosphopeptides: Computational approaches and comparison with experiment. (M.E. Snow, P. Mui, C. McNemar, W. Windsor, A. Prongay, A. Frederick, P.C. Weber) Schering-Plough Research Institute, Kenilworth, NJ 07033

The recognition of specific phosphotyrosine-containing peptide sequences by SH2 domains plays an essential role in many cell-signaling processes. A thermodynamic understanding of these peptide-protein interactions might assist in the design of novel compounds which bind specifically to a given SH2 domain.

We have studied the energetics of the interaction of the Grb2 SH2 domain with the peptide Ac-S-pY-V-N-V-Q-NH_2 (the Y317 peptide from SHC). Three dimensional models of the protein in the free and peptide-complexed form, constructed using three different homology modeling methods, have been used to calculate semi-empirical estimates of the heat capacities, enthalpies and entropies of binding using methodology developed by Gomez and Freire[1]. The calculated heat capacities (-105 to -192 cal/mol K) and enthalpies (-4.6 to -9.6 kcal/mol at 20C) depend on the model used for the calculation but bracket the experimental values determined by isothermal titration calorimetry. Thus, all three models predict that binding is enthalpically favored. The sign of the predicted entropy of binding is model dependent, but is consistently smaller in magnitude than ΔH. The experimental entropy of binding is small and favorable.

[1]Gomez, J. and Freire, E. (1995) J. Mol. Biol., in press

M-Pos438

COMPUTER SIMULATION OF A TYPE I ANTIFREEZE PROTEIN AT THE ICE/WATER INTERFACE. ((J.D. Madura[a], W.A. Ward[b], S. Murrill[b], and A. Wierzbicki[a])) [a]Department of Chemistry, [b]Department of Computer and Information Science, University of South Alabama, Mobile, AL 36688.

Nature has, in certain instances, provided particular organisms with inherent protective mechanisms that either retard and/or inhibit the formation of ice crystals *in vivo* preventing possible cellular damage. One of these protective mechanism, directly dependent upon the presence of antifreeze glycoproteins r antifreeze proteins (AFPs), is known to function in certain species of polar fish. An interesting aspect of this phenomena is the interactions between the surface and the protein at the solid-liquid interface.

The preliminary results from a molecular dynamics simulation of a Type I antifreeze protein at the ice/water interface will be presented. The simulation consists of the winter flounder AFP at the interface between (201) ice face and water. Results will be presented in terms of the various solvent-solvent as well as the solvent-protein interactions. Comparison of our previous work on the protein/ice interactions with the data from the current simulation will also be discussed. This work will also be compared to earlier ice/water simulations done by others.

M-Pos439

INVESTIGATIONS OF STEREOSPECIFITY OF BINDING OF TYPE I ANTIFREEZE PROTEINS TO ICE ((A. Wierzbicki[1], M.S. Taylor[1], C.A. Knight[2], J.D. Madura[1], C.S. Sikes[3] and J.P. Harrington[1])) [1]Department of Chemistry, University of South Alabama, Mobile, Alabama 36688, [2]National Center for Atmospheric Research, Boulder, Colorado 80307, and [3]Department of Biological Sciences, University of South Alabama, Mobile, Alabama 36688.

Using ice crystal growth and etching techniques together with molecular modeling and energy minimization, we investigate mechanisms of stereospecific binding of Type I Antifreeze Proteins (AFP) to ice. This binding mechanism appears to be based on the protein crystal enantioselective recognition that utilizes not only matching of polar/charged residue side chains with specific water molecule positions in the ice surface, but also α-helical protein backbone matching to the ice surface topography. Binding analysis of various Type I AFPs is presented and analyzed to verify the proposed mechanism of Type I AFP binding to ice.

M-Pos440

COMPARISON OF SOLVENT-INDUCED INTERACTIONS BETWEEN HYDROPHILIC AND HYDROPHOBIC GROUPS IN A SIMPLE MODEL COMPOUND. ((S.R. Durell and A. Wallqvist)) Lab of Math. Biol., NCI, NIH. Bethesda MD 20892. (Spon. by S.R. Durell)

Previously, we examined the role of solvent water molecules in inducing forces between two simple hydrophilic and hydrophobic solutes. In short, it was found that the solvent-induced component of the interaction energy was considerably more negative for the hydrophilic version of the solutes than for the non-charged, hydrophobic counterparts. However, inclusion of the direct interaction energy component equalizes the magnitudes of the favorable interactions between the hydrophilic and hydrophobic solute pairs. In this study, we extend this work to the two hydroxyl functional groups of a model phenol derivative which has a methanol group added at either the ortho or meta positions. Molecular dynamics simulations of the solute in water are used to determine the potential of mean forces for the rotatable bonds, which are representative of the solvent-induced interactions between the two hydroxyl groups. Thermodynamic integration is used to calculate the relative free energies of the ortho and meta isomers inorder to investigate the atomic basis for the experimentally determined differences in the energy of solvation. The results of this work are relevant to determining the relative importance of the different factors responsible for macromolecular folding, association and ligand binding.

M-Pos441

ACCELERATED COMPUTER SIMULATIONS OF ASSOCIATION OF BIOLOGICAL MACROMOLECULES. ((G.A. Huber and S. Kim)) Chemical Engineering Department, University of Wisconsin, Madison, WI 53706-1691

Two complementary computational methods, Free Energy Valley Encounter Reactions (FEVER) and Weighted Ensemble Brownian (WEB) Dynamics, are proposed to speed up computer simulations of association kinetics (enzyme–substrate, antibody–antigen). Brownian dynamics simulations have been hindered by free energy barriers and long range electrostatic interactions that necessitate the employment of a large termination radius and lengthy simulations. The new approach, FEVER, is a flux–overpopulation method with the key information on the probability distribution function captured by its moments. A hierarchy of interlinked moment equations is obtained, but the hierarchy may be truncated by introduction of a closure scheme. For configurations close to the docking configuration, the approximations break down and WEB Dynamics are employed instead. WEB Dynamics invokes a weighted ensemble of trajectories in CS, with energy levels dictating the correspondence between "particles" and probability. Free energy barriers are surmounted rapidly (infrequent events are observed immediately) by spawning trajectories of "child" particles.

The overall paradigm for speeding up enzyme–substrate simulations can thus be summarized as FEVER in the far field, WEB Dynamics in the near field, and special boundary conditions at the WEB–FEVER interface. The method has been applied to a simple enzyme–substrate association model with electrostatic steering. WEB–FEVER predicts reaction rate constants in agreement with those obtained by direct Brownian simulation, but with a four–thousand fold decrease in the number of force evaluations.

M-Pos442

Finite Element Model of Second Messenger Diffusion in Dendritic Spines ((M. S. Jafri and T.B. Woolf)) Depts of Biomedical Eng. and Physiology, Johns Hopkins Univ, Schl of Med, Baltimore, MD 21205. (Spon by S. Bergling)

Realistically detailed models of diffusion in dendritic spines were constructed using the finite element (FE) method. These diffusional models use the exact analogy between heat conductivity and the diffusion constant. This permits the application of FE software for heat conduction to diffusion problems. Detailed finite element models of dendritic spines require both high resolution experimental reconstructions and an algorithm for mesh generation. The morphological reconstructions were provided from the labs of C.A. Greer and K. Harris for dendritic spines of olfactory bulb granule cells and hippocampal pyramidal cells. The mesh construction used the program INGRID from Lawrence Livermore National Labs (LLNL). This enabled the simulation of the spines as a connected series of cylindrical elements. An example is shown in the figure. The heat transfer code TOPAZ3D from LLNL was used to simulate concentration transients due to a step functional increase in second messenger at the most apical tip of the dendritic spine. The results support the emerging consensus that dendritic spines function to compartmentalize second messengers.

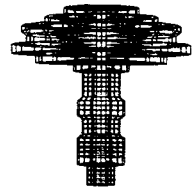

M-Pos443

MOLECULAR DYNAMICS SIMULATIONS OF TWO FATTY ACID BINDING PROTEINS ((M. Tychko and T.B. Woolf)) Depts of Physiology and Biophysics, Johns Hopkins University, School of Medicine, Baltimore, MD 21205

The CHARMM molecular dynamics program was used to explore the dynamics and energetics responsible for fatty acid binding within the adipocyte fatty acid binding protein (A-FABP; *J. Biol. Chem.* **268**:7874-7892) and the human muscle fatty acid binding protein (HM-FABP; *Structure* **2**:523-534). Two 750 psec long trajectories were run to compare the differences between stearic acid in A-FABP and HM-FABP. Two additional trajectories simulated the interactions of HM-FABP complexed with oleate or elaidate (18:1 cis and trans). Initial calculations suggest that the carboxylate headgroup of the fatty acid should be protonated. Each calculation used the all-hydrogen parameter set and an explicit water sphere of 27 Å radius surrounding the FABP. The figure shows an interaction energy distribution for A-FABP:stearate averaged over the trajectory. A total interaction energy of about -60 kcal/mol represents an exceptionally strong protein:lipid interaction. On average, the alkane chain contribution is -2.5 kcal/mol per methylene segment. The headgroup interactions reflect the hydrogen bonding network around the carboxylate of R106, R126, and Y128, which was analyzed in considerable detail. These results suggest ligand selectivity is controlled not only through headgroup interactions but also through a conformation specific VDW component.

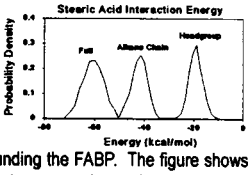

M-Pos444

SAME: A STRATA-BASED APPROXIMATION FOR THE MEMBRANE ENVIRONMENT ((Alan Grossfield, Charles R. Sanders II, Thomas B. Woolf)) Depts. Physiol. and Biophys., Johns Hopkins Univ., Baltimore, MD 21205 & Dept. Physiol. & Biophys., Case Western Reserve Univ., Cleveland, Ohio 44106.

A mean field approximation for the membrane environment has been developed and integrated into the CHARMM molecular mechanics program. The model was developed to extend the work of Sanders and Schwonek, which represented the membrane-water interface as a gradual two-step transition (*Biophys J.* **65**:1207-18). Our routine, SAME (Strata-based Approximation of the Membrane Environment), models the membrane as a continuous series of solvent layers, changing gradually from properties consistent with bulk water to those consistent with bulk hydrocarbon. SAME includes four energy terms rooted in scaled particle theory: a Born-like term, a hard sphere interaction term, a solvent volume term, and a cavity formation term (*Chem. Rev.* **76**:717-26). It also modulates the electrostatic interactions to reflect a continuous variation of the dielectric constant across the membrane. Test cases were evaluated by calculating free energies of transfer for single amino acids and for tripeptides. Further evaluations compared explicit lipid and water simulations for DMDAG and individual bacteriorhodopsin helices to the SAME results. The SAME simulations were typically 80 to 100 times faster than equivalent explicit lipid and water simulations; the relative advantage in speed will enable us to tackle more demanding calculations using this algorithm.

M-Pos445

SIGNAL TRANSDUCTION BY G-PROTEIN COUPLED RECEPTORS: MOLECULAR DYNAMICS OF TRANSMEMBRANE HELICES IN A BILAYER MIMETIC

((Chandra S. Ramanathan[1], Karen Haydock[2], Christopher Haydock[3], Ethan W. Taylor[1], Harel Weinstein[2] and Laurence J. Miller[3])) [1]Department of Medicinal Chemistry, College of Pharmacy, University of Georgia, Athens, GA 30602. [2]Department of Physiology and Biophysics, Mount Sinai School of Medicine, New York, NY 10029. [3]Department of Biochemistry and Molecular Biology, Mayo Foundation, Rochester, MN 55905.

A switch in the conformational state of G-protein coupled receptors transduces ligand binding into a productive coupling of the receptor and G-protein. Experimental results suggest that alanine 293 on the putative intracellular extension of helix 6 of the α_{1B}-adrenergic receptor constrains this receptor in the inactive conformation. Our previous molecular dynamics simulation studies of helix 6 in a bilayer mimetic show transmembrane correlations of the backbone dihedral angles that might correspond to the switch from the inactive to the active state. We are now conducting several new 100 ns simulations of transmembrane helices in the hydrophobic bilayer phase. These simulations give better statistical convergence of the transmembrane correlations and are long enough to apply a new technique that we have developed for measuring the correlations between side chain conformations. We are also examining the effect of helix interactions on the conformational switch from the inactive to the active state by simulating bacteriorhodopsin helices 1 and 7 in a hydrophobic bilayer phase.

M-Pos446

MOLECULAR AND COLLECTIVE DYNAMICS OF MEMBRANE BILAYERS: EVIDENCE FROM NMR RELAXATION.

((Michael F. Brown, Constantin Job and Theodore P. Trouard)) Department of Chemistry, University of Arizona, Tucson, Arizona 85721, USA.

NMR relaxation methods indicate a broad distribution of motions in fluid membranes, including rapid dihedral angle isomerizations, molecular motions, and **collective bilayer excitations.**[1,2] There are two limits depending on the repeat distance d between the layers relative to the wavelength λ of the collective fluctuations. In the high frequency MHz regime where $\lambda << d$ (free membrane or weakly coupled limit), interactions among the bilayers are negligible, and collective excitations are described in terms of a **continuum elastic model** involving twist, splay, and bend disturbances, yielding an $\omega^{-1/2}$ dependence.[3] In the low frequency kHz regime where $\lambda >> d$ (strongly coupled limit), interactions among the various lamellae are treated using a **flexible surface model** involving splay only, leading to an ω^{-1} frequency dependence.[3] Finally the microviscosity of the bilayer hydrocarbon interior is on the order of a few centipoise (cP). These earlier conclusions from experimental NMR relaxation measurements[1,4] are relevant to molecular mechanics simulations of lipid bilayers in the fluid phase.[5,6] With the advent of faster computers, one can investigate more specifically the collective dynamics of bilayer membranes proposed on the basis of NMR spectroscopy. [1]Brown, M.F., et al. (1983), *Proc. Natl. Acad. Sci. USA* **80**, 4325-4329. [2]Trouard, T.P., et al. (1994), *J. Chem. Phys.* **101**, 5229-5261. [3]Brown, M.F., and Chan, S.I. (1995), in *Encyclopedia of Nuclear Magnetic Resonance*, Wiley, in press. [4]Brown, M.F. (1996), in *Membrane Structure and Dynamics*, Birkhäuser, in press. [5]Pastor, R.W., et al. (1991), *Proc. Natl. Acad. Sci. USA* **88**, 892-896. [6]Venable, R.M., et al. (1993), *Science* **262**, 223-226. Supported by NIH grant GM41413.

M-Pos447

A STRUCTURAL BASIS FOR A PHOSPHORAMIDE MUSTARD-INDUCED DNA INTERSTRAND CROSS-LINK AT 5'd(GAC)

((Daniel Barsky†, Qing Dong*, Michael E. Colvin†, Carl F. Meliusŧ, Susan M. Ludeman‡, O. Michael Colvin*, Darell D. Bigner*, Paul Modrich‡, Henry S. Friedman*)) *Depts. of Pathology and Pediatrics; Howard Hughes Med. Inst. and Dept. of Biochemistry, Duke Univ. Med. Center, Durham, NC 27710; †Sandia Nat. Labs, Livermore, CA 94551-0969; and ‡Oncology Center, JohnsHopkins Univ, Baltimore, MD 21287.

Phosphoramide mustard forms DNA interstrand cross-links which are likely to be the basis of anti-tumor activity of phosphoramide compounds. Phosphoramide mustard-induced DNA interstrand cross-links were studied *in vitro* and by computer simulation. The local determinants for the formation of phosphoramide mustard-induced DNA interstrand cross-links were identified by using different pairs of synthetic oligonucleotide duplexes, each of which contained a single potentially cross-linkable site. Phosphoramide mustard was found to cross-link dG-to-dG at a 5'-dGAC-3'. The structural basis for the formation of this 1,3 cross-link was studied by molecular dynamics and quantum chemistry. Molecular dynamics indicated that the geometrical proximity of the binding sites favored a 1,3 dG-to-dG linkage over a 1,2 dG-to-dG linkage in a 5'-dGCC-3' sequence. While the enthalpies of 1,2 and 1,3 mustard cross-linked DNA were found to be very close, a 1,3 structure was more flexible and may therefore be in a considerably higherentropic state.

M-Pos448

COMPUTER SIMULATION OF BIMOLECULAR RATE CONSTANTS FOR SITE-SPECIFIC PROTEIN-DNA INTERACTIONS.

((J.D. Dwyer[1] and V.A. Bloomfield[2])) [1]Department of Chemistry, College of St. Catherine, St. Paul, MN 55105; [2] Department of Biochemistry, University of Minnesota, St. Paul, MN 55108

We have developed a Brownian dynamics algorithm for simulating the time dependent bimolecular rate constant for specific protein-DNA interactions. In our method, based on that originally described by Zhou (J. Phys. Chem. 94 (1990), 8794-8800), protein molecules are modeled by spheres of equivalent hydrodynamic radius and DNA is modeled as a charged cylinder containing a single reactive segment. Protein Brownian trajectories are propagated in a simulation cell containing the DNA chain and are terminated when either the protein reacts or a predetermined cutoff time is reached. A numerical solution to the Poisson-Boltmann equation for a charged cylinder is used to govern the electrostatic interaction between the protein and the DNA. The time dependent rate constant is obtained as the product of two terms: 1) a space dependent component related to the magnitude of the interaction potential at the surface of the reactive patch and an adjustable reactivity parameter; and 2) a time dependent component which is obtained from the survival statistics of the Brownian trajectories. We test this algorithm on several systems for which analytical results are available to demonstrate the validity of the method. The program is then used to study the lac repressor-DNA interaction. We find that a reasonable set of model parameters leads to simulation results for the steady state rate constant that are in good agreement with available experimental data. Simulation results for the ionic strength dependence of the rate constant are presented and discussed.

M-Pos449

MINOR GROOVE DNA CONFORMATIONS OF THE N^2 GUANINE ADDUCT OF 2-ACETYLAMINOFLUORENE (AAF): DIFFERING ORIENTATIONS IN DIFFERENT SEQUENCE CONTEXTS.

((Grad, R.*, Shapiro, R.*, Hingerty, B.E.** and Broyde, S.*)) *Biology and *Chemistry Depts., New York University, New York, NY 10003 and **Health Sciences Research Division, Oak Ridge National Laboratory, Oak Ridge, TN 37831.

In vitro and *in vivo* studies of the carcinogenic aromatic amine AAF have afforded two adducts, one bound to C8 of guanine and a minor product (5-15% of total) bound to N^2 of guanine. The minor adduct may be important in carcinogenesis because it persists, while the major adduct is rapidly repaired (1). Primer extension studies of the minor adduct, N-(deoxyguanosin-N^2-yl)-2-acetylaminofluorene, have indicated that it blocks DNA synthesis, with some bypass and misincorporation of adenine opposite the lesion (2). No experimental structural information is available for this adduct. We have used extensive minimized potential energy searches to study the conformation of this adduct in two sequences: CGCG(AAF)CGC•GCGCGCG and CTAG(AAF)TCA•TGACTAG. In the first sequence AAF was located in the minor groove in the two structures of lowest energy. In the lowest energy form, AAF pointed in the 3' direction (with reference to the modified strand) and the acetyl in the 5' direction. These orientations were reversed in the second structure. These two structures differed in energy by 1.4kcal/mol. Watson-Crick hydrogen bonding was intact in both structures. In the two low energy structures for the second sequence, AAF was also located in the minor groove with Watson-Crick hydrogen bonding intact. However, in the lowest energy form, the AAF pointed in the 5' direction (with reference to the modified strand) and the acetyl in the 3' direction. The potential energy of the structure with opposite orientation (AAF pointed in the 3' direction of the modified strand) differed in energy by 5.1 kcal/mol. A similar study of this second sequence, but with A opposite the modified guanine, provided a lowest energy form with features similar to those of the modified duplex with the normal C partner. The AAF was oriented in the 5' direction of the modified strand. Watson-Crick hydrogen bonding was intact for the entire duplex except at the modification site, where the mispaired adenine was in a syn orientation with Hoogsteen pairing to the modified guanine, as proposed by Shibutani and Grollman (2). These findings suggest that the orientation of the AAF in the minor groove may be dependent on the DNA sequence.

(1) F.A. Beland, K.L. Dooley and C.D. Jackson, Cancer Research 42, 1348 (1982).
(2) S. Shibutani and A. Grollman. Chem. Res. Toxicol. 6, 819 (1993).

Supported by DOE

M-Pos450

WATER IN A CHANNEL, MOBILE PROTONS, AND GATING.

((J. Lu and M. E. Green)) Chemistry Department, City College of CUNY, New York NY 10031

A model we have proposed (e.g., *Biophys J.*62, 101 (1992); 68, A48(1995)) for gating of ion channels is extended to show the effect of motion of protons in the channel wall. The model depends on the distribution of charges in the wall of the channel. We now show that the charges, if taken to be protons in a series of energy wells, can be localized by a field comparable to a few mV across a membrane. The wells are taken to be harmonic and one dimensional, but spaced as amino acid side chains would be. When the levels are just matched, possible as the membrane depolarizes, the protons can tunnel on a time scale comparable to gating. The motion of the protons couples both to other protons and to the potentials produced by ions in the channel. Monte Carlo simulation is used to obtain the behavior of the water in the presence of the ions (we now have 1 or 2 K^+ ions) and the charges. The net force on a K^+ ion in the channel can depend, therefore, on the position of another ion, on the wall charges, and on the water. The mobility of the water depends on the potentials as well. Our calculated fields exceed 10^9 V m^{-1} locally, which is in the expected range; this field strongly orients the water and affects its density in a tapered section of the model, approximately like the pore in a channel. We will show the energy as a function of the position of the K^+ ions and of the charge configuration in the wall, to illustrate how the motion of charges, coupled to the water in the channel, can act as the channel gate. In certain configurations the force pushes an ion down the channel, while in others the ion would experience no net force, or would be trapped in a site defined by the potential, and the channel would be closed.

M-Pos451

STRUCTURE AND DYNAMICS OF WATER WITHIN MODEL TRANSBILAYER PORES.

((M.S.P. Sansom, I.D. Kerr, P.C. Biggin & P.A. Mitton))
Laboratory of Molecular Biophysics, University of Oxford, Oxford, U.K.

Ion channel and related transport proteins contain extended columns of water molecules within their transbilayer pores. The dynamic properties of such confined intra-pore water are likely to differ from those of water in its bulk state. Molecular dynamics simulations of model pores have been employed to analyze the structure and dynamics of intra-pore water. Three classes of model pore have been examined:- parallel bundles of Ala_{20} α-helices; parallel bundles of $(Leu\text{-}Ser\text{-}Ser\text{-}Leu\text{-}Leu\text{-}Ser\text{-}Leu)_3$ α-helices; and antiparallel barrels of Ala_{10} β-strands. All three models exhibit substantially reduced translational and rotational mobility of waters within the pore relative to bulk water and water at the mouths of the pore. Waters within pores formed by parallel bundles of α-helices are preferentially oriented such that their dipoles lie anti-parallel to the α-helix dipoles. Preferential orientation of water dipoles relative to the pore axis is not observed for β-barrel models. Molecular dynamics simulations in the presence of a trans-pore electrostatic field (ie. a voltage drop along the pore axis) have been used to estimate the resultant polarization (due to reorientation) of the intra-pore water, and hence to estimate the local dielectric constant within the pore.

SEDIMENTATION

M-Pos452

RAPID MOLECULAR WEIGHT DETERMINATION BY SEDIMENTATION VELOCITY ANALYSIS. ((Walter F. Stafford)) Boston Biomedical Research Institute, 20 Staniford Street, Boston MA 02114.

The molecular weight of an ideal, monodisperse macromolecule can be determined from sedimentation velocity analysis if the diffusion coefficient is determined simultaneously. Recently, the precision of sedimentation velocity analysis has been increased by using the time derivative (Stafford(1992), Anal. Biochem 203,295-301). The time derivative is converted to an apparent sedimentation coefficient distribution function, g(s*) vs. s*, where s* is defined as $s^* = (1/\omega^2 t)\ln(r/r_m)$ where ω is the angular velocity of the rotor, t is the effective time of sedimentation, r is the radius and r_m is the radius of the meniscus. A plot of g(s*) has essentially the same properties as the familiar schlieren gradient plots. For an ideal, monodisperse macromolecule, a plot of g(s*) vs s*, to within a very good approximation, is gaussian. It can be shown that the diffusion coefficient of the macromolecule can be related to the standard deviation of the g(s*) vs s* curve by the following relationship: $D=(\sigma r_m \omega^2 t)^2/2t$ where D is the diffusion coefficient, σ is the standard deviation of the g(s*) curve and is determined by fitting to the following equation: $g(s^*) = A \exp(-0.5((s^*-s)/\sigma)^2)$. The ratio of s to D is related to the molecular weight by the Svedberg equation, $s/D = M(1-\bar{v}\rho)/RT$, where s is the sedimentation coefficient given by the maximum position of the g(s*) curve, $\bar{v}$ is the partial specific volume of the macromolecule, ρ is the density of the solvent, R is the gas constant and T is the absolute temperature. The molecular weight determined this way has an uncertainty of about 10%.

M-Pos453

CHARACTERIZATION OF IRON DISTRIBUTIONS IN RECONSTITUTED FERRITIN BY ANALYTICAL ULTRACENTRIFUGATION. ((J.K. Grady*#, N.D. Chasteen* and T.M. Laue#) *Chemistry Dept., #Dept. of Biochemistry and Molecular Biology, Univ. of New Hampshire, Durham, N.H. 03824)

The ferritins are a family of iron storage proteins found in vertebrates, invertebrates, plants and bacteria. Characterization of ferritin reconstituted from Fe(II) and apoferritin has been complicated by its propensity to form inhomogeneous iron distributions. The analytical ultracentrifuge was used to determine the iron distribution among horse spleen ferritin molecules reconstituted *in vitro* under a variety of conditions. Iron distributions were found to be more heterogeneous when iron was added in small increments (< 50 Fe/protein per addition), conditions under which the ferroxidase activity of the protein is not kinetically saturated. More homogeneous samples were formed when iron was added in larger increments (1000-2000 Fe/protein per addition) where iron oxidation principally occurs on the growing mineral surface. The dependence of the iron distributions on the method of iron loading and the ferroxidase activity will be presented.

Supported by NSF BIR 9314040 and NIH R37 GM20194

M-Pos454

The use of gases as test objects for absorbance optical systems in the ultracentrifuge. David A. Yphantis* and Jeffrey W. Lary*.
*# Molecular and Cell Biology, University of Connecticut, Storrs, CT 06269-3125 and * Institute of Molecular Biology and Biotechnology, University of Crete, Heraklion, Crete, Greece.

A gas (or vapor) at sedimentation equilibrium may be used as a test object for the absorbance system of the XLA ultracentrifuge. Such gaseous test objects have a number of advantages over solution test objects since the analog of sedimentation equilibrium (compression by the centrifugal field) is attained virtually instantaneously with gases and since many suitable vapors are readily available in pure form. In these experiments a drop of an appropriate organic liquid whose vapor exhibits both a modest vapor pressure and a convenient optical absorbance is placed in one sector of an ultracentrifuge cell while the other sector is left unsealed. The rotor is run up to speed and the absorbance is measured as a function of position at appropriate wavelengths. At the low vapor pressures used with strongly absorbing molecules the vapors are generally quite ideal and correspond to a single molecular species of accurately known molecular weight. This provides a simple reproducible test object. Preliminary experiments with iodobenzene (MW 204) at 50,000 RPM gave molecular weights within experimental error (about 1%) and indicated small systematic errors in data acquisition. Supported by NSF grants BIR-9218679 and BIR-9318373.

M-Pos455

THE INTERACTION OF LIPOPROTEIN LIPASE WITH HOMOGENEOUS LIPID EMULSIONS. ((C. E. MacPhee, W.H. Sawyer, W.F. Stafford* and G.J. Howlett)) *Department of Biochemistry and Molecular Biology, University of Melbourne, Parkville, VIC 3052 AUSTRALIA. *BBRI Boston, MA 02114-2500, U.S.A.* (Spon W.F.Stafford).

Analytical ultracentrifugation techniques were used to study the interaction of lipoprotein lipase (LpL) with populations of non-hydrolysable lipid emulsions which were homogeneous with respect to size and composition. Emulsions were prepared by sonication and pressure extrusion, and purified by density gradient centrifugation in a 0-5% sucrose gradient. Fractionation of gradients resulted in discrete, highly homogeneous emulsion size fractions. Emulsions were characterised by flotation velocity and flotation equilibrium experiments, and by calculation of the apparent flotation coefficient distribution function (g(s*)).

Studies of mixtures of non-hydrolysable emulsion particles and low concentrations of LpL suggest crosslinking of the lipid particles, and the presence of two sites on the enzyme dimer for binding to the lipid surface. At saturation of emulsion with LpL, the capacity of the particles to bind the enzyme decreased systematically with an increase in average particle size. Populations of average radii of 67, 75 and 79nm bound LpL with stoichiometries of 79, 92 and 102 phospholipid molecules per LpL monomer, respectively. We ascribe this behaviour either to an alteration in phospholipid packing, or to a decrease in the amount of triacylglycerol solubilised in the surface monolayer.

M-Pos456 - M-Pos505

Reserved for High School Student Posters.

STUDIES OF PROTEIN COMPLEXES BY NMR: THE NEXT FRONTIER

Tu-AM-SymI-1

COMPLEXES OF HUMAN THIOREDOXIN AND ITS TARGET PEPTIDES
((A.M. Gronenborn)) NIDDK, NIH, Bethesda, MD 20892

It has recently been shown that human thioredoxin, a 12 kDa cellular redox protein, is involved in the activation of several transcription factors, in particular NFkB and Fos/Jun. Using multidimensional heteronuclear-edited and -filtered NMR spectroscopy, we have solved the solution structure of a complexes of human thioredoxin with target peptides from NFkB and Ref-1, representing kinetically stable mixed disulfide intermediates along the reaction pathway. The NFkB peptide is located in a long boot-shaped cleft on the surface of human thioredoxin delineated by the active site loop, helices α2, α3 and α4, and strands β3 and β4. The peptide adopts a crescent-like conformation with a smooth 110° bend centered around residue 60 which permits it to follow the path of the cleft. The Ref-1 peptide, in contrast, binds in the opposite orientation but uses predominantly the same binding cleft. In addtion to the disulfide bridge between Cys32 of human thioredoxin and the cysteines of the peptides, the complexes are stabilized by numerous hydrogen bonding, electrostatic and hydrophobic interactions with the latter being the most important one for defining the orientation of the peptide.

Tu-AM-SymI-2

STRUCTURES OF PROTEIN-LIGAND COMPLEXES INVOLVED IN SIGNAL TRANSDUCTION.
((S.W. Fesik[1], M.-M. Zhou[1], E.T. Olejniczak[1], A.M. Petros[1], R.P. Meadows[1], M.Sattler[1], J.E. Harlan[1], W.S. Wade[1], S. Crosby[1], K.S. Ravichandran[2], and S.J. Burakoff[2]))
[1]PPD, Abbott Laboratories, Abbott Park, IL 60064 [2]Division of Pediatric Oncology, Dana-Farber Cancer Institute and Department of Pediatrics, Harvard Medical School, Boston, MA 02115.

Signal transduction is a complicated process that may involve several steps mediated by specific intermolecular interactions. Recently, three-dimensional structures of protein/ligand complexes involved in signal transduction have been obtained which have greatly aided in our understanding of these processes at the molecular level. In this presentation, the NMR structure of the phosphotyrosine binding (PTB) domain of the adaptor protein Shc complexed to a phosphopeptide (TrkA) derived from the nerve growth factor receptor will be presented. The structure of the complex reveals an alternative means of recognizing tyrosine-phosphorylated proteins compared to SH2 domains. The PTB domain is structurally similar to pleckstrin homology domains (β-sandwich capped by an α-helix) and binds to acidic phospholipids, suggesting a possible role of this domain in membrane localization.

Tu-AM-SymI-3

NMR STRUCTURAL AND DYNAMIC STUDIES OF SH2 DOMAIN-PHOSPHOPEPTIDE COMPLEXES.
(J.D. Forman-Kay, N.A. Farrow, S.M. Pascal, A.U. Singer, T. Yamazaki, L.E. Kay) Hospital for Sick Children and University of Toronto, Toronto, Ontario, CANADA M5G 1X8.

The C-terminal Src Homology 2 (SH2) domain of phospholipase C-γ1 (PLCγ) binds specifically to the phosphorylated Tyr-1021 of the β-platelet-derived growth factor receptor (PDGFR) as well as to certain phosphorylated tyrosines on other growth factor receptors and to PLCγ itself. The NMR structure of a complex of the C-terminal SH2 domain of PLCγ (PLCC SH2) with a 12-residue peptide encompassing the Tyr-1021 site of the PDGFR (pY1021) has been determined and refined, demonstrating (1) SH2 interactions with residues from the -1 to +6 positions relative to the pTyr of the peptide, (2) bound water molecules, one of which bridges interactions between the SH2 domain and peptide, and (3) the presence of a small cavity. Insights into the interaction have also been derived from pH titrations which demonstrate significanty shifted pKa values for the phosphotyrosine (pTyr) of pY1021 and a conserved histidine near the pTyr-binding site. Backbone and sidechain ^{15}N and novel methyl ^{2}H relaxation experiments have been performed on free and pY1021-complexed PLCC SH2 domain. Dynamics have also been inferred from broadening of resonances and chemical shifts of arginine sidechain resonances. Results show significant μs-ms motion but restriction of ns-ps motion in the pTyr-binding site with the reverse in the hydrophobic binding region responsible for binding specificity through interactions with peptide residues C-terminal to the pTyr. Comparison with binding studies suggests a correlation between ns-ps time scale dynamic behavior and contribution to binding energy.

Tu-AM-SymI-4

Homeodomain-DNA Recognition: the NMR Solution Structure of the *Antennapedia* Homeodomain-DNA Complex.
Y.Q. Qian,[1] M. Billeter,[2] G. Otting,[3] Peter Güntert,[2] Peter Luginbühl,[2] M. Müller,[4] W. Gehring[4] and K. Wüthrich,[2]
[1]*Department of Physical & Structural Chemistry, SmithKline Beecham Pharmaceuticals, Mail Code UW-2940, PO Box 1539, King of Prussia, PA 19406-0939, USA*
[2]*Institut für Molekularbiologie und Biophysik, ETH-Hönggerberg, 8093 Zürich, Switzerland*
[3]*Department of Medical Biochemistry and Biophysics Karolinska Institutet S-171 77 Stockholm Sweden*
[4]*Biozentrum der Universität Basel, Abt. Zellbiologie, Klingelbergstr.70, 4056 Basel, Switzerland.*

Recent results on the determination of the NMR solution structure of the *Antennapedia* homeodomain-DNA complex will be presented. The *Antennapedia* homeodomain was uniformly labeled with ^{13}C or ^{15}N, and two-dimensional [^{1}H,^{1}H]-NOESY spectra, recorded with a $^{15}N(\omega_2)$-half-filter or a $^{13}C(\omega_1, \omega_2)$-double-half-filter, as well as three-dimensional heteronuclear-correlated [^{1}H ^{1}H]-NOESY spectra were used. The two macromolecules were docked using a simulated annealing approach and further refined by short runs of molecular dynamics in a water bath, followed by final energy refinements. The salient structure features are that the recognition helix is located in the major groove of the DNA with the turn of the helix-turn-helix motif outside the protein-DNA contact area, and that the N-terminal arm of the homeodomain penetrates the minor groove of the DNA. Although no constraints were imposed on water molecules during the structure calculations, hydration water molecules are found in the protein-DNA interface of the resulting structure, a feature that coincides with direct NMR observations of hydration waters. A subsequently recorded molecular dynamics trajectory covering 2 ns of the *Antennapedia* homeodomain-DNA-water system, using the program OPAL, further explored the implicated fluctuations of the network of specific protein-DNA interactions. Thus, the interfacial hydration water is short-lived and mediates numerous protein-DNA interactions. Several of the amino acid side chains responsible for specific DNA contacts undergo rapid motions between multiple contact sites on the DNA, indicating that fluctuations of the intermolecular interaction network play an important role.